Effector roles of Granulocytes and B cells during Th2 Inflammation

Effector roles of Granulocytes and B cells during Th2 Inflammation

A dissertation presented by

Daniel Francis Dwyer

to

The Division of Medical Sciences

In partial fulfillment of the requirements

for the degree of

Doctor of Philosophy

in the subject of

Immunology

Harvard University

Cambridge, Massachusetts

May, 2014

Dissertation advisor: Dr. K. Frank Austen Daniel F. Dwyer

Effector roles of Granulocytes and B cells during Th2 inflammation

Abstract

Allergens are complex mixes of proteins and other compounds that have innate signaling capacity leading to Th2 inflammation. Understanding the role of each of these signals is essential to determining what separates allergens from innocuous proteins. Here, we examine two models for Th2 inflammation: infection with the helminth *Trichinella spiralis* and footpad immunization with papain, a cysteine protease structurally similar to proteases found in many common allergens including grass pollen and dust mites and helminth-secreted proteases secreted. Together, these studies highlight previously unappreciated effector roles of accessory cells during Th2 inflammation.

T. spiralis infection recruits both basophils and a previously uncharacterized hypogranular circulating mast cell (MC) to draining mesenteric lymph nodes (MLN). This hypogranular MC is phenotypically similar to MC precursors (MCp) found in the bone marrow and spleen of BALB/c mice, and remains lightly granulated following recruitment to the lymph node, where it produces both IL-4 and IL-6. In contrast, footpad immunization with papain only recruits basophils to the draining popliteal lymph node (PLN). Importantly, anti-FceRI injection, used in past studies to deplete basophils, also depletes these hypogranular MCp. This raises the

possibility that some effects attributed to basophils following mAb depletion that were not reproduced by genetic models may instead be caused by MCp.

In addition to basophil recruitment, papain induces a potent IL4 response directed by T cells in the PLN of mice following footpad immunization directed against the protease. We identify a novel capacity for B cells to rapidly bind and subsequently internalize papain to endosomes in an innate manner not mediated by the specificity of the B cell receptor. B cells subsequently regulate the adaptive immune response by enhancing Inducible T cell Costimulator (ICOS) expression on $CD4^+$ T cells and amplifying both Th2 cell and T follicular helper cell induction. Antibody blockade of ICOS ligand, expressed by PLN B cells but not DC at the peak of the immune response, inhibits Th2 and Tfh induction in WT but not B cell-deficient μMT mice. Thus, B cells play a critical role in amplifying adjuvant-dependent T cell responses following non-canonical acquisition and internalization of cysteine protease.

Acknowledgements

I would like to first and foremost thank my mentors, K. Frank Austen and Michael Gurish, for giving me the freedom to follow where my experiments lead me and their support and guidance along the way. Together they created an intellectually stimulating environment that allowed me to thrive, and their excitement with each new result has propelled me throughout my studies.

I'd also like to thank my lab mates past and present, Anne Liu, Lora Bankova, and Tatiana Jones. They've helped me so much along the way in helping with experiments and bouncing ideas around. I also wouldn't have been able to do this without the support of so many others in the Brigham and Woman's Rheumatology, Immunology and Allergy department, including Joshua Boyce, Michael Brenner, Howard Katz, Yoshihide Kanaoka, Nora Barrett, and Tanya Laidlaw.

I'm very grateful to my collaborators Matthew Woodruff and Michael Carroll for all their help with the papain project. Our project just wouldn't be the same without the insight gained from their imaging studies.

My thesis defense advisory committee members, Arlene Sharpe, Jonathan Kagan, and Shannon Turley, have been incredibly insightful and supportive as my project has evolved over the course of my degree. Their guidance has been instrumental over the last four years. I'd also like to thank my thesis examiners, Shiv Pillai, Hans Oettgen, and David Center.

I'd like to thank the Harvard Immunology program for giving me this incredible opportunity and all of my friends at Harvard for making graduate school such a memorable experience. I'd especially like to thank my former roommates

Dmitriy Kolodin, Jonathan Sitrin, Marshall Thomas, and Kevin Bonham for loud conversations in the kitchen, late nights at the Penguin, and great afternoons around the grill.

I'm grateful to my parents, William Dwyer and Linda Sanderson, my sister Allison and my brother Michael for all their love and support throughout the years. I wouldn't have gotten to where I am without all of you.

Finally, I'd like to thank my wife, Jamie Schafer. Completing a Ph.D. isn't a simple task, but having somebody to go through it all with makes it little bit easier. Thanks for sharing all the great times with me but also putting up with me when I'm in a grumpy mood and being there for me when things aren't going as well. I'm so glad that we did this together.

Table of Contents

List of Figures

Chapter 1, Host Th2 responses to infections and allergens

1.1. Overview

The Th1/Th2 paradigm, through which naïve T cells polarize to take on different transcriptional programs depending on the type of pathogenic threat faced by the host, was first described almost 30 years ago, when Mosmann and colleagues demonstrated that murine helper T cells could be divided into two distinct subsets based on their cytokine production profile (1). The first, termed Th1, was characterized by interferon gamma production, and was later shown to differentiate in vivo in response to IL-12 secreting dendritic cells. The second, termed Th2, produced IL-4, and later studies showed that it could be induced in vitro through a T cell stimulus plus IL-4 (2, 3). Subsequent studies by other groups showed that the Th1 program was stabilized by the master transcription factor t-bet (4), while the Th2 program was directed by GATA3 (5). These two transcription factors act to stabilize the Th1 and Th2 element by both enhancing the production of each program's signature cytokines and opposing each other's activity(6, 7).

In the years since, other stable transcriptional programs, including Th17 cells, regulatory T cells (Tregs), and follicular helper T cells (Tfh), have been discovered, each controlled by their own master transcription factor (8-10) and each carrying out distinct roles within the immune system. The innate signals and processes through which a naïve T cell differentiates into many of these phenotypes have been established both in vitro and later in vivo, along with the specific antigen

presenting cell (APC) subsets responsible for polarizing each of these phenotypes (11-14).

Despite the fact that it was one of the first two transcriptional programs described for T cells, the innate signals, specific APCs, and mechanisms leading to Th2 polarization in vivo are not yet fully understood. However, the pathological consequences of this branch of the immune system activating inappropriately are quite well characterized. While the Th1 and Th17 branches, when inappropriately activated, can lead to the immune system directly attacking host tissue (15), the Th2 branch does not tend to directly attack host tissue when inappropriately activated. Rather, a misdirected Th2 responses targets exogenous proteins that are not directly harmful to the host, triggering an immune response that, although not directly cytotoxic, can nonetheless damage host tissue. Th2 inflammation has been implicated in allergic rhinitis, asthma and hives. In these diseases, initial exposure to an allergen sensitizes the immune system and subsequent exposure to the allergen can lead to Th2 inflammation (16). While symptoms of these diseases can be mild, as in rhinitis, in more extreme cases systemic allergic responses can cause systemic blood pressure drops with fatal shock, a process known as anaphylaxis. In other cases, anaphylaxis can lead to edematous swelling of the upper airway or severe bronchial constriction leading to inadequate oxygenation and collapse. While historically not common, asthma allergies are on the rise in western society, prompting a strong need to better understand the immunological processes behind initiating and maintaining Th2 responses. The hygiene hypothesis for increasing allergic diseases emphasizes the lack to exposures inducing Th1 protection but

could also involve an indoor existence with more exposure to mucosal allergens carrying their own adjuvants.

In this thesis, I explore two models of Th2 inflammation, infection with the parasitic helminth *T. spiralis* and immunization with the allergenic cysteine protease papain, and identify previously unappreciated effector roles for accessory cells in each model. The first study focuses on lymph node recruitment of two types of granulocytes, basophils and mast cells precursors (MCp), in both models and highlights a previously unappreciated capacity for the minimally granular MCp to produce cytokines. The second study identifies a novel capacity for B cells to acquire papain in a non-BCR mediated manner and subsequently amplify Th2 polarization in an ICOS-L dependent manner. This introduction will initially focus on the innate signals associated with Th2 inflammation and the cellular processes leading to Th2 polarization and immunoglobulin responses. The second part of this introduction will review what is currently known about the T. Spiralis and papain models.

1.2. Innate recognition signals leading to Th2 inflammation

Before any immune response can be initiated, the immune system must evaluate and determine the nature of the threat it is facing in order to appropriately direct the host response. This is achieved through recognition of factors that are highly conserved among families of pathogens, termed pathogen-associated molecular patterns (PAMPs) through innate pattern recognition receptors (PRR). For bacteria, these factors can include extracellular components of bacteria shed during the bacterial life cycle, such as lipopolysaccharide (LPS), a component of the

outer membrane of gram negative bacteria recognized by the PRR toll-like receptor (TLR)-4 (17, 18), and LTA, a component of gram positive bacterial cell walls, through TLR2 in complex with TLR6 (19, 20). While viral PAMPS can also include viral proteins, many viral sensors detect cytosolic viral double stranded and single stranded RNA as well as unmethylated DNA (21). Fungi, although they are eukaryotic cells similarly to mammalian cells, possess a thick cell wall that protects them against the extracellular environment (22). Components of this cell wall, such as zymosan, can potently activate macrophages and neutrophils as well as the plasma complement pathway. At the cellular level, recognition involves the TLR2/6 heterodimer (23) and carbohydrate receptors such as Dectin 1 (24) and Dectin 2 (25), which recognize B-glucan and a-mannan rich carbohydrates, respectively (26-28).

Recognizing helminthes, a class of parasitic worms, present a different set of challenges. Helminthes are a broad class of complex multicellular parasites that are not known to uniformly express any PAMP (29). However, our immune system can target key points in their life cycle for recognition. Several species of helminths lay eggs that contain high levels of chitin (30) and chitin can also make up part of the mouth structure of some helminthes (29). Thus, our immune system has evolved the ability to recognize chitin, which serves as a potent activator of the innate immune system(31). Helminthes also secrete several classes of proteases as part of their natural life cycle, which can also serve as a source of immune recognition. For example, infective larvae of the trematode *F. hepatica* use the secreted proteases cathepsin B and cathepsin L1 to penetrate the host intestinal wall after hatching, the

immature stage worms use cathepsins L1 and L2 to migrate through the host to their target tissue, the liver, while mature worms use cathepsins L1, L2, and L5 to penetrate the bile duct and to digest red blood cells (32). Proteases are similarly important to other helminthes such *S. mansoni* and *T. regenti*, highlighting their broad relevance in helminth biology (33, 34). The mammalian host also contains many proteases, but these are generally either localized to specific organs like the stomach, kept in an inactive form under steady state conditions such as the proteases involved in the clotting cascade, or sequestered intracellularly in the case of cysteine proteases like cathepsin S (35).

Another important family of helminth-derived Th2 initiating PAMPs are glycans. Immunization of mice with extracts from either the parasitic nematode *B. malayi* and the free-living nematode *C. elegans* are capable of inducing antigen-specific IL-4 responses. These responses are completely ablated following sodium periodate treatment, which alters glycan structure(36). Similarly, metaperiodate treatment of schistosome egg antigen ablates its ability to induce host Th2 as well as IgE and IgG1 responses (37). Glycans may also be important in allergic diseases. A glycan associated with the allergenic dust mite *D. Farrinae* acts as a potent Th2 initiating factor (38), activating Dectin-2 on DCs and leading to cysteinyl leukotriene production and T cell Th2 polarization(39).

Understanding the nature of these innate signals associated with helminthic infection and the receptors that recognize them is important not just for unraveling how the immune system deals with helminthic infection and how helminths can avoid the immune system, but also for understanding how allergic responses are

initiated. Allergens either have direct adjuvant activity of their own or are encountered in the context of other adjuvants. Thus, an allergenic protein with adjuvant activity can stimulate a Th2 response either directly against itself or against other proteins encountered alongside in experimental settings, such as ovalbumin. One prime example of this is the house dust mite cysteine protease DerP1. This protease is the immunodominant target of IgE responses in patients allergic to dust mites and is thus a potent allergenic antigen (40), but can also be used to sensitize mice against innocuous proteins such as ovalbumin in experimental settings (41).

1.3. The Th2 response and follicular helper T cells

A Th2 response is believed to begin with the DC. Dendritic cells sense innate signals conferring the presence of a parasitic infection and carry associated antigen to the local draining lymph node. In contrast to DCs exposed to bacterial antigens that robustly upregulate MHC-II and costimulatory factors(42), exposure to helminth-associated antigens only weakly activates DCs (43, 44). MHC-II, CD80 and CD86 are upregulated to a much lesser degree than following exposure to bacterial antigens (45). However, it is evident that these DCs are receiving activating stimuli. In one model of DC stimulation with N. brasiliensis antigen, DCs treated with antigen promote Th2 responses both in vitro and in vivo, while heat treatment of the antigen renders the DC incapable of triggering Th2 responses, indicating that they must be receiving heat-sensitive adjuvant stimulation (46). Furthermore, in this

model upregulation of other costimualtory factors such as Ox40 ligand can be observed despite there being no observable changes in MHC-II or CD80.

This limited upregulation of antigen presentation molecules may be directly relevant to subsequent Th2 polarization, as in vitro studies have shown that culturing naïve transgenic ova-specific OT-II T cells with DCs and low concentration of ovalbumin can induce Th2 polarization, while higher concentrations of ovalbumin lead to Th1 polarization.(47). As helminthes are generally present in limited numbers and reproduce slowly relative to other microbial threats like viruses, bacteria, and fungi, it is unlikely that high levels of helminth-associated antigens would be present in any physiological setting. Further supporting the physiological relevance of limited antigen presentation in Th2 polarization, several studies have shown that Omega 1, a secreted T2 ribonuclease associated with schistosomal egg extract, can directly diminish the antigen presentation potential of DC (48, 49). This factor is alone sufficient to serve as a Th2 adjuvant in an in vitro system using ovalbumin and transgenic OT-II cells, and also can block upregulation of costimulatory factors by the DC following exposure to the strong adjuvant LPS. Omega 1 treatment further impacts DC cytoskeletal arrangement, inducing a rounded phenotype with fewer dendritic protrusions than seen following LPS exposure or even in naïve DC. Thus, this limited activation phenotype might be the direct result of DC recognition of helminth-associated factors rather than a lack of these factors fully activating the DC.

Th2 cells were initially thought to traffic to the B cell follicle to interact with cognate B cells, secreting B cell-activating cytokines such as IL-4 and leading to B

cell class switching to IgG1 and IgE (50). However, within the past decade this paradigm has been found to be incorrect. Rather, a second subset of CD4+ T cells, follicular helper T cells (Tfh), is responsible for interactions with B cells (51). These cells are known to be dependent on ICOS-L signaling from CD11c+ cells to begin their differentiation (52), and are controlled by the master regulatory transcription factor BCL6 (10). After an initial DC-mediated differentiation event, the Tfh migrates to the B cell follicle. Here, its phenotype will be stabilized by B cells that have acquired antigen through their B cell receptor and present it on MHC-II. Similar to the initial interaction with CD11c+ cells, this interaction is known to also be dependent on ICOS-ICOSL interactions (53). Thus, the Tfh needs to see ICOS-L twice during its differentiation process, once from the DC that directs its initial polarization and then a second time from a cognate B cell.

If the Tfh sees its cognate antigen presented by B cells in the context of MHC-II and ICOS-L along with SLAM, it will begin to secrete cytokines, including IL-4 (54). In the case of a Th2-polarized overall immune response, these signals will direct the B cell to class switch to IgE or IgG1 and ultimately differentiate into an antibody-producing plasma cell. These immunoglobulins will circulate throughout the host, where they will both bind to free antigen and parasitic invaders, impacting ongoing infections and helping to direct the immune response against the current threat. Immunoglobulins also bind to circulating and sentinel immune cells, preparing them to react rapidly to subsequent infections.

An initial study by the Medzhitov laboratory using the CD11c DTR mouse suggested that the DC was not required for at least one model of Th2 polarization

induced through footpad injection of the cysteine protease papain (55). In this mouse, the human DTR is expressed under the CD11c promoter and DCs can be ablated through the injection of diphtheria toxin. Repeated injection or usage of high doses of DT into these mice is lethal due to expression of the DTR on a non-hematopoietic cell type (56). Thus many groups including the Medzhitov laboratory lethally irradiate WT mice and then reconstitute them with CD11c DTR bone marrow rather than using the intact CD11c DTR mouse. Subsequent work by the Pulendran group using the intact CD11c DTR mouse showed that there was a requirement for DCs to induce Th2 polarization in the papain model (57). The discrepancy in results was resolved when the latter group showed that a radiation-resistant dermal DC subset was actually responsible for directing Th2 polarization, and thus would not have been eliminated through lethal irradiation of the WT mouse.

A later study by the Medzhitov group demonstrated that this Th2-inducing DC was an IRF-4 dependent cell expressing both CD301b and PDL2 and could be found in both the skin-draining and mesenteric lymph nodes. Specific deletion of IRF-4 in CD11c+ cells strongly impaired both papain-induced Th2 polarization and IgE and IgG1 responses (58). This cell was simultaneously described by the Iwasaki group who then depleted this cell by generating a CD301b-DTR mouse. They showed that depletion of the CD301b DC population completely eliminated Th2 responses but left immunoglobulin responses against both papain and *N. brasiliensis* intact (59). Taken together, these two studies suggest that Th2 cells are dependent on a CD301b+ DC subset and are completely abolished in the models studied when

this cell is depleted. Immunoglobulin responses appear to be independent of the CD301b DC but are severely impacted by deletion of DC IRF4 expression, suggesting that Tfh responses are mediated by a different DC subset than the CD301b+ DC that is IRF-4 dependent.

Although traditionally thought of as the cells responsible for generating antibodies, several studies have pointed to a more active role for B cells in directing Th2 responses that suggests the original observations of Th2 cells migrating to the B cell follicle may not have been completely mistaken. In a model of *N. brasiliensis* infection, Gause and colleagues showed that the appearance of both peripheral and lymph node Th2 cells was significantly impaired in the absence of B cells (60) using the μMT mouse, a strain in which the membrane-bound form of the IgM B cell receptor is deleted, arresting B cells at the pre-B stage and eliminating mature B cells in the periphery (61). Th2 cell responses could be restored through adoptive transfer of splenic B cells from a WT mouse but not one from a mouse deficient in CD80 and CD86, highlighting a role for B cell costimulation in the generation of Th2 cells and strongly suggesting that B cell antigen presentation plays a role in augmenting Th2 responses. Hernandez et al, in a model of *S. mansoni* infection, showed a large impairment of T cell generated Th2 cytokines in B cell deficient JHD mice but no deficiency in Th1 cytokines (62). In a more recent study of *H. polygyrus* infection, Leon et al showed that B cells can act to coordinate interactions between naïve T cells and DC during Th2 responses through the secretion of chemokines, highlighting an additional way through which B cells can help coordinate Th2 responses (63).

1.4. Mast cells and basophils, key players in allergic immunity

In addition to T and B cells, many non-lymphoid cells play critical roles during Th2 responses. An important myeloid family of effector cells that participate in Th2 responses are granulocytes, including mast cells and basophils. These cells are termed "granulocytes" because they are filled with granules containing pre-formed mediators, allowing a rapid response against any threat once detected.

Mast cells have been described from histological standpoint as either connective tissue or mucosal, based on their location within tissue. Morphologically, both mast cell subsets are large cells filled with granules containing pre-formed mediators including histamine, TNF-α, and serotonin (rodents only) as well as multiple mast cell-specific proteases (64). The specific protease content of any given mast cell is determined by their tissue of residence rather than their mucosal vs. connective tissue localization (65, 66). In addition to their granular content, mast cells are potent sources of both inflammatory cytokines and lipid mediators.

The connective tissue mast cells found in the skin are seeded by a circulating progenitor derived from the fetal liver, migrating to the skin during embryogenesis (67). Experiments involving lethal irradiation of C57BL/6 mice and reconstitution with BM from the C57BL-beige strain show poor engraftment of donor-derived MC in the skin and mesentery at 6 months after transplant (68), suggesting that these cells are long lived rather than constantly replenished by the BM. By contrast, the vast majority of mast cells in mucosal tissues, including the caecum and stomach, were donor derived after 6 months, indicating that these cells turn over much more rapidly and are seeded by the BM. Inflammation in mucosal surfaces including the

lung (69) and intestine (70, 71) can also recruit circulating progenitors in a T cell-dependent manner that subsequently mature into granulated mucosal mast cells. These precursors also constitutively home to the intestinal mucosa in a beta 7 integrin-dependent manner (72) and a sizable pool of mast cell precursors can be found in the intestine (73), poised to quickly mature following inflammation.

In addition to the contents of the granules, mast cells are potent sources of cytokines and lipid mediators, giving them a robust ability to influence inflammation in the surrounding tissue (64). Mast cells express several TLRs and other pattern recognition receptors allowing them to serve as sentinel cells in peripheral tissue and identify microbial threats (74). Additionally, mast cells express the high affinity IgE receptor FcεRI a along with Fc receptors for IgG1, endowing them with a capacity to recognize targets of the adaptive immune system(75, 76). Signaling through these receptors will induce degranulation of mast cells, causing them to release their pre-formed mediators into the surrounding tissue.

The basophil is another important granulocyte in allergic immunity that is closely related to the mucosal mast cell. Both the basophil and the circulating mast cell progenitor arise from a common bone marrow precursor cell, and C57BL/6 mice also have a precursor in the spleen capable of giving rise to each cell type (77). Basophils have a multi-lobed nucleus and are filled with small granules, although to a much lesser degree than mast cells, and are quite short-lived cells, with a half-life of only a few days after leaving the bone marrow (78). Basophil granules primarily contain histamine as well as the protease mcpt8. Similarly to mast cells, basophils express high levels of FcεRI a. Signaling through this receptor induces degranulation

of the basophil accompanied by rapid generation of the lipid mediator LTC4 and potent generation of the cytokines IL-4 and IL-13 (79, 80). Basophils are also recruited to peripheral tissue during allergic inflammation but, in contrast to mast cells, the basophil is a terminally differentiated cell that retains its phenotype after infiltrating tissue.

While basophils are readily observable in the circulation of both humans and mice, their role within the greater immune system is poorly understood. A trio of papers published in 2009 posited a role for basophils in antigen presentation in initiating Th2 polarization in three separate models, namely injection of papain into the footpad(55), exposure to schistosome egg antigen(81), and injection with ova-IgE immune complexes (82). These studies all used mAb depletion of basophils, but their findings were not born out by a subsequent study using a basophil knockout model generated through overexpression of Cre recombinase driven by the mcpt8 promoter(83). Some of this discrepancy may be due to the manner of basophil depletion, namely mAb-mediated depletion using the MAR-1 antibody, which targets FcεRI a. As this receptor is also expressed by MCp and mature mast cells, off target effects may account for some of the controversy. Subsequently, studies using basophil-deficient mice showed an essential and non-redundant role for basophils in IgE-mediated tick rejection (84) and a key role for these cells in secondary *N. brasiliensis* rejection and chronic allergic dermatitis (83).

1.5. *T. spiralis*, a model of helminth infection

The helminth *Trichenella spiralis* is capable of infecting a wide range of mammalian hosts, including humans, and causes the disease trichinosis. *T. spiralis* has a multi-phase life cycle in which it inhabits multiple tissues. The infective larvae of the worm reside within the skeletal muscle tissue of infected hosts. When muscle tissue from this host is eaten by another potential host, the infective larvae enter the digestive tract of the new host where they rapidly mature and invade the mucosa of the small intestine (85). During this early phase of infection, the host immune response is primarily Th1 polarized (86). After maturation, the adult worms sexually reproduce and females release newborn larvae that disseminate throughout the host after entering into the circulation and lymphatic systems.

The host Th2 response begins during this second phase of infection. This response is associated with rapid T cell-dependent recruitment of mast cell precursors to the small intestine and their maturation into fully granulated mucosal mast cells (87). This phase of infection is accompanied by a mast cell-dependent accumulation of fluid in the intestinal lumen (88). Mast cell prostaglandins and histamines increase secretion by epithelial cells (89) and the mast cell chymase MCPT1 increases paracellular permeability (90), which may increase influx of antibodies and other mediators to the intracellular niche in which the parasite resides (91). This process, when combined with increased muscle contraction, is thought to aid in expelling adult worms from the intestine. Mice deficient in MCPT1 exhibit significantly delayed expulsion of adult worms coupled with increased accumulation of larvae in skeletal muscle (92).

After entering systemic circulation through the lymphatic drainage (85), the newborn larvae will home to host skeletal muscle tissue and invade a muscle fiber. Once in the intracellular environment, the larvae convert the muscle fiber into a structure known as a "nurse cell," dramatically altering the muscle fiber. The nurse cell releases angiogenic factors, increasing blood flow to the fiber (93), and finally the cell produces collagen, creating a capsule wall to separate it from the surrounding host tissue(94). Satellite cells residing within the capsule constantly renew the nurse cell (95). Infection of skeletal muscle also induces a robust regulatory T cell response in the local environment, limiting the inflammatory response to intracellular t. spiralis (96). It is unclear currently whether this represents a case of immune invasion by the helminth or rather results from the host immune system trying to limit tissue damage in the area surrounding the infective larvae. Thus encapsulated, the worm matures into an infective larva and awaits a fresh host to begin its life cycle anew, residing for the lifetime of smaller hosts such as rodents and pigs or for years within larger hosts like humans.

While the biology of *T. spiralis* infection in host tissue has been well characterized, they have almost all been focused on peripheral tissue, namely the small intestine or muscle. Few studies have looked at the immunological effects of infection in the draining mesenteric lymph nodes and the cell populations recruited to the MLN and their effects on the immune response have not been well characterized. One such study by the Artis laboratory showed that basophils were recruited to the mesenteric lymph node in a TSLP-dependent manner and concluded that they influenced Th2 polarization following mAb depletion (97).

However, the mAb used did not distinguish between basophils and mast cells, and the relevant mechanisms through which an FcεRI a cell influences Th2 immunity are still unclear.

1.6 The cysteine protease papain, a model of Th2 polarization

Several studies within the past few years have focused on one family of proteases, cysteine proteases, as a potentially important class of proteases in both helminthic infection and in allergic responses. Papain-family cysteine proteases are produced by several different types of helminthes, including the liver fluke *F. Hepatica* and the blood fluke *S. Mansoni*, and are important components of host infection, as inhibition of these proteases drastically reduces worm burden (98, 99). These proteases can be secreted at multiple points during the helminthic life cycle. Helminth larvae can use these proteases to open space between intestinal epithelial cells to enter into the host from the intestinal lumen and to migrate within the host to their preferred target tissue, while the adult worm uses secreted cysteine proteases for feeding once they've arrived at their target tissue (32)

Papain family cysteine proteases are also components of several of the most common human allergens. DerP1 is a cysteine proteases that is a major component of the allergenic house dust mite *D. pteronyssinus* originating in the animal's gut (40). DerP1 is a major common target of IgE responses in patients with house dust mite allergy, with up to 75% of dust mite-specific IgE targeting this protease (100). Grass pollen, another major allergen also contains a major cysteine protease component (101). These proteins are all called "papain family" due to the homology

of their proteolytically active site to that found in papain (102), a cysteine protease derived from the papaya fruit and commonly used as a meat tenderizer. Papain itself can also serve as a potent allergen in humans. One study of workers regularly exposed to airborne papain in the workplace reported that 17 out of 33 developed asthmatic symptom and 34.5% exhibited IgE-mediated sensitization to papain (103).

The innate receptors responsible for cysteine protease recognition are not currently well understood. DerP1 has been shown to cleave the extracellular portions of both protease-activated receptor (PAR)-1 and PAR-2 (104). With PAR-1, this cleavage deactivates the receptor, making it unlikely that this receptor would serve as a recognition receptor for cysteine protease activity. In contrast, DerP1 cleavage of PAR-2 is activating in nature (104), and cleavage of PAR-2 by papain can lead to the activation of naïve T cells and production of cytokines and chemokines (105). As PAR-2 can be activated by multiple cysteine proteases in multiple cell types, this raises the possibility that PAR-2 may serve as a general PRR for cysteine proteases. However, human eosinophils degranulate in response to papain in a non-PAR2 mediated manner, indicating that there must be other innate receptors that recognize papain (106).

In addition to direct effects on cellular activation, cysteine proteases may also influence the immune response through other mechanisms. DerP1 has been shown to cleave alpha subunit of CD25 on T cells, greatly impairing their proliferative capacity and ability to produce IFN-g and potentially helping to shape the immune response towards a more Th2-balanced response (107). DerP1 can also

cleave CD23, the low affinity IgE receptor, from B cells (107), which may lead to increased levels of IgE in circulation, thus improving overall host responses to parasites.

When injected into the rear footpad of mice, papain leads to a strong local Th2 response in the draining popliteal lymph node (108). This immune response is dependent on the protease activity of papain, as inhibition of papain through either pharmacological blockage of the active site using e64, a specific cystine protease inhibitor, or heat inactivation of the protease completely halts the immune response as measured by T cell Th2 polarization and host IgE responses. The papain response is characterized by rapid expansion of the T and B cell compartments as well recruitment of basophils from the circulation. This basophil recruitment peaks at three days following papain immunization and is mediated by direct effects of papain on naïve T cells in a PAR-2 mediated manner. It is unclear if DCs play a role in basophil recruitment, as different groups have given conflicting reports (55, 57, 81, 82). The recruited basophils are strongly positive for IL-4 transcript, leading to the possibility that these cells may secrete IL-4 in situ(108). Further supporting this possibility, papain is able to directly activate basophils, causing them to secrete cytokine and degranulate(108). However, work by others has suggested that, while positive for IL-4 transcript, LN basophils do not actually produce any IL-4 protein (109).

Depletion of basophils via a monoclonal antibody (mAb) directed against the high affinity IgE receptor FcεRI a inhibited Th2 responses following papain immunization (108), and subsequent studies showed that basophils were positive

for MHC-II and were able to phagocytose and present soluble ovalbumin when stimulated with papain(55). This, coupled with experiments questioning the role of the DC as the primary APC in the papain response, lead several groups to suggest that basophils could act as a primary APC in Th2 responses by both presenting antigen to naïve t cells in the context of MHC-II and secreting IL-4, leading to Th2 polarization (55, 81, 82). However, a follow-up study using basophil deficient mice showed no impairment in Th2 responses in the models (83), and studies by several other groups have pointed to a necessary role for the DC in papain-induced Th2 polarization (57, 59). Sullivan et al showed that basophils engage in stable interactions with antigen-specific T cells in peripheral tissue that leads to cytokine production by both cell types (109), suggesting that basophils may indeed act as APCs but only in peripheral tissue and for polarized T cells.

While understanding of the papain model of Th2 inflammation moved rapidly following the publication of the trio of 2009 papers describing basophils as APCs (55, 81, 82), some questions remain. Although subsequent studies highlighted the importance of the DC, a seminal and unresolved finding from the Medzhitov study was that Th2 polarization was greatly impaired in mice that lacked MHC-II expression on CD11c- cells, indicating that antigen presentation by a cell other than the DC was important in this model. Supporting this, the Iwasaki paper showed that the CD301b+ DC was necessary but not sufficient for inducing Th2 polarization and concluded that an additional ancillary cell was required. No subsequent studies have clearly identified this cell, leaving it an important unanswered question.

CONCLUSIONS

Broadly, the goal of this thesis project is to better understand the cells involved in lymph node Th2 inflammation. To accomplish this, we first examined differential recruitment of granulocytes to the lymph node in two models, *T. spiralis* infection and papain immunization. During the course of this study, we observed a previously unrecognized recruitment of MCp to the MLN following *T. spiralis* infection. Strikingly, these cells did not mature and granulate following recruitment to the MLN as they do in peripheral tissue but rather remained hypogranular and produced cytokines, raising the possibility that they directly influence the Th2 immune response. A subsequent study in the papain model sought to identify the CD11c- MHC-II+ ancillary cell required for maximal Th2 polarization in the PLN following immunization. Experiments using fluorescently labeled papain identified large numbers of B cells as rapidly acquiring and internalizing papain following immunization in a non-BCR mediated manner. Follow up experiments using the B cell deficient μMT strain indicated that Tfh responses and Th2 polarization was impaired in μMT. Blockade of ICOS-L impaired Tfh and Th2 responses in WT but not μMT mice, strongly implying that ICOS-L expression by B cells was important for their amplification of Th2 polarization. Thus, the two studies reported here have expanded our understanding of recruited ancillary cells during Th2 inflammation.

1.7. References

1. Mosmann, T. R., H. Cherwinski, M. W. Bond, M. A. Giedlin, and R. L. Coffman. 1986. Two types of murine helper T cell clone. I. Definition according to profiles of lymphokine activities and secreted proteins. *J Immunol* 136: 2348-2357.

2. Le Gros, G., S. Z. Ben-Sasson, R. Seder, F. D. Finkelman, and W. E. Paul. 1990. Generation of interleukin 4 (IL-4)-producing cells in vivo and in vitro: IL-2 and IL-4 are required for in vitro generation of IL-4-producing cells. *J Exp Med* 172: 921-929.

3. Swain, S. L., A. D. Weinberg, M. English, and G. Huston. 1990. IL-4 directs the development of Th2-like helper effectors. *J Immunol* 145: 3796-3806.

4. Szabo, S. J., S. T. Kim, G. L. Costa, X. Zhang, C. G. Fathman, and L. H. Glimcher. 2000. A novel transcription factor, T-bet, directs Th1 lineage commitment. *Cell* 100: 655-669.

5. Zheng, W., and R. A. Flavell. 1997. The transcription factor GATA-3 is necessary and sufficient for Th2 cytokine gene expression in CD4 T cells. *Cell* 89: 587-596.

6. Usui, T., J. C. Preiss, Y. Kanno, Z. J. Yao, J. H. Bream, J. J. O'Shea, and W. Strober. 2006. T-bet regulates Th1 responses through essential effects on GATA-3 function rather than on IFNG gene acetylation and transcription. *J Exp Med* 203: 755-766.

7. Ouyang, W., S. H. Ranganath, K. Weindel, D. Bhattacharya, T. L. Murphy, W. C. Sha, and K. M. Murphy. 1998. Inhibition of Th1 development mediated by GATA-3 through an IL-4-independent mechanism. *Immunity* 9: 745-755.

8. Ivanov, II, B. S. McKenzie, L. Zhou, C. E. Tadokoro, A. Lepelley, J. J. Lafaille, D. J. Cua, and D. R. Littman. 2006. The orphan nuclear receptor RORgammat directs the differentiation program of proinflammatory IL-17+ T helper cells. *Cell* 126: 1121-1133.

9. Hori, S., T. Nomura, and S. Sakaguchi. 2003. Control of regulatory T cell development by the transcription factor Foxp3. *Science* 299: 1057-1061.

10. Yu, D., S. Rao, L. M. Tsai, S. K. Lee, Y. He, E. L. Sutcliffe, M. Srivastava, M. Linterman, L. Zheng, N. Simpson, J. I. Ellyard, I. A. Parish, C. S. Ma, Q. J. Li, C. R. Parish, C. R. Mackay, and C. G. Vinuesa. 2009. The transcriptional repressor Bcl-6 directs T follicular helper cell lineage commitment. *Immunity* 31: 457-468.

11. Brewig, N., A. Kissenpfennig, B. Malissen, A. Veit, T. Bickert, B. Fleischer, S. Mostbock, and U. Ritter. 2009. Priming of CD8(+) and CD4(+) T Cells in Experimental Leishmaniasis Is Initiated by Different Dendritic Cell Subtypes. *Journal of Immunology* 182: 774-783.

12. Guilliams, M., K. Crozat, S. Henri, S. Tamoutounour, P. Grenot, E. Devilard, B. de Bovis, L. Alexopoulou, M. Dalod, and B. Malissen. 2010. Skin-draining lymph nodes contain dermis-derived CD103(-) dendritic cells that constitutively produce retinoic acid and induce Foxp3(+) regulatory T cells. *Blood* 115: 1958-1968.

13. Igyarto, B. Z., K. Haley, D. Ortner, A. Bobr, M. Gerami-Nejad, B. T. Edelson, S. M. Zurawski, B. Malissen, G. Zurawski, J. Berman, and D. H. Kaplan. 2011. Skin-Resident Murine Dendritic Cell Subsets Promote Distinct and Opposing Antigen-Specific T Helper Cell Responses. *Immunity* 35: 260-272.

14. King, I. L., M. A. Kroenke, and B. M. Segal. 2010. GM-CSF-dependent, CD103(+) dermal dendritic cells play a critical role in Th effector cell differentiation after subcutaneous immunization. *Journal of Experimental Medicine* 207: 953-961.

15. Dardalhon, V., T. Korn, V. K. Kuchroo, and A. C. Anderson. 2008. Role of Th1 and Th17 cells in organ-specific autoimmunity. *J Autoimmun* 31: 252-256.

16. Umetsu, D. T., and R. H. DeKruyff. 1997. TH1 and TH2 CD4+ cells in human allergic diseases. *J Allergy Clin Immunol* 100: 1-6.

17. Medzhitov, R., P. Preston-Hurlburt, and C. A. Janeway, Jr. 1997. A human homologue of the Drosophila Toll protein signals activation of adaptive immunity. *Nature* 388: 394-397.

18. Poltorak, A., I. Smirnova, X. He, M. Y. Liu, C. Van Huffel, O. McNally, D. Birdwell, E. Alejos, M. Silva, X. Du, P. Thompson, E. K. Chan, J. Ledesma, B. Roe, S. Clifton, S. N. Vogel, and B. Beutler. 1998. Genetic and physical mapping of the Lps locus: identification of the toll-4 receptor as a candidate gene in the critical region. *Blood Cells Mol Dis* 24: 340-355.

19. Schwandner, R., R. Dziarski, H. Wesche, M. Rothe, and C. J. Kirschning. 1999. Peptidoglycan- and lipoteichoic acid-induced cell activation is mediated by toll-like receptor 2. *J Biol Chem* 274: 17406-17409.

20. Triantafilou, M., F. G. Gamper, R. M. Haston, M. A. Mouratis, S. Morath, T. Hartung, and K. Triantafilou. 2006. Membrane sorting of toll-like receptor (TLR)-2/6 and TLR2/1 heterodimers at the cell surface determines heterotypic associations with CD36 and intracellular targeting. *J Biol Chem* 281: 31002-31011.

21. Goubau, D., S. Deddouche, and C. Reis e Sousa. 2013. Cytosolic sensing of viruses. *Immunity* 38: 855-869.

22. Figueiredo, R. T., L. A. Carneiro, and M. T. Bozza. 2011. Fungal surface and innate immune recognition of filamentous fungi. *Front Microbiol* 2: 248.

23. Underhill, D. M., A. Ozinsky, A. M. Hajjar, A. Stevens, C. B. Wilson, M. Bassetti, and A. Aderem. 1999. The Toll-like receptor 2 is recruited to macrophage phagosomes and discriminates between pathogens. *Nature* 401: 811-815.

24. Brown, G. D., J. Herre, D. L. Williams, J. A. Willment, A. S. Marshall, and S. Gordon. 2003. Dectin-1 mediates the biological effects of beta-glucans. *J Exp Med* 197: 1119-1124.

25. Robinson, M. J., F. Osorio, M. Rosas, R. P. Freitas, E. Schweighoffer, O. Gross, J. SjefVerbeek, J. Ruland, V. Tybulewicz, G. D. Brown, L. F. Moita, P. R. Taylor, and C. R. E. Sousa. 2009. Dectin-2 is a Syk-coupled pattern recognition receptor crucial for Th17 responses to fungal infection. *Journal of Experimental Medicine* 206: 2037-2051.

26. Taylor, P. R., S. V. Tsoni, J. A. Willment, K. M. Dennehy, M. Rosas, H. Findon, K. Haynes, C. Steele, M. Botto, S. Gordon, and G. D. Brown. 2007. Dectin-1 is required for beta-glucan recognition and control of fungal infection. *Nature Immunology* 8: 31-38.

27. Saijo, S., N. Fujikado, T. Furuta, S. H. Chung, H. Kotaki, K. Seki, K. Sudo, S. Akira, Y. Adachi, N. Ohno, T. Kinjo, K. Nakamura, K. Kawakami, and Y. Iwakura. 2007. Dectin-1 is required for host defense against Pneumocystis carinii but not against Candida albicans. *Nature Immunology* 8: 39-46.

28. Saijo, S., S. Ikeda, K. Yamabe, S. Kakuta, H. Ishigame, A. Akitsu, N. Fujikado, T. Kusaka, S. Kubo, S. H. Chung, R. Komatsu, N. Miura, Y. Adachi, N. Ohno, K. Shibuya, N. Yamamoto, K. Kawakami, S. Yamasaki, T. Saito, S. Akira, and Y. Iwakura. 2010. Dectin-2 Recognition of alpha-Mannans and Induction of Th17 Cell Differentiation Is Essential for Host Defense against Candida albicans. *Immunity* 32: 681-691.

29. Perrigoue, J. G., F. A. Marshall, and D. Artis. 2008. On the hunt for helminths: innate immune cells in the recognition and response to helminth parasites. *Cell Microbiol* 10: 1757-1764.

30. Arnold, K., L. J. Brydon, L. H. Chappell, and G. W. Gooday. 1993. Chitinolytic activities in Heligmosomoides polygyrus and their role in egg hatching. *Mol Biochem Parasitol* 58: 317-323.

31. Reese, T. A., H. E. Liang, A. M. Tager, A. D. Luster, N. Van Rooijen, D. Voehringer, and R. M. Locksley. 2007. Chitin induces accumulation in tissue of innate immune cells associated with allergy. *Nature* 447: 92-96.

32. Robinson, M. W., J. P. Dalton, and S. Donnelly. 2008. Helminth pathogen cathepsin proteases: it's a family affair. *Trends Biochem Sci* 33: 601-608.

33. Dalton, J. P., K. A. Clough, M. K. Jones, and P. J. Brindley. 1997. The cysteine proteinases of Schistosoma mansoni cercariae. *Parasitology* 114 (Pt 2): 105-112.

34. Kasny, M., L. Mikes, J. P. Dalton, A. P. Mountford, and P. Horak. 2007. Comparison of cysteine peptidase activities in Trichobilharzia regenti and Schistosoma mansoni cercariae. *Parasitology* 134: 1599-1609.

35. Riese, R. J., P. R. Wolf, D. Bromme, L. R. Natkin, J. A. Villadangos, H. L. Ploegh, and H. A. Chapman. 1996. Essential role for cathepsin S in MHC class II-associated invariant chain processing and peptide loading. *Immunity* 4: 357-366.

36. Tawill, S., L. Le Goff, F. Ali, M. Blaxter, and J. E. Allen. 2004. Both free-living and parasitic nematodes induce a characteristic Th2 response that is dependent on the presence of intact glycans. *Infection and Immunity* 72: 398-407.

37. Okano, M., A. R. Satoskar, K. Nishizaki, M. Abe, and D. A. Harn. 1999. Induction of Th2 responses and IgE is largely due to carbohydrates functioning as adjuvants on Schistosoma mansoni egg antigens. *Journal of Immunology* 163: 6712-6717.

38. Barrett, N. A., A. Maekawa, O. M. Rahman, K. F. Austen, and Y. Kanaoka. 2009. Dectin-2 recognition of house dust mite triggers cysteinyl leukotriene generation by dendritic cells. *J Immunol* 182: 1119-1128.

39. Barrett, N. A., O. M. Rahman, J. M. Fernandez, M. W. Parsons, W. Xing, K. F. Austen, and Y. Kanaoka. 2011. Dectin-2 mediates Th2 immunity through the generation of cysteinyl leukotrienes. *J Exp Med* 208: 593-604.

40. Tovey, E. R., M. D. Chapman, and T. A. Platts-Mills. 1981. Mite faeces are a major source of house dust allergens. *Nature* 289: 592-593.

41. Gough, L., H. F. Sewell, and F. Shakib. 2001. The proteolytic activity of the major dust mite allergen Der p 1 enhances the IgE antibody response to a bystander antigen. *Clin Exp Allergy* 31: 1594-1598.

42. Reis e Sousa, C., S. Hieny, T. Scharton-Kersten, D. Jankovic, H. Charest, R. N. Germain, and A. Sher. 1997. In vivo microbial stimulation induces rapid CD40 ligand-independent production of interleukin 12 by dendritic cells and their redistribution to T cell areas. *J Exp Med* 186: 1819-1829.

43. MacDonald, A. S., A. D. Straw, B. Bauman, and E. J. Pearce. 2001. CD8- dendritic cell activation status plays an integral role in influencing Th2 response development. *J Immunol* 167: 1982-1988.

44. Thomas, P. G., M. R. Carter, O. Atochina, A. A. Da'Dara, D. Piskorska, E. McGuire, and D. A. Harn. 2003. Maturation of dendritic cell 2 phenotype by a helminth glycan uses a Toll-like receptor 4-dependent mechanism. *J Immunol* 171: 5837-5841.

45. Maizels, R. M., A. Balic, N. Gomez-Escobar, M. Nair, M. D. Taylor, and J. E. Allen. 2004. Helminth parasites - masters of regulation. *Immunological Reviews* 201: 89-116.

46. Balic, A., Y. Harcus, M. J. Holland, and R. M. Maizels. 2004. Selective maturation of dendritic cells by Nippostrongylus brasiliensis-secreted proteins drives Th2 immune responses. *Eur J Immunol* 34: 3047-3059.

47. Yamane, H., J. Zhu, and W. E. Paul. 2005. Independent roles for IL-2 and GATA-3 in stimulating naive CD4+ T cells to generate a Th2-inducing cytokine environment. *J Exp Med* 202: 793-804.

48. Everts, B., G. Perona-Wright, H. H. Smits, C. H. Hokke, A. J. van der Ham, C. M. Fitzsimmons, M. J. Doenhoff, J. van der Bosch, K. Mohrs, H. Haas, M. Mohrs, M. Yazdanbakhsh, and G. Schramm. 2009. Omega-1, a glycoprotein secreted by Schistosoma mansoni eggs, drives Th2 responses. *J Exp Med* 206: 1673-1680.

49. Steinfelder, S., J. F. Andersen, J. L. Cannons, C. G. Feng, M. Joshi, D. Dwyer, P. Caspar, P. L. Schwartzberg, A. Sher, and D. Jankovic. 2009. The major component in schistosome eggs responsible for conditioning dendritic cells for Th2 polarization is a T2 ribonuclease (omega-1). *J Exp Med* 206: 1681-1690.

50. Romagnani, S. 1996. Th1 and Th2 in human diseases. *Clin Immunol Immunopathol* 80: 225-235.

51. Crotty, S. 2011. Follicular helper CD4 T cells (TFH). *Annu Rev Immunol* 29: 621-663.

52. Choi, Y. S., R. Kageyama, D. Eto, T. C. Escobar, R. J. Johnston, L. Monticelli, C. Lao, and S. Crotty. 2011. ICOS receptor instructs T follicular helper cell versus

effector cell differentiation via induction of the transcriptional repressor Bcl6. *Immunity* 34: 932-946.

53. Nurieva, R. I., Y. Chung, D. Hwang, X. O. Yang, H. S. Kang, L. Ma, Y. H. Wang, S. S. Watowich, A. M. Jetten, Q. Tian, and C. Dong. 2008. Generation of T follicular helper cells is mediated by interleukin-21 but independent of T helper 1, 2, or 17 cell lineages. *Immunity* 29: 138-149.

54. Yusuf, I., R. Kageyama, L. Monticelli, R. J. Johnston, D. Ditoro, K. Hansen, B. Barnett, and S. Crotty. 2010. Germinal center T follicular helper cell IL-4 production is dependent on signaling lymphocytic activation molecule receptor (CD150). *J Immunol* 185: 190-202.

55. Sokol, C. L., N. Q. Chu, S. Yu, S. A. Nish, T. M. Laufer, and R. Medzhitov. 2009. Basophils function as antigen-presenting cells for an allergen-induced T helper type 2 response. *Nat Immunol* 10: 713-720.

56. Zammit, D. J., L. S. Cauley, Q. M. Pham, and L. Lefrancois. 2005. Dendritic cells maximize the memory CD8 T cell response to infection. *Immunity* 22: 561-570.

57. Tang, H., W. Cao, S. P. Kasturi, R. Ravindran, H. I. Nakaya, K. Kundu, N. Murthy, T. B. Kepler, B. Malissen, and B. Pulendran. 2010. The T helper type 2 response to cysteine proteases requires dendritic cell-basophil cooperation via ROS-mediated signaling. *Nat Immunol* 11: 608-617.

58. Gao, Y., S. A. Nish, R. Jiang, L. Hou, P. Licona-Limon, J. S. Weinstein, H. Zhao, and R. Medzhitov. 2013. Control of T helper 2 responses by transcription factor IRF4-dependent dendritic cells. *Immunity* 39: 722-732.

59. Kumamoto, Y., M. Linehan, J. S. Weinstein, B. J. Laidlaw, J. E. Craft, and A. Iwasaki. 2013. CD301b(+) dermal dendritic cells drive T helper 2 cell-mediated immunity. *Immunity* 39: 733-743.

60. Liu, Q., Z. Liu, C. T. Rozo, H. A. Hamed, F. Alem, J. F. Urban, Jr., and W. C. Gause. 2007. The role of B cells in the development of CD4 effector T cells during a polarized Th2 immune response. *J Immunol* 179: 3821-3830.

61. Kitamura, D., J. Roes, R. Kuhn, and K. Rajewsky. 1991. A B cell-deficient mouse by targeted disruption of the membrane exon of the immunoglobulin mu chain gene. *Nature* 350: 423-426.

62. Hernandez, H. J., Y. Wang, and M. J. Stadecker. 1997. In infection with Schistosoma mansoni, B cells are required for T helper type 2 cell responses but not for granuloma formation. *J Immunol* 158: 4832-4837.

63. Leon, B., A. Ballesteros-Tato, J. L. Browning, R. Dunn, T. D. Randall, and F. E. Lund. 2012. Regulation of T(H)2 development by CXCR5+ dendritic cells and lymphotoxin-expressing B cells. *Nat Immunol* 13: 681-690.

64. Metcalfe, D. D., D. Baram, and Y. A. Mekori. 1997. Mast cells. *Physiol Rev* 77: 1033-1079.

65. Friend, D. S., N. Ghildyal, M. F. Gurish, J. Hunt, X. Hu, K. F. Austen, and R. L. Stevens. 1998. Reversible expression of tryptases and chymases in the jejunal mast cells of mice infected with Trichinella spiralis. *J Immunol* 160: 5537-5545.

66. Xing, W., K. F. Austen, M. F. Gurish, and T. G. Jones. 2011. Protease phenotype of constitutive connective tissue and of induced mucosal mast cells in mice is regulated by the tissue. *Proc Natl Acad Sci U S A* 108: 14210-14215.

67. Hayashi, C., T. Sonoda, T. Nakano, H. Nakayama, and Y. Kitamura. 1985. Mast-cell precursors in the skin of mouse embryos and their deficiency in embryos of Sl/Sld genotype. *Dev Biol* 109: 234-241.

68. Kitamura, Y., M. Shimada, K. Hatanaka, and Y. Miyano. 1977. Development of mast cells from grafted bone marrow cells in irradiated mice. *Nature* 268: 442-443.

69. Jones, T. G., J. Hallgren, A. Humbles, T. Burwell, F. D. Finkelman, P. Alcaide, K. F. Austen, and M. F. Gurish. 2009. Antigen-induced increases in pulmonary mast cell progenitor numbers depend on IL-9 and CD1d-restricted NKT cells. *J Immunol* 183: 5251-5260.

70. Kamal, M., D. Wakelin, A. J. Ouellette, A. Smith, D. K. Podolsky, and Y. R. Mahida. 2001. Mucosal T cells regulate Paneth and intermediate cell numbers in the small intestine of T. spiralis-infected mice. *Clin Exp Immunol* 126: 117-125.

71. Friend, D. S., N. Ghildyal, K. F. Austen, M. F. Gurish, R. Matsumoto, and R. L. Stevens. 1996. Mast cells that reside at different locations in the jejunum of mice infected with Trichinella spiralis exhibit sequential changes in their granule ultrastructure and chymase phenotype. *J Cell Biol* 135: 279-290.

72. Gurish, M. F., H. Tao, J. P. Abonia, A. Arya, D. S. Friend, C. M. Parker, and K. F. Austen. 2001. Intestinal mast cell progenitors require CD49dbeta7 (alpha4beta7 integrin) for tissue-specific homing. *J Exp Med* 194: 1243-1252.

73. Crapper, R. M., and J. W. Schrader. 1983. Frequency of mast cell precursors in normal tissues determined by an in vitro assay: antigen induces parallel

increases in the frequency of P cell precursors and mast cells. *J Immunol* 131: 923-928.

74. Sandig, H., and S. Bulfone-Paus. 2012. TLR signaling in mast cells: common and unique features. *Front Immunol* 3: 185.

75. Tigelaar, R. E., N. M. Vaz, and Z. Ovary. 1971. Immunoglobulin receptors on mouse mast cells. *J Immunol* 106: 661-672.

76. Shimizu, A., I. Tepler, P. N. Benfey, E. H. Berenstein, R. P. Siraganian, and P. Leder. 1988. Human and rat mast cell high-affinity immunoglobulin E receptors: characterization of putative alpha-chain gene products. *Proc Natl Acad Sci U S A* 85: 1907-1911.

77. Arinobu, Y., H. Iwasaki, M. F. Gurish, S. Mizuno, H. Shigematsu, H. Ozawa, D. G. Tenen, K. F. Austen, and K. Akashi. 2005. Developmental checkpoints of the basophil/mast cell lineages in adult murine hematopoiesis. *Proc Natl Acad Sci U S A* 102: 18105-18110.

78. Ohnmacht, C., and D. Voehringer. 2009. Basophil effector function and homeostasis during helminth infection. *Blood* 113: 2816-2825.

79. Gibbs, B. F., H. Haas, F. H. Falcone, C. Albrecht, I. B. Vollrath, T. Noll, H. H. Wolff, and U. Amon. 1996. Purified human peripheral blood basophils release interleukin-13 and preformed interleukin-4 following immunological activation. *Eur J Immunol* 26: 2493-2498.

80. Warner, J. A., S. P. Peters, L. M. Lichtenstein, W. Hubbard, K. B. Yancey, H. C. Stevenson, P. J. Miller, and D. W. MacGlashan, Jr. 1989. Differential release of mediators from human basophils: differences in arachidonic acid metabolism following activation by unrelated stimuli. *J Leukoc Biol* 45: 558-571.

81. Perrigoue, J. G., S. A. Saenz, M. C. Siracusa, E. J. Allenspach, B. C. Taylor, P. R. Giacomin, M. G. Nair, Y. Du, C. Zaph, N. van Rooijen, M. R. Comeau, E. J. Pearce, T. M. Laufer, and D. Artis. 2009. MHC class II-dependent basophil-CD4+ T cell interactions promote T(H)2 cytokine-dependent immunity. *Nat Immunol* 10: 697-705.

82. Yoshimoto, T., K. Yasuda, H. Tanaka, M. Nakahira, Y. Imai, Y. Fujimori, and K. Nakanishi. 2009. Basophils contribute to T(H)2-IgE responses in vivo via IL-4 production and presentation of peptide-MHC class II complexes to CD4+ T cells. *Nat Immunol* 10: 706-712.

83. Ohnmacht, C., C. Schwartz, M. Panzer, I. Schiedewitz, R. Naumann, and D. Voehringer. 2010. Basophils orchestrate chronic allergic dermatitis and protective immunity against helminths. *Immunity* 33: 364-374.

84. Wada, T., K. Ishiwata, H. Koseki, T. Ishikura, T. Ugajin, N. Ohnuma, K. Obata, R. Ishikawa, S. Yoshikawa, K. Mukai, Y. Kawano, Y. Minegishi, H. Yokozeki, N. Watanabe, and H. Karasuyama. 2010. Selective ablation of basophils in mice reveals their nonredundant role in acquired immunity against ticks. *J Clin Invest* 120: 2867-2875.

85. Ilic, N., A. Gruden-Movsesijan, and L. Sofronic-Milosavljevic. 2012. Trichinella spiralis: shaping the immune response. *Immunol Res* 52: 111-119.

86. Ishikawa, N., P. K. Goyal, Y. R. Mahida, K. F. Li, and D. Wakelin. 1998. Early cytokine responses during intestinal parasitic infections. *Immunology* 93: 257-263.

87. Ruitenberg, E. J., and A. Elgersma. 1976. Absence of intestinal mast cell response in congenitally athymic mice during Trichinella spiralis infection. *Nature* 264: 258-260.

88. McDermott, J. R., R. E. Bartram, P. A. Knight, H. R. Miller, D. R. Garrod, and R. K. Grencis. 2003. Mast cells disrupt epithelial barrier function during enteric nematode infection. *Proc Natl Acad Sci U S A* 100: 7761-7766.

89. Madden, K. B., K. A. Yeung, A. Zhao, W. C. Gause, F. D. Finkelman, I. M. Katona, J. F. Urban, Jr., and T. Shea-Donohue. 2004. Enteric nematodes induce stereotypic STAT6-dependent alterations in intestinal epithelial cell function. *J Immunol* 172: 5616-5621.

90. Scudamore, C. L., E. M. Thornton, L. McMillan, G. F. Newlands, and H. R. Miller. 1995. Release of the mucosal mast cell granule chymase, rat mast cell protease-II, during anaphylaxis is associated with the rapid development of paracellular permeability to macromolecules in rat jejunum. *J Exp Med* 182: 1871-1881.

91. Knight, P. A., J. K. Brown, and A. D. Pemberton. 2008. Innate immune response mechanisms in the intestinal epithelium: potential roles for mast cells and goblet cells in the expulsion of adult Trichinella spiralis. *Parasitology* 135: 655-670.

92. Knight, P. A., S. H. Wright, C. E. Lawrence, Y. Y. Paterson, and H. R. Miller. 2000. Delayed expulsion of the nematode Trichinella spiralis in mice lacking the mucosal mast cell-specific granule chymase, mouse mast cell protease-1. *J Exp Med* 192: 1849-1856.

93. Capo, V. A., D. D. Despommier, and R. I. Polvere. 1998. Trichinella spiralis: vascular endothelial growth factor is up-regulated within the nurse cell during the early phase of its formation. *J Parasitol* 84: 209-214.

94. Ritterson, A. L. 1966. Nature of the cyst of Trichinella spiralis. *J Parasitol* 52: 157-161.

95. Wu, Z., L. Sofronic-Milosavljevic, I. Nagano, and Y. Takahashi. 2008. Trichinella spiralis: nurse cell formation with emphasis on analogy to muscle cell repair. *Parasit Vectors* 1: 27.

96. Beiting, D. P., L. F. Gagliardo, M. Hesse, S. K. Bliss, D. Meskill, and J. A. Appleton. 2007. Coordinated control of immunity to muscle stage Trichinella spiralis by IL-10, regulatory T cells, and TGF-beta. *J Immunol* 178: 1039-1047.

97. Giacomin, P. R., M. C. Siracusa, K. P. Walsh, R. K. Grencis, M. Kubo, M. R. Comeau, and D. Artis. 2012. Thymic stromal lymphopoietin-dependent basophils promote Th2 cytokine responses following intestinal helminth infection. *J Immunol* 189: 4371-4378.

98. Alcala-Canto, Y., F. Ibarra-Velarde, H. Sumano-Lopez, J. Gracia-Mora, and A. Alberti-Navarro. 2007. Effect of a cysteine protease inhibitor on Fasciola hepatica (liver fluke) fecundity, egg viability, parasite burden, and size in experimentally infected sheep. *Parasitol Res* 100: 461-465.

99. Abdulla, M. H., K. C. Lim, M. Sajid, J. H. McKerrow, and C. R. Caffrey. 2007. Schistosomiasis mansoni: Novel chemotherapy using a cysteine protease inhibitor. *Plos Medicine* 4: 130-138.

100. Chapman, M. D., and T. A. Platts-Mills. 1980. Purification and characterization of the major allergen from Dermatophagoides pteronyssinus-antigen P1. *J Immunol* 125: 587-592.

101. Grobe, K., W. M. Becker, M. Schlaak, and A. Petersen. 1999. Grass group I allergens (beta-expansins) are novel, papain-related proteinases. *Eur J Biochem* 263: 33-40.

102. Barrett, A. J., and N. D. Rawlings. 2001. Evolutionary lines of cysteine peptidases. *Biol Chem* 382: 727-733.

103. Baur, X., G. Konig, K. Bencze, and G. Fruhmann. 1982. Clinical symptoms and results of skin test, RAST and bronchial provocation test in thirty-three papain workers: evidence for strong immunogenic potency and clinically relevant 'proteolytic effects of airborne papain'. *Clin Allergy* 12: 9-17.

104. Asokananthan, N., P. T. Graham, D. J. Stewart, A. J. Bakker, K. A. Eidne, P. J. Thompson, and G. A. Stewart. 2002. House dust mite allergens induce proinflammatory cytokines from respiratory epithelial cells: the cysteine

protease allergen, Der p 1, activates protease-activated receptor (PAR)-2 and inactivates PAR-1. *J Immunol* 169: 4572-4578.

105. Liang, G., T. Barker, Z. Xie, N. Charles, J. Rivera, and K. M. Druey. 2012. Naive T cells sense the cysteine protease allergen papain through protease-activated receptor 2 and propel TH2 immunity. *J Allergy Clin Immunol* 129: 1377-1386 e1313.

106. Miike, S., and H. Kita. 2003. Human eosinophils are activated by cysteine proteases and release inflammatory mediators. *J Allergy Clin Immunol* 111: 704-713.

107. Schulz, O., H. F. Sewell, and F. Shakib. 1998. Proteolytic cleavage of CD25, the alpha subunit of the human T cell interleukin 2 receptor, by Der p 1, a major mite allergen with cysteine protease activity. *J Exp Med* 187: 271-275.

108. Sokol, C. L., G. M. Barton, A. G. Farr, and R. Medzhitov. 2008. A mechanism for the initiation of allergen-induced T helper type 2 responses. *Nat Immunol* 9: 310-318.

109. Sullivan, B. M., H. E. Liang, J. K. Bando, D. Wu, L. E. Cheng, J. K. McKerrow, C. D. Allen, and R. M. Locksley. 2011. Genetic analysis of basophil function in vivo. *Nat Immunol* 12: 527-535.

Chapter 2 - Mast cells recruited to mesenteric lymph nodes during helminth infection remain hypogranular and produce IL-4 and IL-6

2.1. Author Contribution

Reference (reproduced with permission from the Journal of Immunology)

Anne Y. Liu,* Daniel F. Dwyer,* Tatiana G. Jones, Lora G. Bankova, Shiliang Shen, Howard R. Katz, K. Frank Austen, and Michael F. Gurish (2013). Mast cells recruited to mesenteric lymph nodes during helminth infection remain hypogranular and produce IL-4 and IL-6. Journal of Immunology 190, 1759-1766 (*, equal contributions)

- Anne Liu conceived the study, designed and performed experiments, analyzed and interpreted data, and wrote the manuscript.
- Daniel Dwyer conducted intracellular cytokine staining experiments and MCp isolation, analyzed and interpreted data, and contributed to writing the manuscript.
- Tatiana Jones assisted with experiments.
- Lora Bankova assisted with experiments.
- Shiliang Shen performed histological analysis of samples.
- Howard Katz assisted with experimental design and manuscript preparation.
- K. Frank Austen supervised the project and manuscript writing.
- Michael Gurish supervised the project and manuscript writing.

2.2 Acknowledgements

We would like to thank Dr. Wei Xing for her help in enumeration of mature MC.

2.3 Abbreviations used in this chapter

Ba, basophil; BM, bone marrow; LDA, limiting dilution and clonal expansion analysis; LN, lymph node; mLN, mesenteric LN; MC, mast cell, MCp, MC progenitor; MFI, mean fluorescence intensity; mMCP, mouse MC protease; MMC, mucosal MC.

2.4 Introduction

Mast cells (MC) and basophils (Ba) express the high affinity receptor for IgE and have been appreciated and characterized for their respective effector roles in the Th2 host response to helminth infection (1, 2). Although Ba are detected in bone marrow (BM), spleen, and lymph nodes (LN) by flow cytometry as $Fc\varepsilon RI^{+}CD49b^{+}KIT^{-}$ cells in various models of immune responses (2-4), the paucity of MC in these tissues has been demonstrated only by histochemical assessment. MC are long lived as connective tissue MC (CTMC) (5) but transient when induced in the intestine as mucosal MC (MMC) (6, 7). While mature MC are not detected in blood and are rare in the parenchyma of BM, LN and spleen, MC progenitors (MCp) are readily detected in cell suspensions from BM, spleen and small intestine of naïve mice when assayed by limiting dilution and clonal expansion/maturation assays (LDA) (8-11). MCp are recruited to intestine and mesenteric LN (mLN) during Th2-mediated helminth-induced inflammation (12-15) or in response to hyperimmunization (9, 16). Nonetheless, as MCp cannot be detected

histochemically, their presence has not been directly assessed in many models of inflammation.

We used the LDA assay with stem cell factor (SCF) and IL-3 as growth and maturation factors to demonstrate the absence of jejunal MCp in mice lacking β7-integrin (11). We further demonstrated that MCp migration from the BM to jejunum is constitutive and requires a4b7 integrin, as revealed by the depletion of jejunal MCp in WT mice treated for a week with mAb to this integrin (11, 17). This constitutive basal homing from BM to intestine provides a dynamic reservoir of MCp in naïve mice from which MMC are induced with helminth infection (18). Such basal homing is minimal to lung, but recruitment of MCp to lung parenchyma occurs during Th2-mediated pulmonary inflammation using interdependent adhesion and migration pathways (19, 20). This recruitment precedes the induction of mucosal MC (MMC) in the trachea and large airways (21). Because MCp reside in tissues of naïve mice and can be recruited to peripheral tissues with inflammation, their predominant function has been viewed as providing a reservoir for MMC expansion and attendant secretory functions.

Numerous recent studies have been focused on the role of the Ba in the immune response (reviewed in (22)) and yet the role of the MCp in these studies is rarely considered. Furthermore, the analysis of MCp numbers by the in vitro LDA does not distinguish between the committed $FceRI^{+}KIT^{+}$ cells and those earlier multipotential cells capable of entering into the lineage. We turned to flow cytometric analysis without sorting to study the development and distribution of MC and Ba during an inflammatory response, with the goal of identifying both

progenitor and more mature populations. These studies included mice in the naïve state as well as mice injected locally with papain or infected systemically with the helminth *Trichinella spiralis*. MC lineage cells and mature Ba resided in BM and spleen of naïve BALB/c mice. Ba could be recruited to local LN with both papain and *T. spiralis* infection while only the infection elicited a LN MC lineage population. Forward and side scatter analysis by flow cytometry of these FceRI^{+}KIT^{+}CD49b^{-} MC revealed that they were small hypogranular cells. The parallel assessment of their numbers by LDA, which requires maturation, indicated that they were MCp at d 6 and d 13 of infection. The hypogranular phenotype of these local nodal MCp at d 6 of infection was dramatically different from the appearance of fully granulated intestinal MMC in the same mice at the same time. Moreover, the hypogranular MCp in LN and spleen exhibited IL-4 mRNA which increased during *T. spiralis* infection in 4get reporter mice. Furthermore, in infected BALB/c mice, this population of MCp could produce IL-4 and IL-6 as determined by flow cytometric detection. Our findings suggest that MCp are not simply a developmental stage, but rather may be a tissue population with independent functions in locations where granulation is not needed or desirable.

2.5 Material and Methods

Mice

7-18 wk old BALB/c, and 4get (C.129-*Il4*^{tm1Lky}/J) mice were obtained from Taconic Farms or the Jackson Laboratory. IL-3$^{-/-}$ mice are maintained in house at the Dana Farber Cancer Institute (23). The use of mice for these studies was in accordance

with institutional guidelines with review and approval by the Animal Care and Use Committee of the Dana Farber Cancer Institute.

Antibodies

Fluorescently labeled monoclonal antibodies (mAb) directed against FceRIa (MAR-1), mouse IgE (23G3), CD49b (DX5), B220 (RA3-6B2), CD3 (145-2C11), CD19 (6D5), CD4 (RM4-5), Ly-6G/Ly-6C (Gr-1) (RB6-8C5), TCRβ (H57-597), IL-4 (11B11), IL-6 (MP5-20F3) and TNF-α (MP6-XT22) were obtained from Biolegend (San Diego, CA). Anti-FcγRII/III (2.4G2), -KIT (2B8), and -β7 integrin (M293) mAb were obtained from BD Biosciences (San Diego, CA). Monoclonal anti-mouse MC protease (mMCP)-1 was obtained from R&D Systems (Minneapolis, MN). Anti-mMCP-5 is a rabbit anti-peptide preparation made against a specific peptide (24).

Papain administration

Fifty μg of papain (Sigma-Aldrich, St Louis, MO) in HBSS was injected subcutaneously into bilateral footpads at a concentration of 1 mg/ml 3 days prior to harvest of popliteal LN (3).

Trichinella spiralis infection

Mice were infected with 450 larvae of *T. spiralis* by gavage as previously described (6).

Identification of MCp and Ba and intracellular cytokines by flow cytometry

Single cell suspensions of spleen, BM, and LN were obtained by grinding tissues through 70-μm cell strainers (BD Biosciences) into RPMI1640, with 10% fetal calf serum, L-glutamine, penicillin, streptomycin, gentamicin, HEPES buffer, sodium pyruvate, and 2-mercaptoethanol (Sigma-Aldrich). Peripheral blood was collected by cardiac puncture into syringes containing 100 μL 0.5M EDTA. Erythrocytes in spleen and blood were lysed (1-2 min in 0.1 mM EDTA, 2.0 g/L potassium bicarbonate, 16.6 g/L ammonium chloride). Peritoneal cells were collected by peritoneal lavage with 10 ml of RPMI. Non-specific mAb uptake was blocked with CD16/32 (2.4G2) (BD Biosciences) for 10 min, and appropriate mAb were added for 30 min. Cells were analyzed on a FACS Canto flow cytometer (BD Biosciences) using FACSDiva acquisition software. FlowJo software (Tree Star, Ashland, OR) was used for data analysis. Positive cells were defined as those having fluorescence intensities >99% of cells incubated with isotype control mAb. For exclusion of other cell types, we used mAb against CD19, CD3, CD4, B220, TCRβ, and Gr-1. In experiments with naïve mice or papain-injected mice, anti-FcεRIa was used to identify FcεRI$^+$ cells. After *T. spiralis* infection, anti-IgE mAb was used for identification of FcεRI$^+$ cells.

For isolation of MCp from the mesenteric LN in order to examine their morphology, the nodes were removed from *T. spiralis* infected mice on d 6 post-infection. The single cell suspensions were fractionated on a 44%/67% Percoll gradient and the interface cells harvested and incubated with biotinylated anti-CD19 and anti-CD3 (Biolegend) for 30 minutes, after which they were washed and

incubated with biotin binder Dynabeads (Invitrogen) for 30 minutes according to the manufacturer's protocols. The cells were then placed on a Dynabead magnet (Invitrogen) for 5 minutes, and the unbound cells were collected and stained with anti-FceRI, anti-CD117, and anti-CD49b. FceRI^{+} CD117^{+}CD49b^{-} cells were collected using a BD FACSAria II (BD), affixed to slides using a CytoSpin (Thermo Scientific) and stained with either Diff-Quick (Siemens Healthcare Diagnostics) or toluidine blue.

To assess for intracellular cytokine production by MCp, mLN cells were cultured for 1 h in culture media supplemented with IL-3 (1-10 ng/ml) to improve viability and then for 4 h with 1 μg/ml Brefeldin A in the same cell culture media. After 5 h in culture, cells were spun down, fixed and permeabilized using a BD Cytofix/Cytoperm kit according to the manufacturer's directions and stained for flow cytometry. Production of a specific cytokine was identified as an increase in the mean fluorescence relative to that obtained from the same cells stained with an isotype control mAb in parallel. The mean fluorescence intensity (MFI) index was defined as the MFI from the anti-cytokine mAb minus the MFI from the isotype control and then divided by the MFI from the isotype control.

To develop BM derived MC (BMMC), BM cells were cultured in complete RPMI with 10 ng/ml each of SCF and IL-3. Non-adherent cells were passed weekly and the BMMC were used after 4- 6 weeks in culture.

Identification of MCp by limiting dilution and clonal expansion

The limiting dilution and clonal expansion assay (LDA) was performed as previously described with inclusion of SCF with IL-3 to improve viability and maturation (9, 11). Mononuclear cells (MNC) were obtained by Percoll (Sigma-Aldrich) gradient fractionation of harvested cells by using the 44%/67% Percoll interface. After LDA, the original MC progenitor concentration is expressed as the number of MCp per 10^6 MNC isolated from the tissue.

Histochemical and immunohistochemical evaluation of MC

Tissues and isolated cells were evaluated for mature MC numbers by chloroacetate esterase (CAE) reactivity and immunohistochemistry for the mouse MC-specific proteases (mMCP) (21). Briefly, tissue was harvested, fixed in 4% paraformaldehyde overnight and then embedded in paraffin for evaluation of mMCP expression or in glycol methacrylate for evaluation of CAE reactivity. To quantify the number of mature MC in the lymph node preparations, cytospins of ~200,000 cells per slide were stained for CAE reactivity and counted for CAE^+ cells with morphologic characteristics consistent with mature MC.

Antibody-mediated cell depletion

Injection of anti-FcεRIa (MAR-1 from eBioscience, San Diego, CA and Biolegend) was performed essentially as described by others (4, 25). Mice were injected with 10 μg of MAR-1 intraperitoneally 72, 48, and 24 hours prior to *T. spiralis* infection. In initial studies with naïve mice, this protocol depleted most of

the Ba in spleen and BM. In studies of *T. spiralis*-infected mice, BM, spleen and LN were harvested at the times noted and analyzed for MC lineage cells by clonal expansion or flow cytometry and for Ba lineage cells by flow cytometry.

Statistics

Data are expressed as the mean ± SEM when derived from three or more values. Significance was determined with a two-tailed Student's *t* test where three or more values were available for analysis. Significance was determined with the Mann-Whitney U test when values did not follow a normal distribution. Values of $p < 0.05$ were considered significant.

2.6 Results

Identification of two Ba and two MC lineage populations in BALB/c BM and a single phenotype for each lineage in peripheral tissues

Earlier studies by our group and others with BM-derived cells cultured *in vitro* demonstrated that commitment to the MC and Ba lineages was closely followed by *de novo* expression of the high affinity IgE receptor detected either by mAb to the α chain or the ability to bind IgE (26-29). Differentiation along the MC lineage was associated with the continued expression of KIT, the receptor for stem cell factor (SCF), whereas this receptor was down regulated with Ba lineage development (29). To follow the parallel lineage development of MC and Ba *in vivo*, we analyzed the non-B, non-T cells (by excluding cells expressing CD19 or CD3) in BALB/c BM for expression of FceRIa and KIT (CD117), as well as CD49b as a Ba

marker (30-32). Within the non-B, non-T population there were two contiguous populations of cells positive for both FcεRI and CD49b expression (pentagonal and ovoid gates in Figure 2.1A). These cells showed a 10-fold range in the fluorescence intensities of FcεRI expression, and the population of cells expressing the highest levels of FcεRI (ovoid gate in Figure 2.1A) had a 10-fold range in expression of CD49b. A third population of cells was negative for CD49b expression and intermediate in FcεRI expression (rectangular gate in Figure 2.1A), and was predominantly KIT$^+$ (Figure 2.1A, top histogram) suggesting a committed MC lineage identity. The CD49b$^+$ population that expressed intermediate levels of FcεRI (pentagonal gate in Figure 2.1A) uniformly lacked KIT expression (Figure 2.1A, bottom histogram), suggesting a committed Ba identity. The cells expressing high levels of FcεRI (ovoid gate) with a range of CD49b expression were heterogeneous in their KIT expression (Figure 2.1A, middle histogram) suggesting at least two different precursor populations.

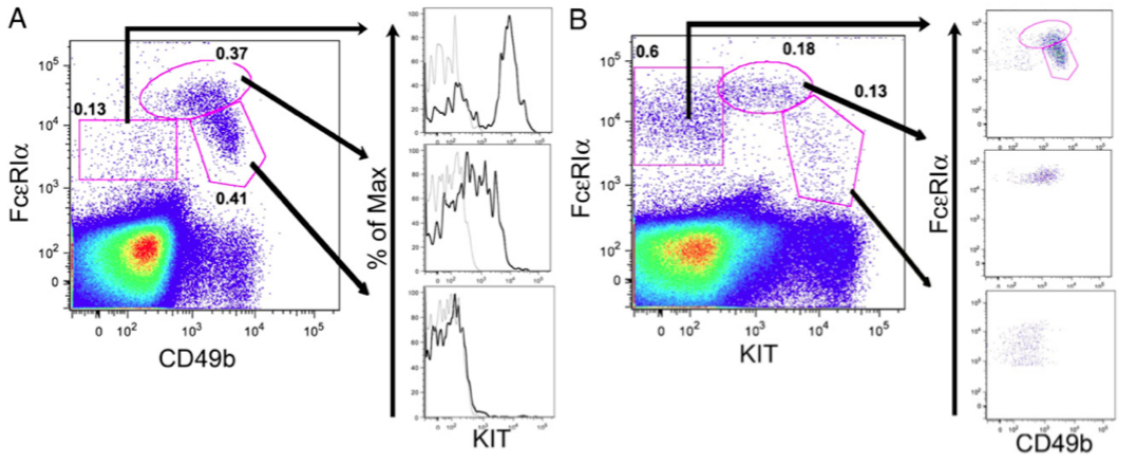

Figure 2.1. BM Ba and MC lineage populations in BALB/c mice defined by flow cytometric analysis of FcεRI, CD49b and KIT expression. BALB/c BM cells were

(Figure 2.1, continued) analyzed for expression of FcεRI, CD49b, and KIT after exclusion of $CD3^+$ and $CD19^+$ (non-T, non-B) cells. **A**. Three populations are defined (polygons) by FcεRI and CD49b expression. The frequencies of the populations are shown as a percent of non-T, non-B cells. Each of the three populations is further analyzed for KIT expression (black histograms) compared with isotype control (gray histograms). **B**. Analysis of FcεRI and KIT expression within the non-T, non-B cells as in panel *A*. Indicated populations are further analyzed for FcεRI and CD49b expression (right panels). Data are representative of 6-9 mice in 3 experiments. Isotype control values were less than 5% of the indicated values.

To further classify these BM cell populations, we reanalyzed the non-B, non-T cells for FcεRI and KIT expression, and then assessed CD49b expression (Figure 2.1B). We identified a KIT^- population (rectangle gate in Figure 2.1B) that was predominantly $CD49b^+$ (Figure 2.1B, top dot plot) suggesting it is mostly composed of Ba lineage cells also identified in the oval and pentagonal gates in Fig 2.1A. The population of cells expressing high levels of KIT and intermediate levels of FcεRI (Figure 2.1B, pentagon) was largely $CD49b^-$ (Figure 2.1B, bottom dot plot) compatible with MC commitment. The population of cells with intermediate KIT and high FcεRI expression (Figure 2.1B, ovoid gate) was heterogeneous for CD49b suggesting two different precursor populations (Figure 2.1B, middle dot plot) similar to the cells in the oval gate identified in Fig 1A. Together, the $FcεRI^+$ populations make up about 0.9% of non-B, non-T cells in BALB/c BM.

Using the same three cell surface markers, we compared the phenotypes of MC ($FcεRI^+KIT^+CD49b^-$) and Ba ($FcεRI^+KIT^-CD49b^+$) within the non-B, non-T cells of BALB/c spleen, blood, and popliteal lymph nodes (LN) with those in the BM, using injection of papain in the footpads to elicit Ba in popliteal LN (3). In the spleen, there was only a single population of $FcεRI^+KIT^+$ cells expressing intermediate levels of FceRI in both naïve and papain-treated mice (Figure 2.2A, top panel, rectangular gate). Few or no $FceRI^+KIT^+$ cells were detected in blood or popliteal LN of naïve and papain-injected mice (Figure 2.2A, middle and bottom panels). There also was only a single population of $FcεRI^+CD49b^+$ cells expressing intermediate levels of FceRI in the spleen and blood of both naïve and papain injected mice (Figure 2.2B, top and middle panels). This $CD49b^+$ population corresponds to the unmarked population of $FceRI^+KIT^-$ cells seen in Figure 2.2A. There were very few LN Ba in naïve mice, but papain administration induced an influx of Ba into LN (Figure 2.2B, bottom panels) as previously noted (3). The $KIT^+FcεRI^{hi}$ and $KIT^-FcεRI^{hi}$ populations seen in BM were notably undetectable in these peripheral tissues.

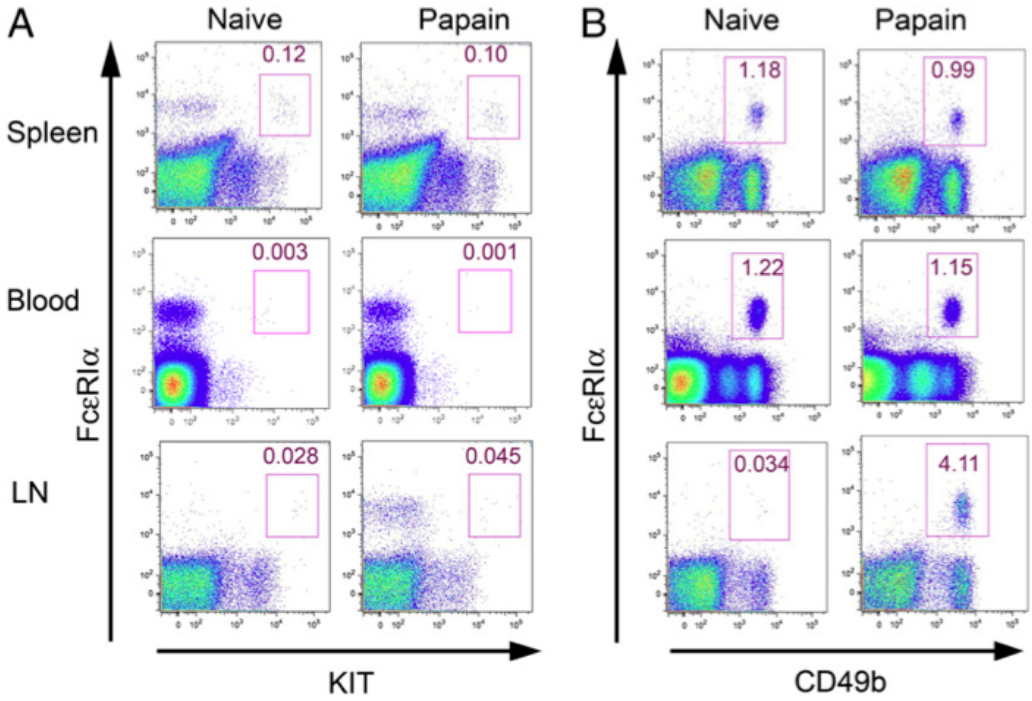

Figure 2.2. Identification of MC and Ba lineage populations in spleen, blood, and LN of naive and papain-injected BALB/c mice. **A.** Three d after papain or PBS injection, MC lineage cells were identified as FcεRI$^+$KIT$^+$ cells in spleen, blood, and popliteal LN. **B**. Three d after papain or PBS injection, Ba lineage cells were identified as non-T, non-B, FcεRI$^+$CD49b$^+$KIT$^-$ cells in spleen, blood, and popliteal LNs. Data are representative of 9-12 mice in 3 experiments. Numbers indicate the frequency of MCp and Ba as a percentage of the non-T, non-B cells isolated from the indicated tissues. Isotype control values were less than 5% of the indicated values.

Infection with T. spiralis expands MC and Ba lineage populations and recruits them to mLN

To directly study recruitment of MC lineage progenitors to LN as predicted by LDA (12-15), we employed a *T. spiralis* infection in which tissues were harvested

in the middle of (d6-7) and toward the end of (d12-14) the acute phase of intestinal infection. In contrast to the studies with papain, we used anti-IgE rather than anti-FcεRI to monitor FcεRI expression during *T. spiralis* infection to avoid any competing effects of host IgE on the assessment of $FcεRI^+$ cells (33). IgE^+KIT^+ MC lineage populations in naïve mice were present in BM and spleen but were rare in mLN (Figure 2.3A, top). The unmarked IgE^+KIT^- Ba population can be seen directly to the left of the gated MCp (Figure 2.3A). After *T. spiralis* infection, there were significant increases in the frequency of BM $IgE^+KIT^+CD49b^-$ MC at d6 and d12 (Figure 2.3A, B). Further, distinct IgE^+KIT^+ MC lineage populations of similar phenotype appeared in spleen and mLN (Figure 2.3A). There were concurrent significant rises in these splenic and LN populations on d6 and d12 (Figure 2.3B). Ba populations identified as IgE^+CD49b^+ cells also significantly expanded in BM on d6 and d12 (Figure 2.3C). Splenic Ba numbers lagged at d6 but had a significant increase at d12. The number of Ba in the mLN was significantly increased at d6 and d12. In the mLN, MC lineage cells constituted a larger (~2 fold) fraction of the population than Ba at each time point.

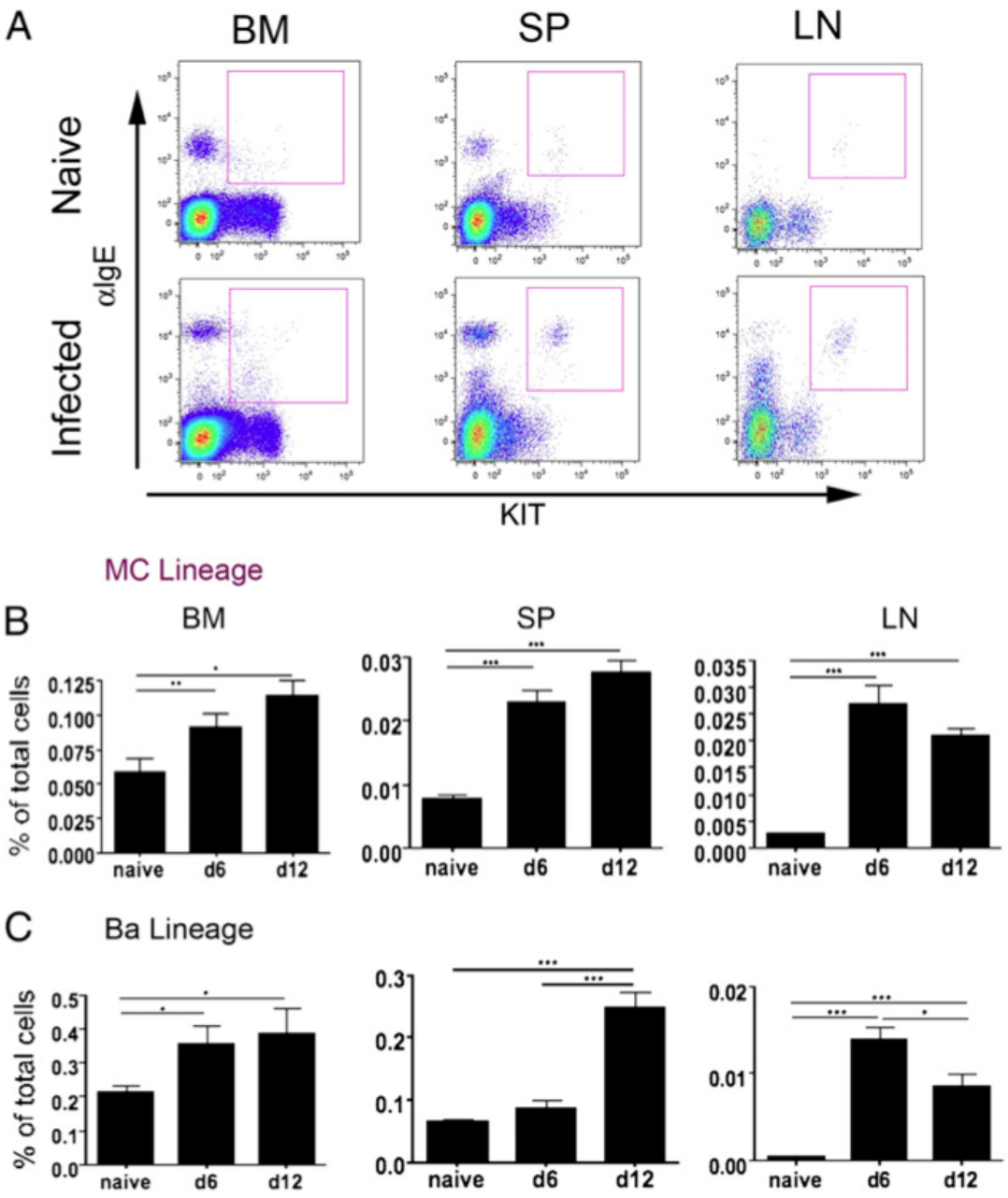

Figure 2.3. *T. spiralis*-infected BALB/c mice recruit MC and Ba to mesenteric LN and expand spleen and BM lineage pools. **A.** Dot plots of BM, spleen, and LN cells from naïve and d12 infected BALB/c mice show the $IgE^{+}KIT^{+}$ MC lineage populations (square gate). Dot plots are representative of data from 4 experiments. **B.** Frequencies of MC lineage populations from naïve, d6 and d12 post-infection mice

(Figure 2.3, Continued) are shown as a percent of total cells isolated from BM, spleen, and LN. **C.** Frequencies of Ba lineage populations (IgE^+CD49b^+) in the BM, spleen, and LN as in panel B. Data in panels B and C represent means ± SEM, n = 13 mice per group, 4 experiments. * $p<0.05$, ** $p<0.001$, ***$p<0.0001$.

LN MCp assessed by flow cytometry are highly immature and correspond in number to MCp assessed by limiting dilution and clonal expansion.

To determine if the numbers of lineage committed MCp in mLN detected directly by their distinct cell surface phenotype in flow cytometry are comparable to the numbers of MCp assayed indirectly ex vivo by LDA, we compared these numbers in naïve mice and in mice 13 d after *T. spiralis* infection by both assays using the MNC fraction. There were very few MCp in naïve mLN with either assay (55.8 and 56.4 MCp/10^6 MNC, mean from 2 experiments, 5 mice). At 13 d post infection there were significant increases in the number of MCp detected by flow cytometry (6.2 fold, $p<0.001$) and by LDA (8.7 fold, $p< 0.01$) (Figure 2.4A). There was no significant difference between the measurements of MCp per million MNC obtained by the two methods in either naïve or infected mice. The trend toward higher numbers obtained by LDA may reflect the lower specificity of this assay attributable to participation by myeloid lineage cells that differentiate into MC colonies in the presence of IL-3 and SCF (34).

To assess the maturity of LN MCp detected by flow cytometry, we analyzed the numbers of MCp in the LN obtained by cytometry before and after density gradient fractionation and compared them to the numbers of granulated MC

detected by histochemistry. It had been established previously using peritoneal cells obtained by lavage that density gradient isolation of MNC yields a cell preparation enriched for MCp and depleted of mature MC which sediment in the pellet (17). *T. spiralis*-infected mLN harvested at d13 post infection yielded 281 ± 57 MCp (IgE^+KIT^+) cells per 10^6 LN cells (mean ± SEM, n= 8, 2 experiments). Histochemical evaluation of granulated MC in these and one additional mLN cell preparation yielded 12.5 ± 3.1 CAE^+ MC per 10^6 LN cells (mean ± SEM, n= 11, 3 experiments). After isolation of the MNC fraction, there were 332 ± 40 MCp per 10^6 MNC by flow cytometry and 7.5 ± 1.0 CAE^+ MC per 10^6 MNC cells by histochemistry. Thus, 96% and 98% of the LN cells identified as IgE^+KIT^+ were histochemically hypogranular MCp before and after isolation of the MNC fraction, respectively.

The majority of mLN MCp appeared in a low SSC gate, with only a scant few mature MC in a high SSC gate (Figure 2.4B). In contrast, the majority of IgE^+KIT^+ cells recovered from peritoneal lavage appeared to be mature MC in the high SSC gate, with few MCp in the low SSC gate (Figure 2.4B). The finding of low granularity for the MCp is consistent with the low density of helminth-induced LN MCp reported by Jarboe et al. (14). When we compared mLN and splenic MCp populations from d6 post *T. spiralis* infection, these induced MCp were virtually identical in size (forward scatter profile) and granularity (SSC profile) and greater than the lymphocyte population in these parameters. Of note, these induced MCp were lower in both assessments than immature BMMC derived with IL-3 and SCF emphasizing their relative agranularity (Supplemental Fig 2.1). Thus, although the recruited LN MCp, splenic MCp, BMMC, and peritoneal MC exhibit the same surface marker phenotype,

when identified by flow cytometry, they are different in regard to size (forward scatter) and granularity (SSC).

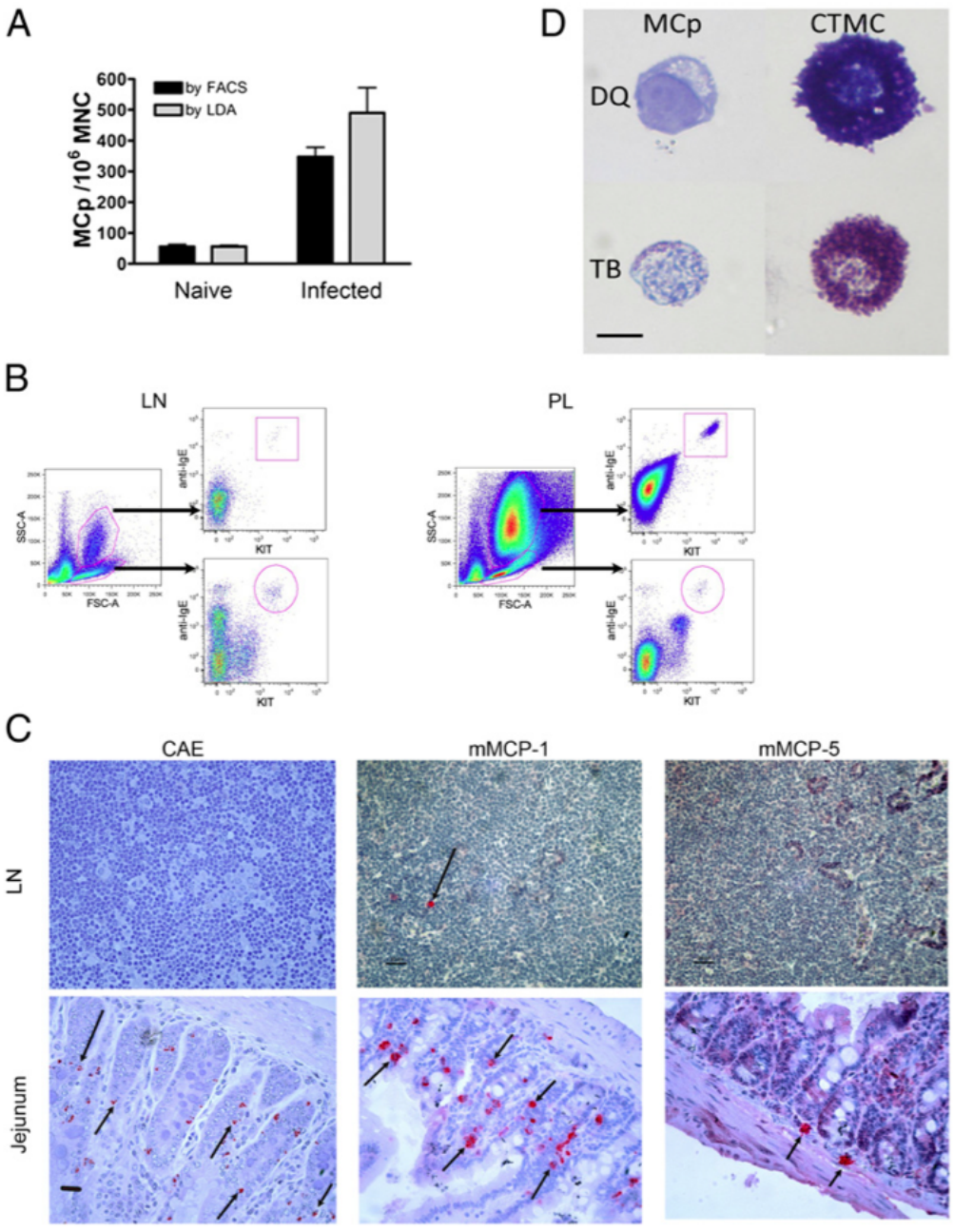

Figure 2.4. Comparison of MC and MCp populations in various tissues of naïve and *T. spiralis*-infected mice analyzed by flow cytometry, limiting dilution analysis, histochemical staining and immunohistochemistry. Mesenteric LN cells were

(Figure 2.4, Continued) isolated from BALB/c mice before and 13 d after *T. spiralis* infection. **A**. Enumeration of MCp in the MNC fraction of LN cells by flow cytometry (FACS) and by the limiting dilution/maturation assay (LDA) to quantitatively compare the 2 methods in naïve and infected mice. Data shown are means ± SEM, n = 5-7 mice per group, from 2 experiments. **B**. Cells from mesenteric LN and peritoneal lavage (PL) isolated 13 d after *T. spiralis* infection were allocated as high and low side scatter (SSC) by flow cytometry and evaluated separately for IgE binding and KIT expression (gates shown in left panel for each tissue). Data are representative of 12 mice, from 3 experiments. **C**. Mesenteric LN and jejunal sections from BALB/c mice obtained 13 d after *T. spiralis* infection were evaluated for MC by CAE reactivity, and by immunohistochemistry for mMCP-1 and mMCP-5. Arrows indicate positively stained cells. **D**. Comparison of the morphology of LN MCp to peritoneal CTMC from BALB/c mice. MCp (left panels) were isolated by FACS from 6 d post *T. spiralis* infected mice and CTMC (right panels) were obtained by peritoneal lavage. The top panels (Diff-Quik stain, DQ) shows only empty vesicles in the MCp and the bottom panels (toluidine blue stain, TB) shows only a few metachromatic granules in MCp while the CTMC has a large number of cytoplasmic granules by both stains. Data shown in A – C are representative of 5 experiments. Micrographs are taken at 400X (C), and 630X (D); black scale bars represent 50 and 10 mm, respectively.

In a histological examination of the parenchyma of mLN for MC we used CAE reactivity as well as immunohistochemistry to mMCP-1 and mMCP-5 to detect mature MC and evaluate their protease phenotype. In the intestine after *T. spiralis* infection, mMCP-1 and mMCP-5 identify the induced MMC and the constitutive submucosal MC, respectively (6, 7, 21). The LN parenchyma from naïve mice demonstrated virtually no CAE reactivity or immunoreactivity for mMCP-1 or mMCP-5 (data not shown). After *T. spiralis* infection, there was little CAE reactivity in the LN as compared to the distinct MMC staining in the jejunum. There were only rare cells immunoreactive for mMCP-1 or mMCP-5 in parenchyma of mLN (Figure 2.4C, top panels) while the intraepithelial MMC from the jejunum of the same mice expressed mMCP-1 and the submucosal MC expressed mMCP-5 (Figure 2.4C, bottom panels). These observations support the findings by flow cytometry that with *T. spiralis* infection, dispersed mLN parenchymal cells harbor very few mature MC in concert with a dominant hypogranular subset of MCp.

To directly visualize the morphology of this recruited subset, we sorted them from the mesenteric nodes of *T. spiralis* infected mice at d6 based on their distinct phenotype. After depleting the $CD3^{+}CD19^{+}$ cells, the sorted $KIT^{+}FceRI^{+}CD49b^{-}$ cells were stained with Diff-Quick or toluidine blue.The LN MCp are small cells with a prominent nucleus and a cytosol which contains numerous empty vesicles after staining with Diff-Quick and reveals a few toluidine blue positive granules (Figure 2.4D). By comparison, CTMC from the peritoneal cavity are large and heavily granulated cells by either Diff-Quik or toluidine blue staining.

Depletion of MCp by administration of anti-FcεRI mAb with T. spiralis infection

Depletion of Ba by systemic administration of anti-FcεRI mAb (MAR-1) to assess their role in mouse models of inflammation (3, 4, 25, 32) is based on a protocol by Denzel *et al.* (33) in which Ba depletion is not accompanied by a change in the number of mature peritoneal MC. To assess the effect of this treatment on MCp, we administered anti-FcεRI mAb intraperitoneally to BALB/c mice prior to infection with *T. spiralis* and then enumerated the numbers of MCp in mLN, spleen and BM. MCp were identified as β7-integrin$^+$KIT$^+$ cells, a combination that was equivalent to anti-IgE$^+$KIT$^+$ identification of MCp in isotype-treated infected mice (data not shown). Six days after infection, the b7-integrin$^+$KIT$^+$ MCp were significantly reduced by ~70% (from 471 to 141 MCp per 10^6 nucleated LN cells) as compared to isotype control injected mice (Figure 2.5A). The fold-reduction was similar when assessed by LDA in which cell numbers were reduced from 860 to 260 MCp per 10^6 LN MNC (Figure 2.5B). In contrast, the numbers of MCp in the BM and spleen at d6 post infection were not reduced by this treatment when assessed by flow cytometry or by LDA. The number of b7-integrin$^+$KIT$^+$ MCp in isotype control mAb versus MAR-1 injected mice in the BM and spleen was 2020 ± 328 versus 2058 ± 157 MCp per 10^6 BM cells (mean ± SEM, n=3) and 534 ± 48 versus 837 ± 227 MCp per 10^6 splenic MNC, respectively (mean ± SEM, n=3). By LDA, we found 624 ± 63 MCp per 10^6 MNC in the spleens of isotype control injected mice versus 750 ± 128 MCp per10^6 MNC in the spleens of MAR-1 injected mice (mean ± SEM, n=6, 2 experiments).

To address the possibility that the influx of Ba influenced the recruitment of MCp to draining nodes, we evaluated the response in the IL-3$^{-/-}$ strain which had been reported to lack Ba in their mesenteric LN by FACS analysis after *N. brasiliensis* infection (35). The number of LN MCp in the IL3$^{-/-}$ versus the BALB/c mice 6 d after infection with *T spiralis* was not different (0.70 ± 0.15 % versus 0.68 ± 0.05 % of non-B, non-T LN cells, respectively, n=4 mice per genotype in a single experiment) while the increase in the number of Ba in these same mice was reduced by 77 % (0.03 ± 0.01 % versus 0.15 ± 0.05 %, respectively). We obtained similar results in a second experiment indicating the independence of MCp recruitment to the DLN.

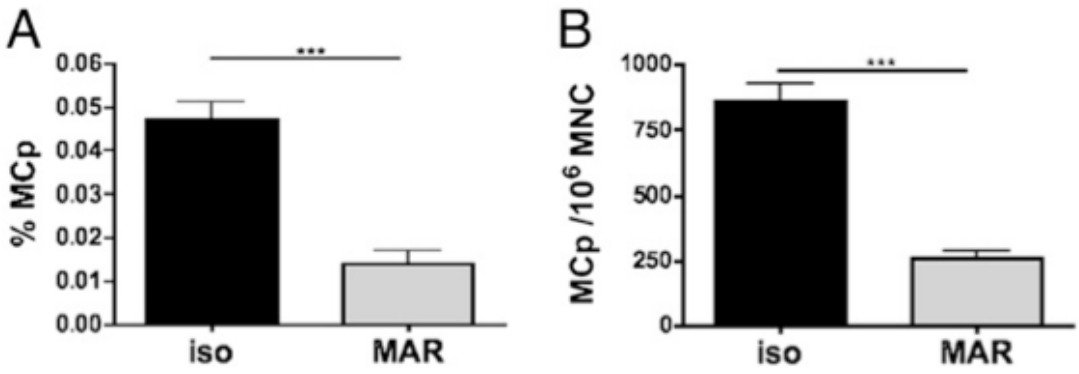

FIGURE 2.5. Administration of anti-FcεRI mAb depletes LN MCp. BALB/c mice were injected i.p. with anti-FcεRI mAb (MAR-1) daily for 3 d before being infected with *T. spiralis*. Mesenteric LN were harvested after 6 d and MCp were assayed. **A**. In a flow cytometric assay, MCp were identified as β7 integrin^{+}KIT^{+} cells and enumerated per million live nucleated nodal cells. Data represent means ± SEM, n = 10-11 mice per group, 3 experiments. **B**. In the LDA, MCp were assayed after Percoll gradient

(Figure 2.5, continued) isolation of MNC and expressed per million MNC. Data represent means ± SEM, n = 5-6 mice per group, 2 experiments. ***p<0.0001.

T. spiralis infection increases IL-4 mRNA in mLN MCp of 4get mice

The infection-driven expansion of hypogranular MCp in the draining LN without the appearance of MMC that are so prominent in the intestine, suggests that LN MCp might have a granule-independent function. As many helminth infections generate a substantial Th2 type inflammation with an increased IgE response implicating IL-4, we examined IL-4 mRNA levels in MCp using IL-4/eGFP (4get) reporter mice. In these mice, an eGFP gene is inserted in the 3' untranslated region of the endogenous IL-4 locus such that eGFP is transcribed in parallel with IL-4 and thus serves as a marker of IL-4 mRNA levels. In naïve 4get mice, BM MCp express very little GFP as measured by mean fluorescence intensity (MFI) (184 ± 10.6), consistent with the findings of Gessner *et al.* (36), while splenic MCp express moderate levels of GFP (761.4 ± 50.6), and peritoneal MC express uniformly high levels of GFP (1789 ± 85.3) (Figure 2.6A and B, left panels). Very few naïve LN MCp were detectable but those seen expressed low GFP levels comparable to naïve splenic MCp (Figure 2.6A, black histograms). Six days after *T. spiralis* infection, GFP expression increased in MCp in all tissues (Figure 2.6A, red histograms). The increase in MFI with infection was significant for the MCp in BM, spleen and mLN as well as for peritoneal MC (Figure 2.6B, left panel). The Ba lineage demonstrated initial baseline GFP expression in BM, spleen and LN, and with *T. spiralis* infection, it significantly increased in the BM and splenic Ba. (Figure 2.6A and B, right panels).

Of note, the hypogranular MCp of spleen and LN increased expression of GFP by 2.5, and 3.6 fold, respectively, while the mature granular peritoneal MC increased GFP expression by only 1.3 fold with infection.

T. spiralis infection induces IL-4 and IL-6 production by mLN MCp of WT BALB/c mice

We then evaluated IL-4 and IL-6 production in LN MCp by intracellular cytokine staining in BALB/c mice on d6 after *T. spiralis* infection. The LN MCp from a typical infected mouse showed expression of IL-4 and IL-6 as indicated by the right shift in the histograms of intracellular cytokine staining for both cytokines (Figure 2.6C). The range of expression in all mice at d6 post infection is presented in Figure 2.6D and shows detectable levels of IL-4 in 9 of 13 and of IL-6 in 11 of 13 mice. Importantly, the hypogranular MCp can exhibit cytokine-generating function without being subjected to further *ex vivo* stimulation.

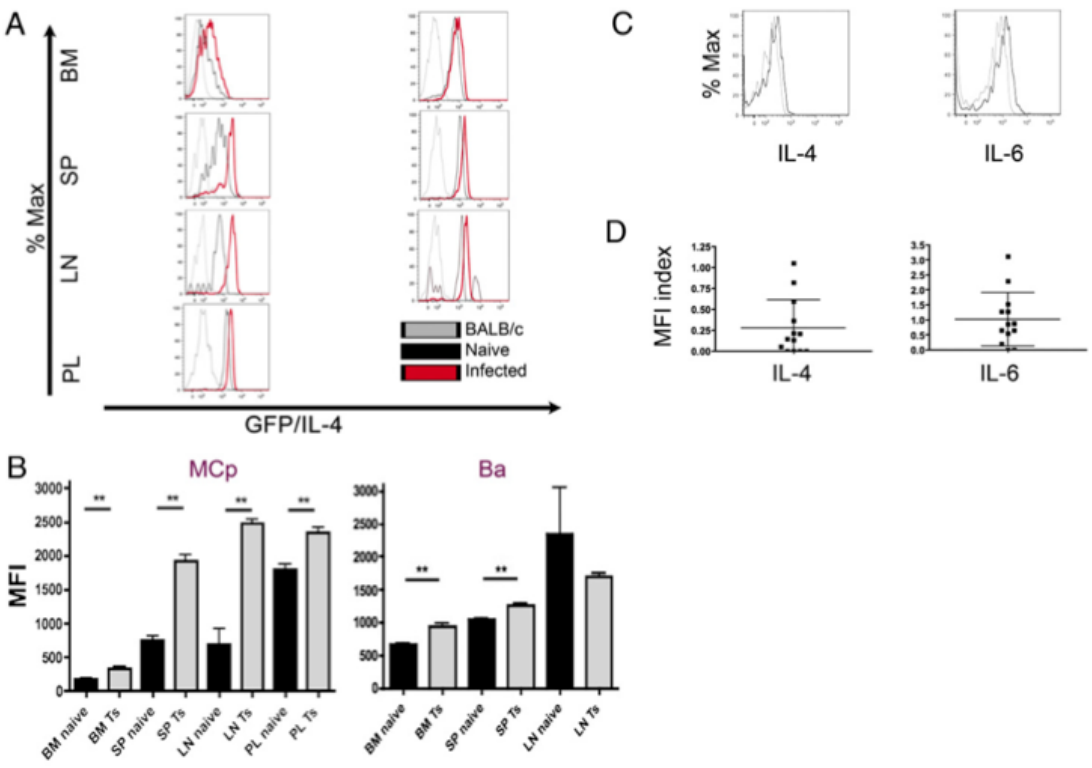

FIGURE 2.6. Increased IL-4 transcription in 4get mice and production of IL-4 and IL-6 by LN MCp after *T. spiralis* infection of BALB/c mice. **A**. BM, spleen, mesenteric LN, and peritoneal lavage (PL) fluid were harvested from naïve BALB/c and 4get mice, and from 4get mice on d6 post *T. spiralis (Ts)* infection. The single cell suspensions were assessed for GFP expression within the MC and Ba lineage populations. Histograms of GFP expression are shown for MC (left) and Ba (right) from each tissue as indicated. Histogram colors represent: gray, naïve BALB/c mice; black, naïve 4get mice; red, *T. spiralis*-infected 4get mice. Naïve LN data are based on very few events. **B**. Mean fluorescence intensities (MFI) of GFP in the indicated MC (left) or Ba (right) lineage populations from 4get mice represent mean ± SEM, n = 13-14 mice, 3 experiments. ** $p < 0.0005$, calculated by the Mann-Whitney U test. **C**. Intracellular cytokine staining for the indicated cytokines in mLN MCp d6 post

(Figure 2.6, Continued) infection in a representative BALB/c mouse. The gray lines are the isotype control, and black lines are the indicated cytokine. Histograms are from one mouse whose response was close to the mean shown in D. **D***.* MFI index of intracellular cytokine staining for IL-4 and IL-6 in mLN MCp, showing individual values and mean values ± SEM (bars), d6 post infection, 13 mice per group, 5 experiments.

2.7 Discussion

We have addressed the parallel *in vivo* responses of MC and Ba from BM to blood, spleen and regional LN using flow cytometry in mice subjected to local or systemic inflammation as compared to naïve controls. Unlike other myeloid lineage cells, MC are released from BM as a progenitor which is devoid of the secretory granules that define the mature tissue resident cells. Thus, we first established that their cytometric detection and enumeration as $FceRI^{+}KIT^{+}CD49b^{-}$ MCp corresponded in numbers with their classical assay in tissues by limiting dilution and clonal expansion with maturation to granulated immature MC (34, 37). We then observed that the size (FSC) and granularity (SSC) of MCp by cytometric assay were more than that observed for lymphocytes and demonstrably less than these parameters for culture-derived immature BMMC. These finding were also confirmed by histochemistry in which MC in the jejunum were readily observed using either CAE reactivity or immuno-histochemistry for the secretory granule proteases while those in the LN were not detectable by either measure. Turning to a positive definition of the nodal MCp, we sorted this subset by their lineage phenotype and

assessed their morphology on cytospins. As expected nodal MCp are small cells with a prominent nucleus and empty cytoplasmic vesicles by Diff-Quik stain. Toluidine blue staining showed a few granules. The contrast to peritoneal MC by size and granularity was marked, again as expected from the FACS study. Thus, even though the nodal MCp had the same membrane phenotype as mature granulated MC such as those in the peritoneal cavity, they are a novel MC subset with small size and little granularity.

As the MCp recruited to parenchymal tissue of mLN or expanded in spleen with *T. spiralis* infection are granule deficient by cytometric presentation or direct histochemisty, they would not have been directly recognized in prior studies of MC biology. However, their phenotypic definition allows for a dynamic real time assessment of their accumulation with cytometry. While the jejunum was enriched with mMCP-1^{+} MMC likely derived from MCp recruited by the *T. spiralis* infection (12, 13), the nodal MCp were hypogranular and remained as such even as they declined in numbers by d13 when the infection is subsiding and the jejunal MMC are at their peak. Thus, we sought evidence of function in vivo for the hypogranular nodal subset. Exocytosis of preformed secretory granule mediators seemed excluded based on the lack of granules, so we turned to the production of cytokines which is a well-recognized function for BMMC in response to various agonists (38). Using 4get reporter mice, we found upregulation of IL-4 mRNA during helminth infection that increased to a greater degree in mLN MCp than in granulated mature peritoneal CTMC or in the recruited Ba. Importantly, intracellular cytokine staining demonstrated that MCp of WT BALB/c mice had cytokine generating function as

shown by IL-4 and IL-6 production in most mice at d6 post *T. spiralis* infection. We did not need to further activate these LN ex vivo to obtain cytokine generation but did provide IL-3 to maintain their viability during their exposure to brefeldin. We have not yet sought to optimize the post infection time course for MCp cytokine production or surveyed for other cytokines. Rather, our current goal was to demonstrate function for this essentially agranular MC subset prominent in draining LN after *T. spiralis* infection. We appreciate that there is a longer term need to address the role of the MC lineage in afferent as well as the traditional efferent components of adaptive immunity.

Ginsburg and Lagunoff first extrapolated the appearance of MC lineage progenitors in LN of BALB/c mice, using repeated injections of horse serum or hen albumin for systemic sensitization (16). In their study, LN cells cultured on embryonic fibroblast monolayers differentiated into histochemically defined MC at higher rates from immunized mice, and the dependence of this outcome on Ag restimulation during the culture suggested cytokine dependent maturation. Subsequently, Crapper and Schrader used a conditioned media to grow immature MC from putative MCp and used a limiting dilution analysis with clonal expansion to define the levels of MCp in BM, spleen, and LN of naïve CBA mice as well to show an increase in their number following a local immunization (9). Guy-Grand *et al.* used such an assay to indirectly recognize MCp in both the thoracic duct lymph and in the mLN during *Nippostrongylus brasiliensis* infection in BALB/c mice (10). Jarboe *et al*. extended these findings to show that putative MCp harvested from mesenteric LN were of low density and could be expanded and matured with cytokine culture

alone or on a fibroblast monolayer with the latter inducing a histochemical positivity for heparin (14). Similarly, Rennick and colleagues demonstrated that IL-4 and IL-10 promoted expansion and maturation, respectively, of MCp recruited to mesenteric LN with helminth infection and that fibroblast monolayer co-culture induced heparin biosynthesis (15). Thus, the seminal assay of LN MCp from immunized mice by Ginsburg and Lagunoff had components such as added Ag and fibroblast monolayers favoring their maturation to identifiable immature MC. A recent study has suggested that MCp identified by clonal expansion in the LN of helminth-infected mice could be due to the influx of early myeloid progenitors (34). In that study, the authors noted the recruitment of type 2 multipotential progenitors to the LN and their maturation to MC, Ba and macrophages on ex vivo culture. Notably, these prior studies have relied on in vitro culture with MC growth factors to indirectly demonstrate the presence of MC lineage progenitors and this indirect approach does not reveal their relative maturation or purity of their lineage commitment. Our studies provide a direct assay for the MCp and in concert with LDA, demonstrate that the majority of the cells of the MC lineage recruited to the draining LN with helminth infection are committed MCp. However, our findings also point out that the assays of MCp by ex vivo expansion with maturation do not define their hypogranular in vivo phenotype and apparent failure to mature to MMC within the LN parenchyma.

The number of MC subsets is of course not limited to agranular and granular. For example, within the granular subset, the MMC in the intestine induced by helminth infection express mMCP-1 while MMC induced to accumulate in the

trachea by ovalbumin sensitization and challenge express not only mMCP-1, a chymase, but also another chymase, mMCP-4, an elastase, mMCP-5, two tryptases, mMCP-6 and -7 and carboxypeptidase A3 (6, 21). There are also differences in the protease profile of the innate CTMC in intestine and trachea. Taken together it begins to appear that the particular tissue and its microenvironment to which MCp are recruited can determine if there is granulation and as well as the protease profile of those that become granulated (21, 37). This heterogeneity along with the added contexts of cytokine and eicosanoid generation for a lineage with major innate and adaptive immune-induced members suggest that subset recognition is a step toward clarifying the complexities of overall MC lineage function.

As the MCp recruited to parenchymal tissue of mLN and spleen with *T. spiralis* infection were granule deficient by cytometric presentation or histochemistry on cytospins, they would not have been recognized in studies in which mAb to FceRI was used to deplete and thereby recognize a Ba function. Germane to this, recently Giacomin et al (39) evaluated this treatment in C57BL/6 mice infected with *T. spiralis* and noted a decrease in the mucosal MC response in the small intestine which they attributed to attenuation of the Th2 response although they did not evaluate MCp. We observed an approximate 70% reduction in accumulation of LN MCp with administration of mAb to FceRI to mice prior to *T. spiralis* infection. This blocking was selective as there was no significant concomitant reduction of MCp in BM or spleen assessed by either FACS or LDA. We have not yet addressed the kinetics of LN Ba and MCp depletion with mAb to FceRI. Nonetheless, our findings with administration of anti-FcεRI are noteworthy because

the contributions of IL-4 and/or IL-6 production by Ba have been implicated in host Th2 cell and B cell responses (3, 4, 25, 32, 33, 39, 40), whereas our new findings reveal a previously unrecognized possible contribution from LN MCp.

2.8 References

1. Kamiya, M., Y. Oku, H. Itayama, and M. Ohbayashi. 1985. Prolonged expulsion of adult Trichinella spiralis and eosinophil infiltration in mast cell-deficient W/Wv mice. *J. Helminthol.* 59:233-239.

2. Voehringer, D., T. A. Reese, X. Huang, K. Shinkai, and R. M. Locksley. 2006. Type 2 immunity is controlled by IL-4/IL-13 expression in hematopoietic non-eosinophil cells of the innate immune system. *J. Exp. Med.* 203:1435.

3. Sokol, C. L., G. M. Barton, A. G. Farr, and R. Medzhitov. 2008. A mechanism for the initiation of allergen-induced T helper type 2 responses. *Nat. Immunol* 9:310-318.

4. Yoshimoto, T., K. Yasuda, H. Tanaka, M. Nakahira, Y. Imai, Y. Fujimori, and K. Nakanishi. 2009. Basophils contribute to T(H)2-IgE responses in vivo via IL-4 production and presentation of peptide-MHC class II complexes to CD4+ T cells. *Nat. Immunol.* 10:706-712.

5. Fukuzumi, T., N. Waki, Y. Kanakura, J. Nagoshi, S. Hirota, K. Yoshikawa, and Y. Kitamura. 1990. Differences in irradiation susceptibility and turnover between mucosal and connective tissue-type mast cells of mice. *Exp. Hematol.* 18:843-847.

6. Friend, D. S., N. Ghildyal, K. F. Austen, M. F. Gurish, R. Matsumoto, and R. L. Stevens. 1996. Mast cells that reside at different locations in the jejunum of mice infected with Trichinella spiralis exhibit sequential changes in their granule ultrastructure and chymase phenotype. *J. Cell Biol.* 135:279-290.

7. Friend, D. S., N. Ghildyal, M. F. Gurish, J. Hunt, X. Hu, K. F. Austen, and R. L. Stevens. 1998. Reversible expression of tryptases and chymases in the jejunal mast cells of mice infected with Trichinella spiralis. *J. Immunol.* 160:5537-5545.

8. Sonoda, T., Y. Kitamura, Y. Haku, H. Hara, and K. J. Mori. 1983. Mast-cell precursors in various haematopoietic colonies of mice produced in vivo and in vitro. *Br. J. Haematol.* 53:611.

9. Crapper, R. M., and J. W. Schrader. 1983. Frequency of mast cell precursors in normal tissues determined by an in vitro assay: antigen induces parallel increases in the frequency of P cell precursors and mast cells. *J. Immunol.* 131:923-928.

10. Guy-Grand, D., M. Dy, G. Luffau, and P. Vassalli. 1984. Gut mucosal mast cells. Origin, traffic, and differentiation. *Journal of Experimental Medicine* 160:12-28.

11. Gurish, M. F., H. Tao, J. P. Abonia, A. Arya, D. S. Friend, C. M. Parker, and K. F. Austen. 2001. Intestinal mast cell progenitors require CD49dbeta7 (alpha4beta7 integrin) for tissue-specific homing. *Journal of Experimental Medicine* 194:1243-1252.

12. Dillon, S. B., and T. T. MacDonald. 1986. Limit dilution analysis of mast cell precursor frequency in the gut epithelium of normal and Trichinella spiralis infected mice. *Parasite Immunol.* 8:503-511.

13. Parmentier, H. K., J. S. Teppema, H. van Loveren, J. Tas, and E. J. Ruitenberg. 1987. Effect of a Trichinella spiralis infection on the distribution of mast cell precursors in tissues of thymus-bearing and non-thymus-bearing (nude) mice determined by an in vitro assay. *Immunology* 60:565-571.

14. Jarboe, D. L., J. S. Marshall, T. R. Randolph, A. Kukolja, and T. F. Huff. 1989. The mast cell-committed progenitor. I. Description of a cell capable of IL-3-independent proliferation and differentiation without contact with fibroblasts. *J. Immunol.* 142:2405-2417.

15. Rennick, D., B. Hunte, G. Holland, and L. Thompson-Snipes. 1995. Cofactors are essential for stem cell factor-dependent growth and maturation of mast cell progenitors: comparative effects of interleukin-3 (IL-3), IL-4, IL-10, and fibroblasts. *Blood* 85:57-65.

16. Ginsburg, H., and D. Lagunoff. 1967. The in vitro differentiation of mast cells. Cultures of cells from immunized mouse lymph nodes and thoracic duct lymph on fibroblast monolayers. *J. Cell Biol.* 35:685-697.

17. Abonia, J. P., K. F. Austen, B. J. Rollins, S. K. Joshi, R. A. Flavell, W. A. Kuziel, P. A. Koni, and M. F. Gurish. 2005. Constitutive homing of mast cell progenitors to the intestine depends on autologous expression of the chemokine receptor CXCR2. *Blood* 105:4308-4313.

18. Artis, D., N. E. Humphreys, C. S. Potten, N. Wagner, W. Muller, J. R. McDermott, R. K. Grencis, and K. J. Else. 2000. Beta7 integrin-deficient mice: delayed leukocyte recruitment and attenuated protective immunity in the small intestine during enteric helminth infection. *Eur. J. Immunol.* 30:1656-1664.

19. Abonia, J. P., J. Hallgren, T. Jones, T. Shi, Y. Xu, P. Koni, R. A. Flavell, J. A. Boyce, K. F. Austen, and M. F. Gurish. 2006. Alpha-4 integrins and VCAM-1, but not MAdCAM-1, are essential for recruitment of mast cell progenitors to the inflamed lung. *Blood* 108:1588-1594.

20. Hallgren, J., T. G. Jones, J. P. Abonia, W. Xing, A. Humbles, K. F. Austen, and M. F. Gurish. 2007. Pulmonary CXCR2 regulates VCAM-1 and antigen-induced recruitment of mast cell progenitors. *Proc. Natl. Acad. Sci. USA* 104:20478-20483.

21. Xing, W., K. F. Austen, M. F. Gurish, and T. G. Jones. 2011. Protease phenotype of constitutive connective tissue and of induced mucosal mast cells in mice is regulated by the tissue. *Proc. Natl. Acad. Sci. USA* 108:14210-14215.

22. Sawaguchi, M., S. Tanaka, Y. Nakatani, Y. Harada, K. Mukai, Y. Matsunaga, K. Ishiwata, K. Oboki, T. Kambayashi, N. Watanabe, H. Karasuyama, S. Nakae, H. Inoue, and M. Kubo. 2012. Role of Mast Cells and Basophils in IgE Responses and in Allergic Airway Hyperresponsiveness. *J. Immunol.* 188:1809-1818.

23. Jones, T. G., J. Hallgren, A. Humbles, T. Burwell, F. D. Finkelman, P. Alcaide, K. F. Austen, and M. F. Gurish. 2009. Antigen-Induced Increases in Pulmonary Mast Cell Progenitor Numbers Depend on IL-9 and CD1d-Restricted NKT Cells. *J. Immunol.* 183:5251-5260.

24. McNeil, H. P., D. P. Frenkel, K. F. Austen, D. S. Friend, and R. L. Stevens. 1992. Translation and granule localization of mouse mast cell protease-5. Immunodetection with specific antipeptide Ig. *J. Immunol.* 149:2466.

25. Perrigoue, J. G., S. A. Saenz, M. C. Siracusa, E. J. Allenspach, B. C. Taylor, P. R. Giacomin, M. G. Nair, Y. Du, C. Zaph, N. van Rooijen, M. R. Comeau, E. J. Pearce, T. M. Laufer, and D. Artis. 2009. MHC class II-dependent basophil-CD4+ T cell interactions promote T(H)2 cytokine-dependent immunity. *Nat. Immunol.* 10:697-705.

26. Rottem, M., J. P. Goff, J. P. Albert, and D. D. Metcalfe. 1993. The effects of stem cell factor on the ultrastructure of Fc epsilon RI+ cells developing in IL-3-dependent murine bone marrow-derived cell cultures. *J. Immunol.* 151:4950-4963.

27. Yuan, Q., M. F. Gurish, D. S. Friend, K. F. Austen, and J. A. Boyce. 1998. Generation of a novel stem cell factor-dependent mast cell progenitor. *J. Immunol.* 161:5143-5146.

28. Jamur, M. C., A. C. Grodzki, E. H. Berenstein, M. M. Hamawy, R. P. Siraganian, and C. Oliver. 2005. Identification and characterization of undifferentiated mast cells in mouse bone marrow. *Blood* 105:4282-4289.

29. Arinobu, Y., H. Iwasaki, M. F. Gurish, S. Mizuno, H. Shigematsu, H. Ozawa, D. G. Tenen, K. F. Austen, and K. Akashi. 2005. Developmental checkpoints of the basophil/mast cell lineages in adult murine hematopoiesis. *Proc. Natl. Acad. Sci. USA* 102:18105-18110.

30. Voehringer, D., K. Shinkai, and R. M. Locksley. 2004. Type 2 immunity reflects orchestrated recruitment of cells committed to IL-4 production. *Immunity* 20:267-277.

31. Min, B., M. Prout, J. Hu-Li, J. Zhu, D. Jankovic, E. S. Morgan, J. F. Urban, Jr., A. M. Dvorak, F. D. Finkelman, G. LeGros, and W. E. Paul. 2004. Basophils produce IL-4 and accumulate in tissues after infection with a Th2-inducing parasite. *J. Exp. Med.* 200:507-517.

32. Mukai, K., K. Matsuoka, C. Taya, H. Suzuki, H. Yokozeki, K. Nishioka, K. Hirokawa, M. Etori, M. Yamashita, T. Kubota, Y. Minegishi, H. Yonekawa, and H. Karasuyama. 2005. Basophils play a critical role in the development of IgE-mediated chronic allergic inflammation independently of T cells and mast cells. *Immunity* 23:191-202.

33. Denzel, A., U. A. Maus, M. R. Gomez, C. Moll, M. Niedermeier, C. Winter, R. Maus, S. Hollingshead, D. E. Briles, L. A. Kunz-Schughart, Y. Talke, and M. Mack. 2008. Basophils enhance immunological memory responses. *Nat. Immunol.* 9:733-742.

34. Saenz, S. A., M. C. Siracusa, J. G. Perrigoue, S. P. Spencer, J. F. Urban, Jr., J. E. Tocker, A. L. Budelsky, M. A. Kleinschek, R. A. Kastelein, T. Kambayashi, A. Bhandoola, and D. Artis. 2010. IL25 elicits a multipotent progenitor cell population that promotes T(H)2 cytokine responses. *Nature* 464:1362-1366.

35. Kim, S., M. Prout, H. Ramshaw, A. F. Lopez, G. LeGros, and B. Min. Cutting edge: basophils are transiently recruited into the draining lymph nodes during helminth infection via IL-3, but infection-induced Th2 immunity can develop without basophil lymph node recruitment or IL-3. *J. Immunol.* 184:1143-1147.

36. Gessner, A., K. Mohrs, and M. Mohrs. 2005. Mast cells, basophils, and eosinophils acquire constitutive IL-4 and IL-13 transcripts during lineage differentiation that are sufficient for rapid cytokine production. *J. Immunol.* 174:1063-1072.

37. Gurish, M. F., and K. F. Austen. 2012. Developmental origin and functional specialization of mast cell subsets. *Immunity* 37:25-33.

38. Burd, P. R., H. W. Rogers, J. R. Gordon, C. A. Martin, S. Jayaraman, S. D. Wilson, A. M. Dvorak, S. J. Galli, and M. E. Dorf. 1989. Interleukin 3-dependent and -independent mast cells stimulated with IgE and antigen express multiple cytokines. *J. Exp. Med.* 170:245.

39. Giacomin, P. R., M. C. Siracusa, K. P. Walsh, R. K. Grencis, M. Kubo, M. R. Comeau, and D. Artis. 2012. Thymic Stromal Lymphopoietin-Dependent Basophils Promote Th2 Cytokine Responses following Intestinal Helminth Infection. *The Journal of Immunology* 189:4371-4378.

40. Gomez, M. R., Y. Talke, N. Goebel, F. Hermann, B. Reich, and M. Mack. 2010. Basophils Support the Survival of Plasma Cells in Mice. *J. Immunol.* 185:7180-7185.

Chapter 3, B Cells Regulate CD4+ T cell Responses to Papain Following BCR-Independent Papain Uptake

3.1. Author Contribution

Daniel F. Dwyer, Matthew C. Woodruff, Michael C. Carroll, K. Frank Austen, and Michael F. Gurish

- Daniel Dwyer conceived the study, designed and performed experiments, analyzed and interpreted data, and wrote the manuscript.
- Matthew Woodruff performed and analyzed intravital and confocal microscopy experiments and helped prepare figures
- Michael Carroll provided the CR2-/- mice and guidance in experimental design and interpretation
- K. Frank Austen supervised the project and manuscript writing.
- Michael Gurish supervised the project and manuscript writing.

3.2 Acknowledgements

The authors wish to thank Dr. Peter Sage for many helpful conversations.

3.3 Abbreviations used in this chapter

Ba, basophil; BM, bone marrow; DC, Dendritic Cell; ICOS, Inducible T cell costimulator; NS, no significant difference; PD-1, programmed cell death protein 1; PLN, popliteal lymph node; Tfh, Follicular helper T cell; Th2 T helper type 2 cell.

3.4 Introduction

Allergens are a broad class of otherwise innocuous Ags capable of inducing vigorous Th2 responses. Allergens commonly provide adjuvant signals that direct innate and adaptive immune responses against associated proteins. Several common allergens, including grass pollen and house dust mite Ag, contain cysteine protease elements (1, 2), and these elements provide adjuvant effects (3). Infection with parasitic helminths also induces a host Th2 response that assists in parasite clearance (4), and helminth-secreted cysteine proteases play important roles in helminthic life cycles (5). The cysteine protease papain shares structural similarity with proteases found in both helminths (6) and allergens (7) and when injected into the mouse footpad induces a potent Th2 response in the popliteal lymph nodes (PLN) (8).

Although an initial study failed to show a role for dendritic cells (DC) in Th2 polarization following papain immunization (9), subsequent studies established a central DC role in directing this response (10-13). However, the seminal finding that Th2 polarization is impaired in mice with MHC-II expression restricted to $CD11c^+$ cells (9) remains unresolved, indicating the need for a MHC-II expressing cell other than the DC to maximize IL-4 responses. This ancillary role was initially attributed to the basophil (Ba) (9, 14, 15), as mAb depletion of Ba greatly inhibits Th2

polarization, but subsequent studies using Ba-deficient mice have called this finding into question (12).

In the interest of identifying a second MHC-II$^+$ cell involved in the local response to papain, we injected C57BL/6 mice in the footpad with fluorescently labeled papain and followed papain uptake in the PLN by flow cytometry. We found an unexpectedly rapid and strong uptake of papain by B cells that also occurred in transgenic MD4 mice, in which 98% of B cells express a BCR specific for hen egg lysozyme (HEL). This uptake by polyclonal B cells occurred within minutes after injection and B cells subsequently internalized papain into endosomes. These findings suggested that papain acquisition by B cells involved an innate B cell response to cysteine protease activity rather than cognate-specific uptake by the clonotypic BCR.

This prompted a study of papain immunization in B cell-deficient μMT mice (16), which showed normal PLN T cell expansion but significantly impaired peak IL-4 induction in both conventional Th2 cells and follicular helper T cells (Tfh) at d 5-6. Reconstitution of the B cell compartment in μMT mice restored papain-induced development of the Tfh and Th2 compartments. Mechanistic studies pointed to the inducible T cell costimulator (ICOS)/ICOS-Ligand (ICOS-L) pathway as central to this amplification. T cells strongly upregulated ICOS following papain immunization, peaking at d 5 post-immunization, and ICOS-L was expressed on B cells but not by DCs at this time point. T cell ICOS upregulation was partially dependent on B cells, as μMT mice showed normal increases in ICOS expression at d 3 but impaired upregulation on d 4-5 post-immunization. ICOS-L blockade with neutralizing mAb

inhibited IL-4 induction in wild type (WT) mice but did not further reduce the already diminished IL-4 induction in μMT mice. Our findings reveal innate uptake of papain by B cells and suggest that the B cell is the essential MHC-II^{+} auxiliary cell needed for a full primary Th2 response to cysteine protease immunization. The B cell acts at least partially through ICOS-L costimulation, which significantly augments DC-dependent Th2 and IL-4^{+} Tfh induction in response to cysteine protease immunization.

3.5 Materials and Methods

Mice

7 to 12 wk old C57BL/6J, μMT (B6.129S2-*Igh-6*^{tm1Cgn}/J, STAT6$^{-/-}$ (B6.129S2(C)-*Stat6*^{tm1Gru}/J), IL4$^{-/-}$ (B6.129P2-*Il4*^{tm1Cgn}/J), and MD4 (C57BL/6-Tg(IghelMD4)4Ccg/J) mice were obtained from The Jackson Laboratory (Bar Harbor, ME, stock #000664, 002288, 005977, 002253, and 002595, respectively), and maintained in-house at the Dana Farber Cancer Institute. CD21-cre (B6.Cg-Tg(Cr2-cre)3Cgn/J) and tdTomato (B6.Cg-Gt(ROSA)$^{26Sortm14(CAG-tdTomato)Hze}$/J) mice were obtained from The Jackson Laboratory (stock #006368 and 007914, respectively) and housed at Harvard Medical School. CR2$^{-/-}$ mice were housed at Harvard Medical School as previously reported (17). All mice were housed under specific pathogen free conditions, and the use of all mice for these studies was in accordance with institutional guidelines with review and approval by the Animal Care and Use Committee of the Dana Farber Cancer Institute.

Papain administration

Fifty ml of papain diluted to a concentration of 1 mg/ml (Sigma-Aldrich, St. Louis, MO) in HBSS were injected subcutaneously into the bilateral footpads on d 0, and the mice were sacrificed for harvest of the PLN at d 5 unless otherwise noted. For fluorescently labeled papain experiments, papain was labeled with either an AF647 or AF488 labeling kit (Life Technologies, San Diego, CA) according to the manufacturer's protocols and the labeling reaction was stopped using the optional hydroxylamine hydrochloride (Sigma-Aldrich) stopping step. Following labeling, samples were dialyzed for 18 h in 4 changes of HBSS in a Slide-A-Lyzer Dialysis Cassette (Thermo Scientific, Rockford, IL). Prior to injection, any remaining unreacted dye was removed using a Micro Bio-Spin 30 chromatography column (Bio-Rad, Hercules, CA). This process yielded a degree of labeling of approximately 5 moles fluorophores per mole papain. As a control, OVA (Sigma-Aldrich, St Louis, MO)) was labeled in parallel to a similar degree of labeling. For intravital microscopy, mice were injected with 10 ml papain at a concentration of 10 mg/ml.

Flow Cytometric analysis

Fluorescently conjugated mAb directed against the following epitopes (clone) were used for flow cytometric analysis: CD3 (17A2), CD4 (RM4-5), CD19 (6D5), MHC-II (M5/114.15.2), CD11c (N418), CD11b (M1/70), IL-4 (11B11), IFN-g (XMG1.2), FcεRI a (MAR1), CD49b (DX5), ICOS (7E.17G9), ICOS-ligand (HK5.3), CD80 (16-10A1), CD86 (GL-1), PD-1(RMP1-30), CXCR-5(L138D7). Staining with

each mAb was compared to an isotype-matched control using fluorescence minus one. All mAb were purchased from Biolegend.

Single-cell suspensions of spleen and LN were obtained by grinding tissues through 70-mm cell strainers (BD Biosciences, San Diego, CA) into HBSS supplemented with 2% heat-inactivated FBS. Nonspecific mAb binding was blocked with anti-CD16/32 (2.4G2) (BD Biosciences) for 10 min, and appropriate mAb were added for 30 min. Cells were analyzed on a FACSCanto II flow cytometer (BD Biosciences) using FACSDiva acquisition software. FlowJo software (Tree Star, Ashland, OR) was used for data analysis.

To assess intracellular cytokine production by $CD4^+$ T cells, LN cells were resuspended in culture medium supplemented with 10% FBS, L-glutamine, penicillin, streptomycin, gentamicin, HEPES buffer, sodium pyruvate, and 2-mercaptoethanol (Sigma-Aldrich). PMA and Ionomycin (Fisher Scientific) were added for 2 h, after which 1 mg/mL Brefeldin-A (BD Biosciences) was added for an additional 2 h. At this point, cells were harvested, spun down, stained for extracellular markers, fixed and permeabilized using a BD Cytofix/Cytoperm kit according to the manufacturer's protocol, and stained intracellularly for cytokine production. Gating to determine positive cytokine expression was set using samples stained with an isotype control antibody such that 0.1% of isotype control stained events fell in the positive gate.

Sublethal irradiation and bone marrow (BM) reconstitution

μMT mice were irradiated with a sublethal dose of 400 rad and injected i.v. with 10^6 WT BM cells after resting for 24 h. These reconstituted mice, along with non-irradiated μMT littermates and age-matched WT mice, were rested in the Dana Farber animal facility for 8 wks, after which they were immunized in the footpad with papain and their responses analyzed after 5 d.

Confocal Microscopy

PLN from mice immunized with AF647-labeled papain were isolated after 24 h and fixed in 4% paraformaldehyde for 4 h. Fixed PLNs were soaked in 30% sucrose overnight and then embedded in optimal cutting temperature compound for cryostat sectioning. To assess internalization of papain by follicular B cells in the PLN and ensure that only B cells were being analyzed, image sections were chosen based on the presence of B cells and the absence of immunofluorescent staining for macrophages or follicular DC. PLN sections were stained with the indicated mAb and imaged using standard confocal microscopy on an Olympus Fluoview FV1000 confocal microscope. Data was acquired by Olympus Fluoview 1000 software, and basic post-capture processing (brightness/threshold adjustment) was performed in Volocity. Fluorochromes used include Pacific Blue, DyLight405, AF488, FITC, AF568, PE, AF633, and APC. Lenses – Olympus 10x NA: 0.45; 20x NA: 0.7; 60x/W NA: 1.2.

Intravital Multiphoton Microscopy

C57BL/6 mice were given $5x10^6$ naïve B cells isolated from CD21-cre_tdTomato reporter mice by intravenous injection 24 h prior to imaging. Recipient mice were anesthetized with 2% isofluorane, and prepared on a surgical board for PLN live imaging. Exposed PLNs were monitored for physiological temperature maintenance, and imaged using a Zeiss-BioRad Radiance 2100 Multiphoton microscope. Data was acquired by LaserSharp 2000 software. All live imaging data was collected at 34 degrees C as assessed by a temperature probe at the exposed LN site. AF488-labeled papain was injected in the footpad at time point 0, and serial 150 micrometer (mm) depth captures (3 mm steps) were taken every 2 min for at least 60 min following papain injection. 4 dimensional data reconstruction was done using Volocity image analysis software, and subsequent 2-dimensional quantitation was processed using CellProfiler (http://www.cellprofiler.org/citations.shtml). Fluorochromes include Pacific Blue, AF488, and tdTomato. Lenses – Olympus XLUMPlanFl 20x/W NA: 0.95; Leica HC PL Fluotar 10x NA: 0.3.

mAb-mediated blockade

For inhibition of the ICOS/ICOS-L pathway, mice were injected on d 0 with 250 mg of anti-ICOS-L or the appropriate isotype control mAb (BioLegend, San Diego, CA). Mice were then injected in the footpad with papain, and cytokine production in the PLN was assessed after 5 d.

Statistical analysis

Data are expressed as the mean ± SD when derived from 3 or more values. Significance was determined with a two-tailed Student t test where 3 or more values were available for analysis. ANOVA was used to determine statistical significance for intravital microscopy experiments and MFI changes over time. The Pearson product-moment correlation coefficient was used to analyze association of papain with IgD or EEA-1. A p value of $< 0.05\%$ was considered to be significant.

3.6 Results

The majority of papain-binding cells in the PLN within the first 24 h following footpad injection are CD19$^+$ B cells, which subsequently internalize papain.

To determine which MHC-II$^+$ cells were interacting with papain following immunization, papain was labeled with the fluorophore AlexaFluor (AF) 647 and injected bilaterally into the hind footpads of mice. After 24 h, the mice were sacrificed and the draining PLN analyzed via flow cytometry. Analysis of all MHC-II$^+$ cells showed that slightly over 1% were positive for papain and, strikingly, the majority of these papain$^+$ MHC-II$^+$ cells were CD19$^+$ B cells (Figure 3.1A). The remaining papain$^+$, MHC-II$^+$ cells consisted of a mixture of CD11c$^+$ and CD11c$^+$, CD11b$^+$ DC and CD11b$^+$ macrophages (data not shown). Although Ba (CD49b$^+$, FcεRI a$^+$) have been previously reported to act as APC in the papain model (9), and were present in the spleen at baseline and 1 day after immunization, they lacked labeled papain despite the presence of papain+ B cells and DC in the spleen at this time

point (Supplemental Figure 3.1A). No Ba were present in the PLN at day 1 but they were present in the PLN at day 3 following immunization. Again no detectable Ba were carrying labeled papain despite both B cells and DC being papain+ (Supplemental Figure 3.1B).

As this uptake of papain by B cells was both substantial and unexpected, we compared papain uptake to that of labeled OVA, using unlabeled papain as a control. A significant percentage of B cells, 1.48%, were positive for labeled papain at 24 h, while only 0.19% of B cells were positive for OVA, a non-significant increase over unlabeled controls (Figure 3.1B, C). This B cell acquisition of papain could be observed as early as 1 h post-immunization, at which point B cells made up the vast majority of papain$^+$ cells in the PLN (Figure 3.1D).

The B cell preference for papain uptake over OVA suggested that papain acquisition occurred in a manner not mediated by the specificity of the BCR. To confirm this, papain uptake by B cells from WT mice was compared to that of B cells from transgenic MD4 mice, of which 98% carry a BCR specific for HEL (18). MD4 mice also readily acquired papain 1 h after immunization (Figure 3.1E), and no significant difference in papain uptake was observed between WT and MD4 mice (Figure 3.1F). There was also no difference in papain uptake between B cells from WT mice and B cells from mice lacking complement receptor 2 (CR2), another mechanism through which B cells have been reported to acquire Ag (19) (not shown).

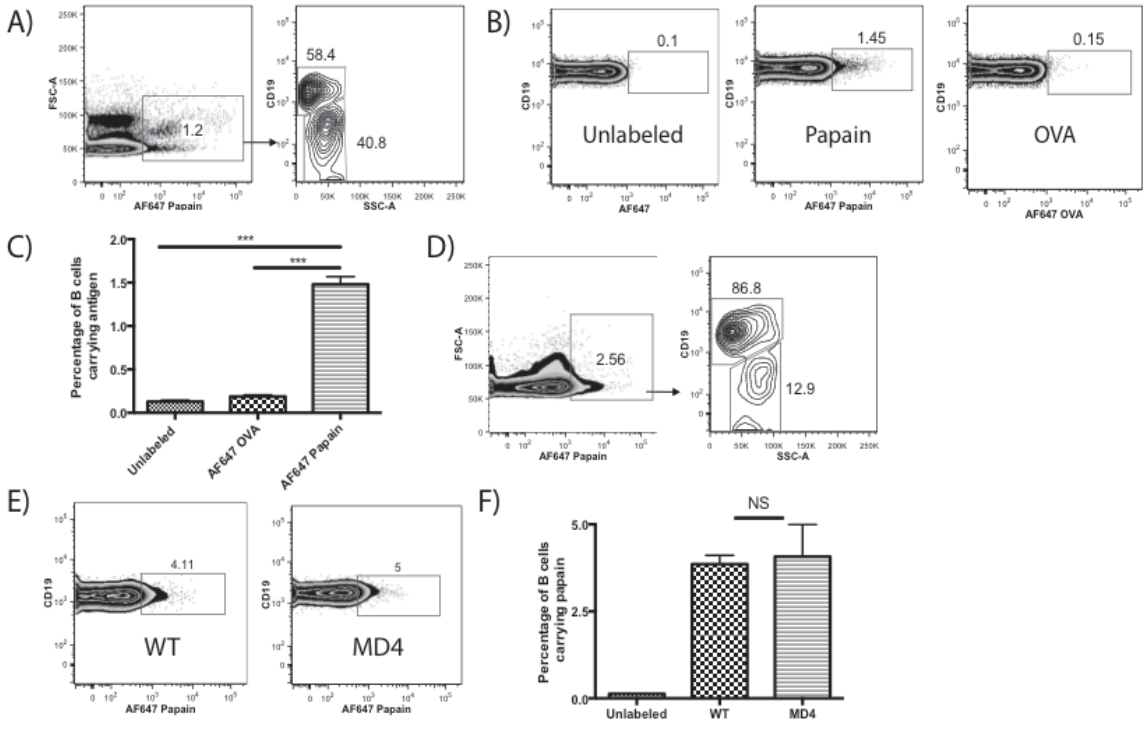

Figure 3.1. CD19⁺ B cells are the major Ag-bearing cell type in the PLN 24 h after footpad injection of papain and acquire papain in a non-BCR mediated manner. **(A)** Representative FACS plots of mice injected in the footpad with 50 mg AF647-labeled papain and sacrificed after 24 h. After gating on MHC-II⁺ cells, cells positive for papain (left panel) were phenotyped, showing that CD19⁺ cells constituted the majority of AF647⁺ cells at 24 h (right panel). **(B)** Representative FACS plots of CD19⁺ B cells from WT mice 24 h after injection with unlabeled papain, AF647-labeled papain, or AF647-labeled OVA. **(C)** Quantification of percentages of B cells binding AF647-labeled Ag compared to unlabeled papain controls as described in B. Bars indicate mean ± SD obtained from 2 experiments with n=3 mice per group experiment, *** indicates $p<0.001$. **(D)** Representative FACS plots of PLN cells from WT mice injected with AF647-labeled papain as described in (A) and analyzed after 1 h. **(E)** Representative FACS plots of B cells from WT and MD4 transgenic mice 1 h

(Figure 3.1, Continued) after injection with AF647-labeled papain. **(F)** Quantification of the percentages of WT and MD4 B cells acquiring AF647-labeled papain as described in (E). Bars indicate mean ± SD obtained from 2 experiments with n=3 mice per group per experiment, NS indicates no significant difference.

We then confirmed B cell acquisition of papain with confocal microscopy. AF647-labeled papain was readily observable in the B cell follicle, colocalizing with B cells in a punctate pattern suggesting the Ag might be in vesicles (Figure 3.2A). To assess whether this pattern indicated internalization of papain by follicular B cells, C57BL/6 mice were injected with AF647-labeled papain in the footpad and the PLNs were harvested and fixed for imaging 24 h following injection. Initial experiments showed that AF647-labeled papain appeared to co-localize with the early endosomal marker endosomal Ag-1 (EEA-1) (20) (Figure 3.2B). This was confirmed by measuring the correlation of the papain signal with EEA-1 versus a general correlation with the B cell membrane, identified using anti-IgD. This revealed a significantly higher correlation with the endosomal marker, indicating that papain in these regions was internalized into endosomes by resident B cells (Figure 3.2C). As papain uptake was not dependent on either CR2 or BCR Ag specificity, this uptake and internalization of a cysteine protease represents a novel innate mechanism of B cell uptake of an allergenic Ag.

Intravital microscopy reveals B cell uptake of papain within minutes following footpad injection

We next used multiphoton intravital microscopy to observe the *in situ* uptake of labeled papain by B cells. To mark the B cells *in vivo*, fluorescently labeled B cells from CD21-cre_tdTomato reporter mice were adoptively transferred into C57BL/6 mice, and 24 h later the mice were injected in the right footpad with AF488-labeled papain. The uptake of papain by tdTomato$^+$ B cells in the PLN was monitored every 2 min for 60 min following injection (Figure 3.2D). The assayed PLN region was bathed in papain within minutes following footpad injection, suggesting Ag entry into the PLN via the conduit network. Overall papain intensity within the PLN increased over time, beginning as early as 10 min and peaking between 30 and 40 min (Figure 3.2E & supplemental movie 3.1). At the same time there was also an increase in papain uptake by individual B cells, reaching a plateau at 40 min and remaining constant at this level for the duration of the experiment (Figure 3.2F). An analysis of all tdTomato$^+$ cells determined that 60% of imaged cells were positive for papain using this technique (Figure 3.2G). An in depth analysis of this response is shown in supplementary Figure 3.2.

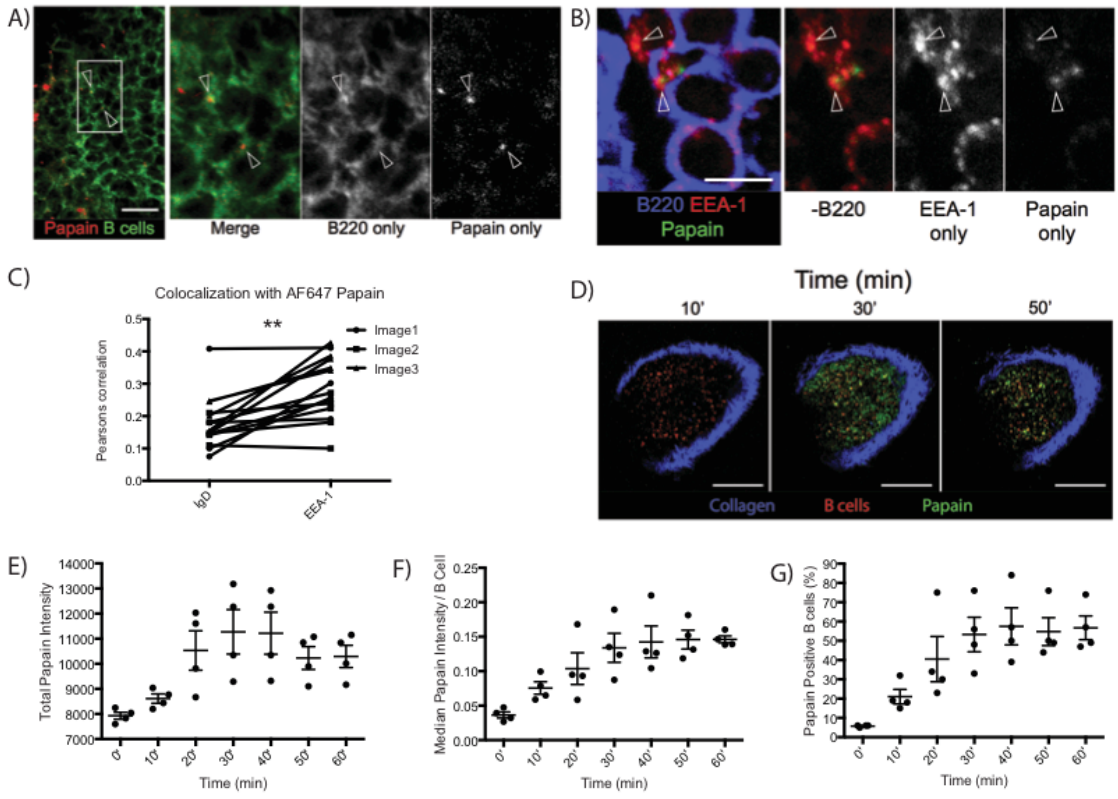

Figure 3.2. Confocal and intravital microscopy reveal that PLN B cells rapidly acquire and subsequently internalize papain after footpad immunization. **(A)** Confocal microscopy indicating colocalization of B cells and AF647-labeled papain at 24 h post-immunization. Green indicates B220, red indicates AF647-labeled papain. Arrows indicate points of colocalization between B220 and AF647-papain. White bar indicates 14 mm. **(B)** Confocal microscopy showing colocalization of AF647-papain and the early endosomal marker EEA-1 in B cells 24 h post-immunization. Blue indicates B220, green indicates AF647-papain, and red indicates EEA-1. Arrows indicate colocalization between EEA-1 and AF647-papain on B220$^+$ B cells, and white bar indicates 5 mm. **(C)** Pearson's correlation comparing the colocalization of AF647-labeled papain with the B cell surface marker IgD versus the early endosomal marker EEA-1, ** indicates $p<0.01$. **(D)** Representative images at a depth

(Figure 3.2, continued) of 30 mm taken from a time course of AF647 uptake by adoptively transferred CD21-cre_tdTomato B cells in PLN of C57BL/6 mice captured at the indicated time points. AF488-papain was injected into the footpad and the PLNs were live-imaged using intravital-multiphoton microscopy. Blue indicates collagen, green indicates papain, and red indicates B cells. White bar indicates 100 mm. **(E)** Time course of total papain intensity in the PLN expressed as median of 4 depths captured as described in (D). Line and error bars indicate mean ± SD, ANOVA $p<0.001$. **(F)** Time course of median papain intensity of CD21-cre_tdTomato cells from the images in (D). Line and error bars indicate mean ± SD, ANOVA $p<0.0005$. **(G)** Time course indicating the percentage of $CD21^+$ cells identified as described in (F) positive for papain. Line and error bars indicate mean ± SD, ANOVA $p<0.0005$.

B cell-deficient μMT mice show no reduction in T cell expansion but markedly reduced induction of $CD4^+$, $IL4^+$ T cells in the PLN following papain immunization

Having identified a previously unreported uptake of papain by B cells, we hypothesized that there may be a role for B cells in the integrated primary PLN immune response in WT mice. Thus, we compared the PLN response in WT mice to that in B cell-deficient μMT mice, which lack mature B cells. In WT mice, both $CD19^+$ B cell and $CD4^+$ T cell expansion peaked between d 4 and 5 post-papain immunization (Figure 3.3A) As PLN hypertrophy could be seen as early as several h following immunization, this peak expansion likely reflected a combination of lymphocyte recruitment and subsequent adaptive proliferation. Despite lacking B

cells, μMT mice showed no reduction in CD4+ T cell numbers at the d 5 peak (Figure 3.3B). At d 4 post-immunization there was no difference in T cell IL-4 expression by CD4+ T cells from WT mice (1.3%) and μMT mice (1.4%) (Figure 3.3C). At d 5 post-immunization, CD4+, IL-4+ T cells increased to a mean of 3.3% in WT mice, similar to the peak levels of CD4+, IL-4+ T cells seen during primary responses to bee venom (21) as well as in OVA immunization using papain as an adjuvant or hookworm infection (10); representative plots from d 5 are shown (Figure 3.3D). However, there was no increase in the percentage of CD4+, IL-4+ T cells in μMT mice between d 4 and 5, with a mean of 1.1% at d 5. At 6 d post-immunization, the percentage of CD4+ T cells expressing IL-4 declined in both strains, to 2.1% in the WT and 0.61% in the μMT. Thus, while B cells did not influence CD4+ T cell expansion following papain immunization, they profoundly amplified IL-4 induction in this cell population.

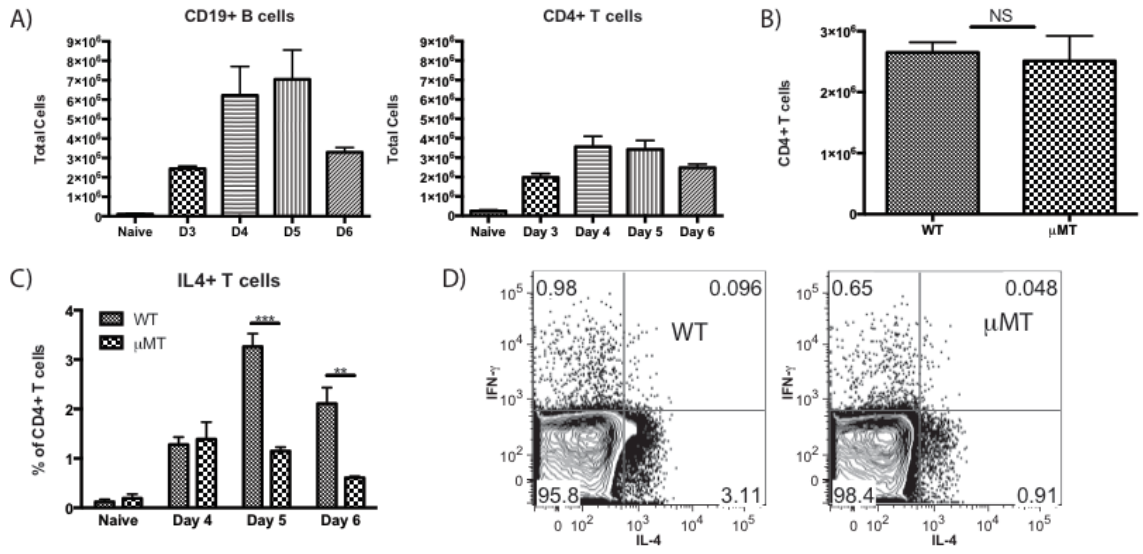

Figure 3.3. B cell deficient μMT mice show no difference in papain-induced T cell expansion but have a marked reduction in CD4+ T cell IL-4 production. **(A)** Total

(Figure 3.3, continued) number of $CD19^+$ B cells and $CD4^+$ T cells in the PLN from naïve mice or papain immunized WT mice 3-6 d post-immunization. Bars indicate mean ± SD from 2-3 independent experiments per time point with n=3 mice per group per experiment. **(B)** Comparison of $CD4^+$ T cell numbers in the PLN at d 5 following papain immunization in WT and μMT mice. Bars indicate mean ± SD from 3 independent experiments with n=3 mice per group. **(C)** Time course showing the percentage of IL-4 expressing PLN $CD4^+$ T cells from naive and papain-injected WT and μMT mice at d 4-6 following papain immunization. Bars indicate mean ± SD from 2-4 independent experiments per time point with n=3-4 mice per group per experiment, NS indicates no significant difference, ** indicates $p<0.01$, *** indicates $p<0.001$. **(D)** Representative plots showing the percentages of IL-4 and IFN-g expressing $CD4^+$ T cells from WT and μMT mice 5 d after papain immunization.

μMT mice show impaired papain-induced Th2 and Tfh cell induction, which is restored through B cell reconstitution

As both effector Th2 cells and Tfh cells are $CD4^+$ T cells capable of producing IL-4, we evaluated the effects of B cell deficiency on each of these compartments. Follicular helper T cells express high levels of the chemokine receptor CXCR5 and the T cell activation marker programmed cell death protein-1 (PD-1) (22) while conventional effector Th2 cells express IL-4 but lower levels of CXCR5 (23). $PD\text{-}1^{hi}$, $CXCR5^{hi}$ Tfh were readily detectable in both WT and μMT mice. IL-4 expression by both Tfh and effector Th2 cells could be observed in both strains, but the induction of IL-4 was reduced in both populations in the absence of B cells (Figure 3.4A). The

expansion of Tfh was also reduced by ~3 fold in μMT (Figure 3.4B), consistent with previous reports in other models showing a B cell dependence for the expansion of Tfh cells (24). In WT mice, effector Th2 cells represented 2.3% of $CD4^+$ T cells and IL-4^+ Tfh cells represented 1% of CD4+ T cells (Figure 3.4C). In the μMT strain, these $CD4^+$ T cell compartments were reduced to 0.65% for Th2 cells and only 0.14% for IL-4^+ Tfh. This represented a 3.5 fold reduction in Th2 cells and a 7-fold reduction in IL-4^+ Tfh in the absence of B cells. Thus, B cell deficiency suppressed both expansion and IL-4 induction in Th2 effector and Tfh cells.

Figure 3.4. μMT mice show impaired Tfh generation and reduced IL-4 induction by both Th2 and Tfh cells. **(A)** Representative FACS plots showing the induction of Tfh ($PD1^{hi}$, $CXCR5^{hi}$) and IL-4 expression by Tfh and conventional T cells ($CXCR5^{lo}$) in (Figure 3.4, continued) WT and μMT mice immunized in the footpad with papain 5 d earlier. **(B)** Quantification of total Tfh as a percentage of all $CD4^+$ T cells in WT and μMT mice on d 5 post-papain immunization. Bars indicates mean ± SD from 2 independent experiments with n=3 mice per group per experiment, *** indicates $p<0.001$. **(C)** Comparison of effector Th2 cells (IL-4^+, CXCR5 low) versus IL-4^+ Tfh cells ($CXCR5^{hi}$, PD-1^{hi}, IL-4^+) as a mean percentage of all $CD4^+$ T cells in WT and μMT mice 5 d post-immunization, calculated by multiplying the percentage of $CD4^+$ T cells represented by $CD4^+$ effector or Tfh cells (left panels in A) by the fraction of each population expressing IL-4 (center and right panels in A). Bars indicate mean ± SD from 2 independent experiments with n=3 mice per group per experiment, *** indicates $p<0.001$.

(Figure 3.4, Continued)

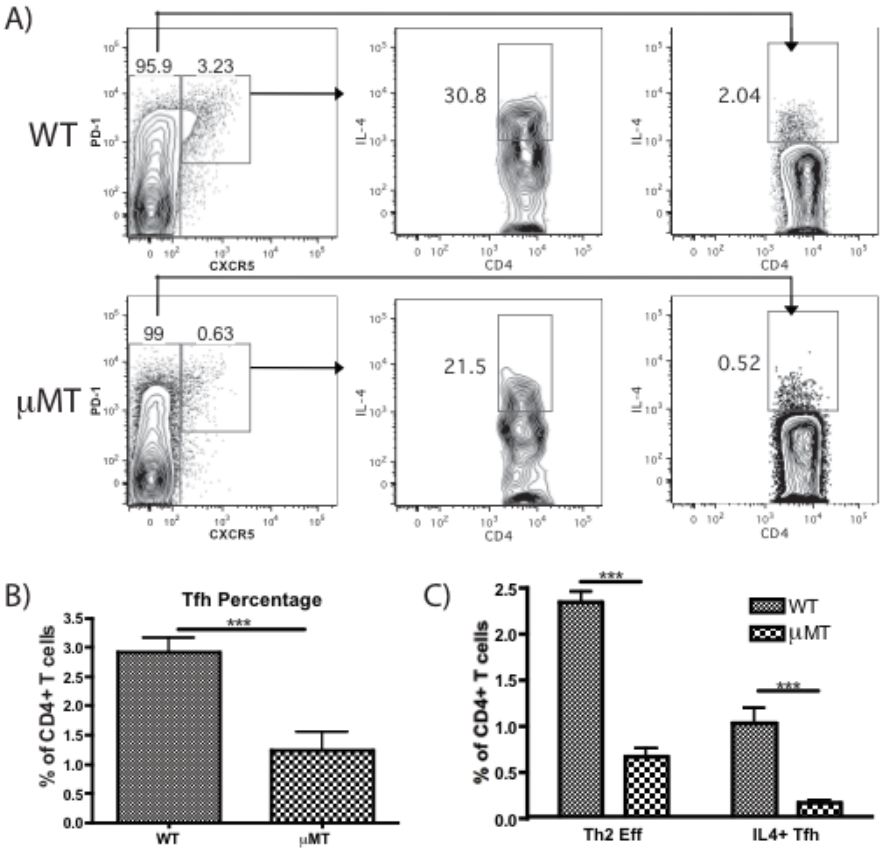

To assess whether the B cell deficiency accounted for these findings, the B cell compartment in μMT mice was restored via sublethal irradiation followed by adoptive transfer of WT BM. After 8 wks, the B cell compartment in both the spleen and PLN was restored to near-WT levels (Supplementary Figure 3.2). Reconstitution of μMT mice restored papain-induced Tfh expansion (Supplementary Figure 3.3A, B), Tfh IL-4 production and Th2 polarization to levels comparable to WT mice (Supplementary Fig 3.3 A, C). Similar results were obtained using lethal irradiation of μMT mice followed by reconstitution with WT BM (not shown).

Papain immunization induces STAT-6-dependent upregulation of MHC-II and CD86 expression by PLN B Cells.

Based on the finding that B cells acquire papain and are important regulators of papain-induced Th2 and Tfh responses, we evaluated MHC-II and CD86 expression on B cells as these proteins are essential to Ag presentation. MHC-II was strongly expressed on naïve B cells and steadily increased in expression between d 3 and d 5, at which point expression had increased 2.7 fold over naïve levels (Figure 3.5A). CD86 expression was barely detectable on naive B cells, increased in expression on d 3-4 post-immunization and reached a peak on d 5 (Figure 3.5B). In both cases this reflected increased expression on most or all B cells in the PLN. Expression of B cell activation markers peaked on the same day as the numbers of IL-4^{+}, CD4^{+} T cells in WT mice.

Despite the fact that less than 2% of B cells were positive for labeled papain at 24 h (Figure 3.1B) and B cells greatly expand between d 0 and d 5 (Figure 3.3A), all B cells in the PLN on d 5 exhibited robust upregulation of MHC-II and CD86 (Figure 3.5A, B), suggesting a soluble signal was responsible. We thus evaluated whether this B cell activation was IL-4 dependent by comparing the MHC-II and CD86 upregulation on B cells from papain immunized WT and STAT6$^{-/-}$ mice, which are unable to respond to IL-4 signaling. STAT6$^{-/-}$ mice immunized with papain showed no increase in these activation markers over naïve levels (Figure 3.5C). The same results were observed in IL-4$^{-/-}$ animals (Figure 3.5D), confirming that PLN B cell MHC-II and CD86 upregulation following papain immunization is an IL-4 dependent process.

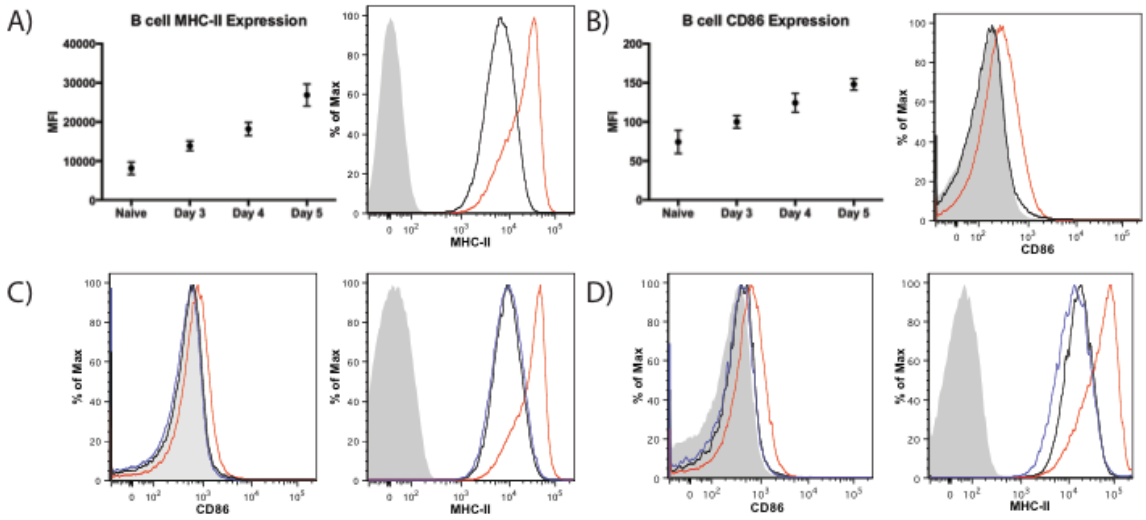

FIGURE 3.5. Papain immunization increases expression of MHC-II and CD86 on PLN B cells in a STAT6 and IL-4 dependent manner. **(A)** Time course of B cell MHC-II MFI in naïve mice and in papain immunized mice 3-5 d post-papain immunization and representative histogram showing B cell MHC-II expression in naïve animals (black) and in mice immunizated with papain 5 d prior (red) compared to isotype control staining (grey). Points indicate mean ± SD and data was obtained from 2 independent experiments with n=3 mice per group per experiment, ANOVA $p<0.0001$. **(B)** Time course of B cell CD86 MFI in naïve mice and in mice at d 3-5 post-papain immunization and representative histogram showing B cell CD86 expression in naïve animals (black) and in mice immunized with papain 5 d prior (red) compared to isotype control staining (grey). Points indicate mean ± SD and data was obtained from 2 independent experiments with n=3 mice per group per experiment, ANOVA $p=0.0001$. **(C)** Representative histograms indicating B cell expression of CD86 (left panel) and MHC-II (right panel) in naïve animals (black)

(Figure 3.5, continued) and in WT (red) and STAT6$^{-/-}$ (blue) mice 5 d post-papain immunization compared to isotype control staining (grey). **(D)** Representative histograms indicating B cell expression of CD86 (left panel) and MHC-II (right panel) in naïve animals (black) and in WT (red) and IL-4$^{-/-}$ (blue) mice 5 d post-papain immunization compared to isotype control staining (grey).

ICOS-L is expressed on B cells but not DC and ICOS is strongly upregulated on CD4$^+$ T cells at d 4-6 following papain immunization of WT Mice

Due to the observed upregulation of MHC-II and CD86 on PLN B cells, we considered whether a TCR-dependent costimulatory signal might contribute to the IL-4$^+$ T cell response. As the costimulatory ligand ICOS-L on APC and ICOS on CD4$^+$ T cells has previously been associated with CD4$^+$ IL-4 induction (25), expression of this costimulatory pair on B cells and T cells was assessed. ICOS-L was present on naïve B cells in the PLN at baseline, persisted to d 3-4 post-papain immunization and then decreased on d 5 post-immunization (Figure 3.6A), suggesting an interaction with ICOS (26). ICOS-L was not expressed on PLN DC at the peak of T cell IL-4 induction (Figure 3.6B). We observed a slow, steady increase in the percentage of CD4$^+$ T cells expressing ICOS between d 0 and 3 in both WT and μMT mice, with 17% of T cells expressing ICOS at this time point in both strains (Figure 3.6C). Between d 4 and 5 there was a significant increase in ICOS expression on CD4$^+$ cells from WT mice such that 40% of CD4$^+$ cells in the LN were ICOS positive at d 5. This increase was significantly blunted in μMT mice, with 26% of CD4$^+$ T cells expressing ICOS at the d 5 peak. By d 6, expression began to decline in both WT and μMT mice,

with WT mice maintaining higher expression than μMT animals. Unlike the uniform changes in B cell MHC-II and CD86 expression (Figure 3.5), the changes in ICOS expression involved only a subset of CD4⁺ T cells (Figure 3.6D). Taken together, the impaired responses for the μMT strain imply a B cell role in the incremental T cell ICOS expression and Th2 polarization seen in WT mice.

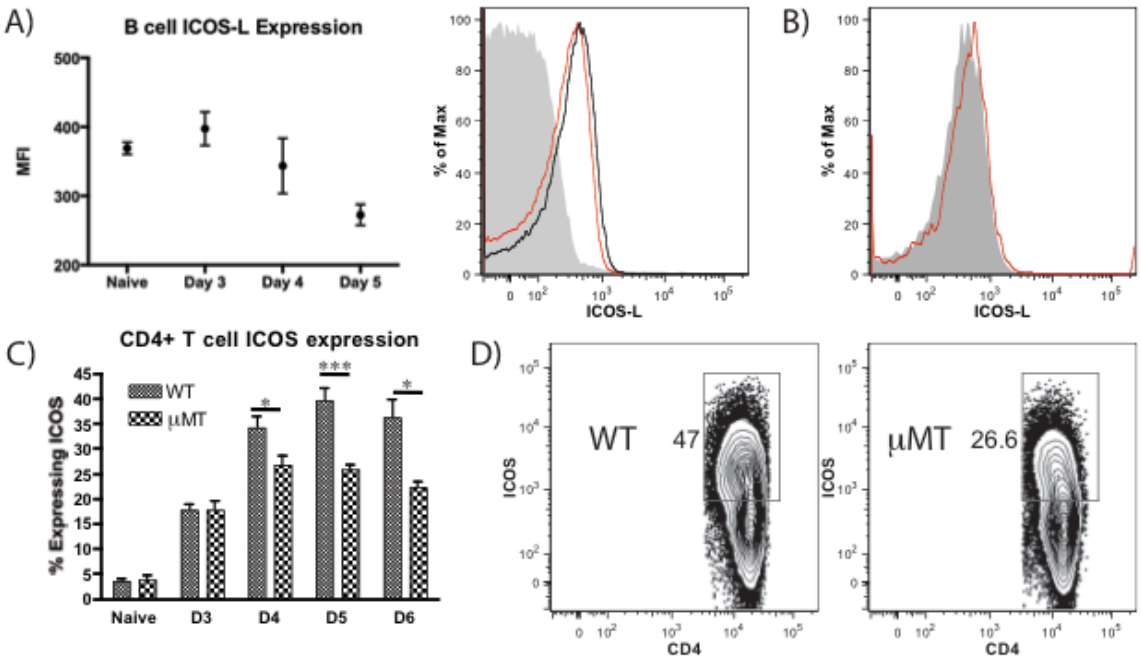

Figure 3.6. PLN B cells express ICOS-L and μMT mice show impaired ICOS upregulation on PLN CD4⁺ T cell after papain immunization. **(A)** Time course of B cell ICOS-L MFI in the PLN of naïve mice and papain-immunized mice 3-5 d post-immunization and representative histogram indicating B cell ICOS-L expression in naïve animals (black) and in mice immunization with papain 5 d prior (red) compared to isotype control staining (grey). Points indicate mean ± SD from 2 independent experiments, n=3 mice per group per experiment. ANOVA $p<0.05$. **(B)**

(Figure 3.6, continued) Representative histogram indicating ICOS-L expression on MHC-II$^+$ CD11c$^+$ DC in mice immunized with papain 5 d previously. Red indicates ICOS-L staining and grey indicates isotype control. **(C)** Time course showing the percentage of ICOS-expressing PLN CD4$^+$ T cells in WT and μMT mice 3-6 d following papain immunization. Bars indicate mean ± SD from 2-3 experiments per time point with n=3 mice per group per experiment. * indicates $p<0.05$, *** indicates $p<0.001$ **(D)** Representative FACS plots of CD4$^+$ T cell ICOS expression in WT and μMT animals 5 d post-immunization, indicating that ICOS upregulation occurs in a subset of T cells.

Monoclonal antibody blockade of ICOS-L inhibits induction of Th2 and Tfh cells in WT but not μMT mice

The findings that ICOS expression and IL-4 induction on CD4$^+$ T cells peaked at d 5 at the same time that B cell MHC-II and CD86 expression peaked and ICOS-L expression declined suggested that ICOS-ICOS-L costimulation could be a mechanism through which B cells influenced papain-induced IL-4 induction. Thus, the functional importance of ICOS-L in papain-induced Th2 polarization was assessed by mAb blockade. WT and μMT mice were injected i.p. with an anti-ICOS-L neutralizing mAb or the appropriate isotype-matched control IgG on d 0 followed by subcutaneous administration of papain into the footpads and analysis of the PLN by cytometry 5 d later. In WT mice, ICOS-L blockade suppressed both the generation of Tfh and their IL-4 production (Figure 3.7A, C), consistent with previous findings establishing the central role of ICOS/ICOSL interactions in the generation of Tfh

(27). ICOS-L blockade also suppressed the generation of Th2 cells in WT mice (Figure 3.7A, D), indicating a role for either ICOS-L or ICOS-L-responsive cells in the generation of Th2 cells. ICOS-L blockade did not further reduce the already impaired generation of Tfh and Th2 responses in μMT mice (Figure 3.7B, D). While ICOS-L blockade significantly impaired both Th2 and Tfh responses, it did not reduce Tfh generation in WT mice to μMT levels (Figure 3.7C), nor did it fully reduce IL-4 production by either Tfh or Th2 cells (Figure 3.7D).

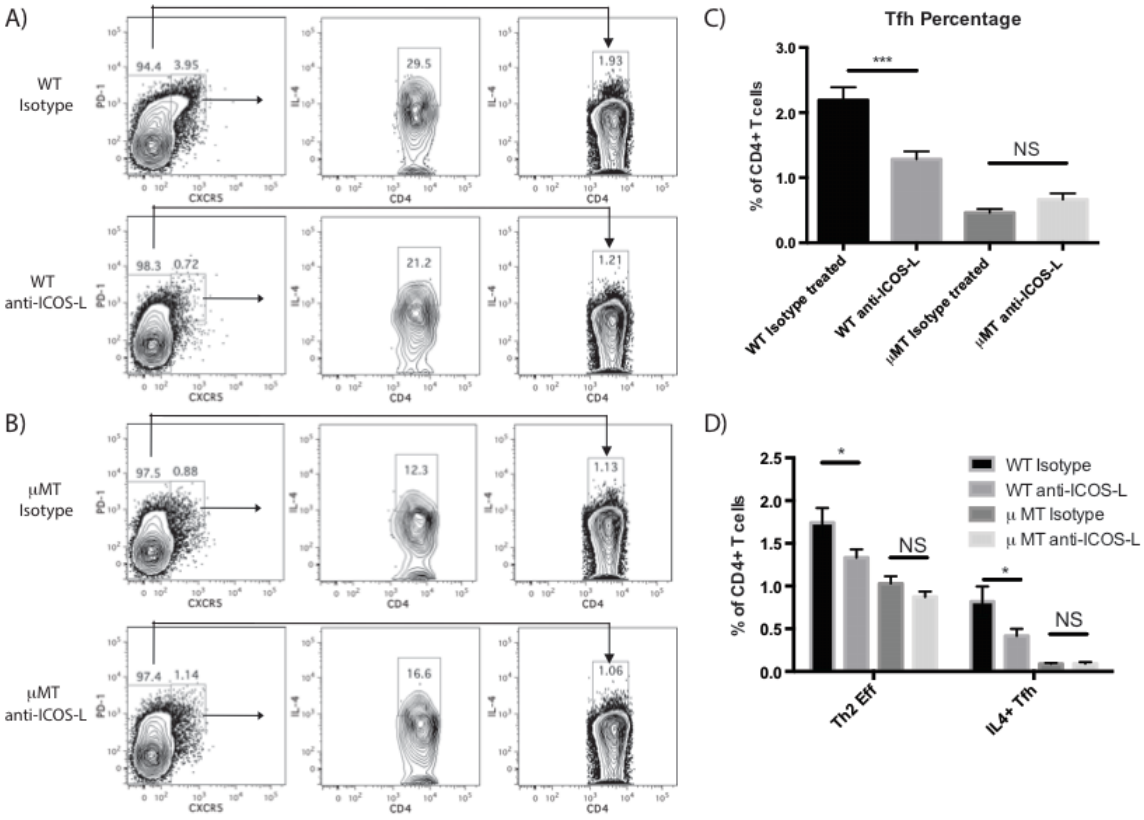

Figure 3.7. mAb blockade of ICOS-L markedly reduces Tfh expansion and IL-4 production by Th2 and Tfh cells following papain immunization in WT but not in μMT mice 5 d post-immunization. **(A)** Representative FACS plots showing the

(Figure 3.7, continued) induction of Tfh cells ($PD1^{hi}$, $CXCR5^{hi}$) and IL-4 expression 5 d post-papain immunization by Tfh and conventional $CD4^+$ T cells ($CXCR5^{lo}$) in WT mice injected i.p. with either isotype control antibody or anti-ICOS-L mAB on d 0. **(B)** Representative FACS plots showing the induction of Tfh and IL-4 expression 5 d post-papain immunization by Tfh and conventional T cells in μMT mice injected i.p. with either isotype control antibody or anti-ICOS-L mAb on d 0. **(C)** Quantification of total Tfh as a percentage of all $CD4^+$ T cells 5 d post-papain immunization in WT and μMT mice injected with either isotype control antibody or anti-ICOS-L. Bars indicate mean ± SD of n=2-3 independent experiments with 3-4 mice per experiment, *** indicates $P<0.001$, NS indicates no significant difference. **(D)** Comparison of effector Th2 cells ($IL\text{-}4^+$, $CXCR5^{lo}$) vs $IL\text{-}4^+$ Tfh cells ($CXCR5^{hi}$, $PD\text{-}1^{hi}$, $IL\text{-}4^+$) as a mean percentage of all $CD4^+$ T cells 5 d post-papain immunization in WT mice injected with either isotype control antibody or anti-ICOS-L. Bars indicate mean ± SD of n=2-3 independent experiments with 3-4 mice per experiment, * indicates $P<0.05$.

3.5 Discussion

We initially examined the papain footpad model because cysteine proteases are components of several common allergens, including house dust mite (2) and grass pollen (1), and there was controversy in the literature as to the involvement of a second cell ancillary to the DC in maximizing the Th2 response to papain in the PLN (9, 11, 12). Furthermore, this model allows a unique opportunity to analyze the cellular events involved in a primary Th2 response in the draining LN to a cysteine

protease Ag with Th2 adjuvant activity (8, 28) through direct assays over a 6 d time period.

We began in an unbiased fashion by injecting naïve mice with fluorescently labeled papain to identify interacting cells that might drive or regulate Th2 polarization. The majority of cells taking up papain in the PLN were B cells by flow cytometric analysis and the percentage of B cells positive for papain was strikingly high compared to OVA uptake, suggesting an innate reaction to the protease activity rather than cognate-specific uptake directed by the BCR. This was confirmed through experiments with the HEL BCR transgenic mouse that revealed papain uptake was unaltered by the HEL specificity of the BCR. Furthermore, after acquiring papain the B cells internalized the Ag and directed it to endosomes. This uptake of papain was not mediated by CR2, another BCR-independent pathway through which B cells have been shown to acquire Ag (19). Intravital multiphoton microscopy highlighted that B cells proximal to the subcapsular sinus rapidly acquired papain from lymphatic flow following immunization, both confirming the flow cytometry findings and adding evidence for a direct mechanism of uptake. Thus, our initial findings recognized a novel innate mechanism through which B cells acquire a cysteine protease Ag.

Although the papain model of Th2 inflammation has been used by numerous groups over the past several years, there is uncertainty regarding the receptors and cell types driving the immune response to papain. However, the proteolytically active site of papain is required for it's immunogenicity, as both heat inactivation and treatment with a specific cysteine protease inhibitor eliminate the immune

responses against papain (8). Liang et al. showed that papain can activate naïve T cells through protease activated receptor (PAR)-2 cleavage, leading to T cell production of cytokines and chemokines (29). As PAR-2 expression by B cells has also been reported (30), papain could be stimulating B cell capture and internalization through a similar mechanism. Additionally, papain's ability to cleave immunoglobulin into Fc and Fab regions has been long established (31), raising the possibility that active site interactions with non-Ag-specific regions of the BCR could lead to internalization. Additionally, other surface proteins found on the B cell such as CD23 can be cleaved by papain-family cysteine proteases such as DerP1 (32).

A comparison of the cellular events leading to IL-4 induction in PLN $CD4^+$ T cells in WT and μMT mice revealed a previously undescribed role for B cells in this process. B cell-deficient mice showed significantly reduced percentages of $IL\text{-}4^+$, $CD4^+$ T cells in the PLN at the d 5 peak of the papain immune response but had no impairment in overall T cell expansion. This deficit in the level of $IL\text{-}4^+$ $CD4^+$ cells represented both a reduction in effector Th2 cell generation and in Tfh expansion and decreased induction of IL-4 in these populations. Restoration of the B cell compartment in μMT mice restored both Th2 and Tfh responses, highlighting the important role for B cells in each compartment.

The finding that B cell upregulation of MHC-II and CD86 are both IL-4 and STAT6-dependent processes strongly suggested a role for Tfh cells in the observed B cell activation. These cells generate IL-4 *in situ* in the B cell follicle (33, 34) and this cytokine was previously described to induce upregulation of both MHC-II and CD86 on B cells (35). As the generation of both $IL\text{-}4^+$ Tfh and Th2 effector cells was

impaired in the absence of B cells, B cells and Tfh play a reciprocal role in activating each other during the immune response to papain, consistent with other findings regarding the interplay between these two cells (36). This interplay is likely necessary for the simultaneous B cell amplification of Th2 polarization, as B cell activation is greatly impaired in STAT6$^{-/-}$ and IL-4$^{-/-}$ mice and B cell costimulatory enhancement of Th2 polarization likely depends on presentation of papain on MHC-II in the context of CD86 and ICOS-L.

While IL-4 is canonically required for optimal Th2 polarization, ligation of costimulatory molecules on the T cell surface can also modulate Th2 polarization. CD86 blockade during leishmania infection can inhibit pathogen-induced Th2 polarization, skewing the immune response to a Th1 phenotype and improving host clearance of the pathogen (37). ICOS ligation on naïve CD4^{+} T cells in conjunction with a TCR signal enhances IL-4 and IL-10 production while inhibiting IL-2 production (25). CD4^{+} cells from mice deficient in ICOS and immunized with KLH and alum show defective IL-4 production following restimulation with KLH, and the in vivo IgE and IgG1 responses in these mice are also impaired (38). Signaling through both ICOS and CD28, the ligand of CD86, is necessary for full Th2 polarization in a model of *S. mansoni* egg Ag-induced airway inflammation (39), suggesting that B-7 family members and ICOS act together to potentiate Th2 polarization. Neither the latter study nor several others examining ICOS-mediated Th2 polarization identified the source of ICOS-L expression (38, 40).

In the papain model, ICOS-L expression on B cells increased modestly but not significantly at d 3-4 before decreasing at d 5, and expression of this costimulatory

receptor was not observed on DCs or any other APC in the PLN during the d 5 peak of the IL-4 response. ICOS upregulation on $CD4^+$ T cells was significantly reduced in μMT mice compared to WT mice at d 4-6 post-papain immunization, with the largest differences occurring during d 5-6, when IL-4 production was also profoundly impaired. These findings suggested a potential link between the ICOS/ICOS-L pathway and subsequent B cell-dependent IL-4 production by LN $CD4^+$ T cells. Supporting this link, administration of an ICOS-L blocking mAb reduced IL-4 production in WT mice but did not further reduce the already impaired Th2 polarization in μMT mice.

While the role of ICOS in supporting the generation of Tfh cells is well characterized (24), its role in supporting effector Th2 polarization is more controversial (41, 42). ICOS-L blockade impaired Th2 polarization in addition to suppressing Tfh responses to papain. Thus, our results support a role for this pathway in the generation of both cell types. However, ICOS-L inhibition did not fully reduce WT Th2 or Tfh responses to the levels seen in the μMT. This could indicate either incomplete inhibition of ICOS-L or point to other pathways also playing an important role in B cell support of Th2 and Tfh responses. The magnitude of the difference in ICOS upregulation in the absence of B cells (<2 fold) was modest compared to the impact on IL-4 induction (~3 fold), further highlighting the effect of B cells on optimizing the Th2 and Tfh responses in this model. Importantly, this pathway acts subsequent to an early DC-dependent event that initiates the development of each cell type as some level of Tfh and Th2 effector cells can be seen in the absence of B cells.

While no studies thus far have posited a role for B cells in papain-induced Th2 polarization, several studies have highlighted a role for B cells in supporting Th2 polarization in parasite infection models. B cell-deficient JHD mice infected with *S. mansoni* exhibit impaired $CD4^+$ T cell IL-4 and IL-10 production accompanied by increased IFN-g and IL-12 generation compared to WT mice, indicating a role for B cells in influencing the Th1/Th2 balance in this model (43). Furthermore, μMT mice infected with *N. brasiliensis* have greatly impaired IL-4 secretion by $CD4^+$ cells, indicating a B cell-dependent Th2 polarization in another infection model (44). The surface costimulatory receptors CD80 and CD86 are central to this B cell-dependent T cell polarization, as reconstitution of B cell-deficient mice with WT B cells restores Th2 polarization while reconstitution with CD80 and CD86 deficient B cells does not. Adoptive transfer of IL-4-deficient B cells fully reconstitutes the Th2 response, showing that B cell production of IL-4 is not a relevant mechanism (44). A role for B cells was also identified in coordinating the colocalization of $CXCR5^+$ DC and both Tfh and Th2 cells during *H. Polygyrus* infection, thereby enhancing IL-4 production by each T cell subset (23).

In summary, our results indicate that during the allergic response to papain, draining LN resident B cells rapidly acquire cysteine protease Ag directly from lymphatic flow following immunization via an innate mechanism dependent on its protease activity and subsequently internalize the Ag. They are later joined by peripheral migratory DC carrying the protease from the site of immunization. The DC plays a major early role in the LN response, likely driving the expansion of the $CD4^+$ T cell population and mediating initial IL-4 induction and expansion of B cells

in the LN. These activated B cells enhance $CD4^+$ T cell ICOS expression beginning on d 4 and then amplify Th2 polarization and Tfh induction in an ICOS-L/ICOS dependent manner during d 5-6. We speculate that the B cells that acquired papain at d 0 in a noncognate manner then process and retain Ag during expansion so as to present the Ag to papain-specific T cells on d 4-5. This cognate presentation occurs in the context of MHC-II along with ICOS/ICOS-L and CD86/CD28 costimulation, thereby amplifying IL-4 production by both effector Th2 cells and Tfh. This IL-4 production by Tfh further activates B cells, increasing their expression of surface proteins associated with Ag presentation and possibly acting to enhance B cell-T cell interactions and subsequent IL-4 induction in both T cell compartments. Taken together, our findings identify a novel non-canonical mechanism through which B cells acquire a cysteine protease Ag with Th2 adjuvant activity and reveal a previously uncharacterized co-stimulatory role for B cells in T cell ICOS expression and Th2 polarization following papain immunization.

3.6 References

1. Grobe, K., W. M. Becker, M. Schlaak, and A. Petersen. 1999. Grass group I allergens (beta-expansins) are novel, papain-related proteinases. *Eur. J. Biochem.* 263: 33-40.

2. Chua, K. Y., G. A. Stewart, W. R. Thomas, R. J. Simpson, R. J. Dilworth, T. M. Plozza, and K. J. Turner. 1988. Sequence analysis of cDNA coding for a major house dust mite allergen, Der p 1. Homology with cysteine proteases. *J. Exp. Med.* 167: 175-182.

3. Gough, L., H. F. Sewell, and F. Shakib. 2001. The proteolytic activity of the major dust mite allergen Der p 1 enhances the IgE antibody response to a bystander antigen. *Clin. Exp. Allergy* 31: 1594-1598.

4. Finkelman, F. D., K. B. Madden, A. W. Cheever, I. M. Katona, S. C. Morris, M. K. Gately, B. R. Hubbard, W. C. Gause, and J. F. Urban, Jr. 1994. Effects of interleukin 12 on immune responses and host protection in mice infected with intestinal nematode parasites. *J. Exp. Med.* 179: 1563-1572.

5. McKerrow, J. H., C. Caffrey, B. Kelly, P. Loke, and M. Sajid. 2006. Proteases in parasitic diseases. *Annu. Rev. Pathol.* 1: 497-536.

6. Robinson, M. W., J. P. Dalton, and S. Donnelly. 2008. Helminth pathogen cathepsin proteases: it's a family affair. *Trends Biochem. Sci.* 33: 601-608.

7. Simpson, R. J., E. C. Nice, R. L. Moritz, and G. A. Stewart. 1989. Structural studies on the allergen Der p1 from the house dust mite Dermatophagoides pteronyssinus: similarity with cysteine proteinases. *Protein Seq. Data Anal.* 2: 17-21.

8. Sokol, C. L., G. M. Barton, A. G. Farr, and R. Medzhitov. 2008. A mechanism for the initiation of allergen-induced T helper type 2 responses. *Nat. Immunol.* 9: 310-318.

9. Sokol, C. L., N. Q. Chu, S. Yu, S. A. Nish, T. M. Laufer, and R. Medzhitov. 2009. Basophils function as antigen-presenting cells for an allergen-induced T helper type 2 response. *Nat. Immunol.* 10: 713-720.

10. Kumamoto, Y., M. Linehan, J. S. Weinstein, B. J. Laidlaw, J. E. Craft, and A. Iwasaki. 2013. CD301b dermal dendritic cells drive T helper 2 cell-mediated immunity. *Immunity* 39:733-743.

11. Tang, H., W. Cao, S. P. Kasturi, R. Ravindran, H. I. Nakaya, K. Kundu, N. Murthy, T. B. Kepler, B. Malissen, and B. Pulendran. 2010. The T helper type 2 response to cysteine proteases requires dendritic cell-basophil cooperation via ROS-mediated signaling. *Nat. Immunol,* 11: 608-617.

12. Ohnmacht, C., C. Schwartz, M. Panzer, I. Schiedewitz, R. Naumann, and D. Voehringer. 2010. Basophils orchestrate chronic allergic dermatitis and protective immunity against helminths. *Immunity* 33: 364-374.

13. Gao, Y., S. A. Nish, R. Jiang, L. Hou, P. Licona-Limon, J. S. Weinstein, H. Zhao, and R. Medzhitov. 2013. Control of T Helper 2 Responses by Transcription Factor IRF4-Dependent Dendritic Cells. *Immunity* 39: 722-732.

14. Perrigoue, J. G., S. A. Saenz, M. C. Siracusa, E. J. Allenspach, B. C. Taylor, P. R. Giacomin, M. G. Nair, Y. Du, C. Zaph, N. van Rooijen, M. R. Comeau, E. J. Pearce, T. M. Laufer, and D. Artis. 2009. MHC class II-dependent basophil-CD4+ T cell interactions promote T(H)2 cytokine-dependent immunity. *Nat, Immunol,* 10: 697-705.

15. Yoshimoto, T., K. Yasuda, H. Tanaka, M. Nakahira, Y. Imai, Y. Fujimori, and K. Nakanishi. 2009. Basophils contribute to T(H)2-IgE responses in vivo via IL-4 production and presentation of peptide-MHC class II complexes to CD4+ T cells. *Nat, Immunol,* 10: 706-712.

16. Kitamura, D., J. Roes, R. Kuhn, and K. Rajewsky. 1991. A B cell-deficient mouse by targeted disruption of the membrane exon of the immunoglobulin mu chain gene. *Nature* 350: 423-426.

17. Gommerman, J. L., D. Y. Oh, X. Zhou, T. F. Tedder, M. Maurer, S. J. Galli, and M. C. Carroll. 2000. A role for CD21/CD35 and CD19 in responses to acute septic peritonitis: a potential mechanism for mast cell activation. *J. Immunol.* 165: 6915-5921.

18. Silveira, P. A., J. Dombrowsky, E. Johnson, H. D. Chapman, D. Nemazee, and D. V. Serreze. 2004. B cell selection defects underlie the development of diabetogenic APCs in nonobese diabetic mice. *J. Immunol.* 172: 5086-5094.

19. Phan, T. G., I. Grigorova, T. Okada, and J. G. Cyster. 2007. Subcapsular encounter and complement-dependent transport of immune complexes by lymph node B cells. *Nat. Immunol.* 8: 992-1000.

20. Mu, F. T., J. M. Callaghan, O. Steele-Mortimer, H. Stenmark, R. G. Parton, P. L. Campbell, J. McCluskey, J. P. Yeo, E. P. Tock, and B. H. Toh. 1995. EEA1, an early endosome-associated protein. EEA1 is a conserved alpha-helical peripheral membrane protein flanked by cysteine "fingers" and contains a calmodulin-binding IQ motif. *J. Biol. Chem.* 270: 13503-13511.

21. Palm, N. W., R. K. Rosenstein, S. Yu, D. D. Schenten, E. Florsheim, and R. Medzhitov. 2013. Bee venom phospholipase A2 induces a primary type 2 response that is dependent on the receptor ST2 and confers protective immunity. *Immunity* 39: 976-985.

22. Haynes, N. M., C. D. Allen, R. Lesley, K. M. Ansel, N. Killeen, and J. G. Cyster. 2007. Role of CXCR5 and CCR7 in follicular Th cell positioning and appearance of a programmed cell death gene-1high germinal center-associated subpopulation. *J. Immunol.* 179: 5099-5108.

23. Leon, B., A. Ballesteros-Tato, J. L. Browning, R. Dunn, T. D. Randall, and F. E. Lund. 2012. Regulation of T(H)2 development by CXCR5+ dendritic cells and lymphotoxin-expressing B cells. *Nat. Immunol.* 13: 681-690.

24. Choi, Y. S., R. Kageyama, D. Eto, T. C. Escobar, R. J. Johnston, L. Monticelli, C. Lao, and S. Crotty. 2011. ICOS receptor instructs T follicular helper cell versus effector cell differentiation via induction of the transcriptional repressor Bcl6. *Immunity* 34: 932-946.

25. McAdam, A. J., T. T. Chang, A. E. Lumelsky, E. A. Greenfield, V. A. Boussiotis, J. S. Duke-Cohan, T. Chernova, N. Malenkovich, C. Jabs, V. K. Kuchroo, V. Ling, M. Collins, A. H. Sharpe, and G. J. Freeman. 2000. Mouse inducible costimulatory molecule (ICOS) expression is enhanced by CD28 costimulation and regulates differentiation of CD4+ T cells. *J. Immunol.* 165: 5035-5040.

26. Logue, E. C., S. Bakkour, M. M. Murphy, H. Nolla, and W. C. Sha. 2006. ICOS-induced B7h shedding on B cells is inhibited by TLR7/8 and TLR9. *J. Immunol.* 177: 2356-2364.

27. Nurieva, R. I., Y. Chung, D. Hwang, X. O. Yang, H. S. Kang, L. Ma, Y. H. Wang, S. S. Watowich, A. M. Jetten, Q. Tian, and C. Dong. 2008. Generation of T follicular helper cells is mediated by interleukin-21 but independent of T helper 1, 2, or 17 cell lineages. *Immunity* 29: 138-149.

28. Pulendran, B., and D. Artis. 2012. New paradigms in type 2 immunity. *Science* 337: 431-435.

29. Liang, G., T. Barker, Z. Xie, N. Charles, J. Rivera, and K. M. Druey. 2012. Naive T cells sense the cysteine protease allergen papain through protease-activated receptor 2 and propel TH2 immunity. *J. Allergy Clin. Immunol.* 129: 1377-1386 e1313.

30. Busso, N., M. Frasnelli, R. Feifel, B. Cenni, M. Steinhoff, J. Hamilton, and A. So. 2007. Evaluation of protease-activated receptor 2 in murine models of arthritis. *Arthritis Rheum.* 56: 101-107.

31. Porter, R. R. 1950. The formation of a specific inhibitor by hydrolysis of rabbit antiovalbumin. *Biochem J* 46: 479-484.

32. Schulz, O., B. J. Sutton, R. L. Beavil, J. Shi, H. F. Sewell, H. J. Gould, P. Laing, and F. Shakib. 1997. Cleavage of the low-affinity receptor for human IgE (CD23) by a mite cysteine protease: nature of the cleaved fragment in relation to the structure and function of CD23. *Eur. J. Immunol.* 27: 584-588.

33. Liang, H. E., R. L. Reinhardt, J. K. Bando, B. M. Sullivan, I. C. Ho, and R. M. Locksley. 2012. Divergent expression patterns of IL-4 and IL-13 define unique functions in allergic immunity. *Nat. Immunol.* 13: 58-66.

34. King, I. L., and M. Mohrs. 2009. IL-4-producing CD4+ T cells in reactive lymph nodes during helminth infection are T follicular helper cells. *J. Exp. Med.* 206: 1001-1007.

35. Marshall-Clarke, S., L. Tasker, M. P. Heaton, and R. M. Parkhouse. 2003. A differential requirement for phosphoinositide 3-kinase reveals two pathways for inducible upregulation of major histocompatibility complex class II

molecules and CD86 expression by murine B lymphocytes. *Immunology* 109: 102-108.

36. Nutt, S. L., and D. M. Tarlinton. 2011. Germinal center B and follicular helper T cells: siblings, cousins or just good friends? *Nat. Immunol.* 12: 472-477.

37. Brown, J. A., R. G. Titus, N. Nabavi, and L. H. Glimcher. 1996. Blockade of CD86 ameliorates Leishmania major infection by down-regulating the Th2 response. *J. Infect. Dis.* 174: 1303-1308.

38. Dong, C., A. E. Juedes, U. A. Temann, S. Shresta, J. P. Allison, N. H. Ruddle, and R. A. Flavell. 2001. ICOS co-stimulatory receptor is essential for T-cell activation and function. *Nature* 409: 97-101.

39. Shilling, R. A., B. S. Clay, A. G. Tesciuba, E. L. Berry, T. Lu, T. V. Moore, H. S. Bandukwala, J. Tong, J. V. Weinstock, R. A. Flavell, T. Horan, S. K. Yoshinaga, A. A. Welcher, J. L. Cannon, and A. I. Sperling. 2009. CD28 and ICOS play complementary non-overlapping roles in the development of Th2 immunity in vivo. *Cell. Immunol.* 259: 177-184.

40. Tafuri, A., A. Shahinian, F. Bladt, S. K. Yoshinaga, M. Jordana, A. Wakeham, L. M. Boucher, D. Bouchard, V. S. Chan, G. Duncan, B. Odermatt, A. Ho, A. Itie, T. Horan, J. S. Whoriskey, T. Pawson, J. M. Penninger, P. S. Ohashi, and T. W. Mak. 2001. ICOS is essential for effective T-helper-cell responses. *Nature* 409: 105-109.

41. Watanabe, M., S. Watanabe, Y. Hara, Y. Harada, M. Kubo, K. Tanabe, H. Toma, and R. Abe. 2005. ICOS-mediated costimulation on Th2 differentiation is achieved by the enhancement of IL-4 receptor-mediated signaling. *J. Immunol.* 174: 1989-1996.

42. Tesciuba, A. G., S. Subudhi, R. P. Rother, S. J. Faas, A. M. Frantz, D. Elliot, J. Weinstock, L. A. Matis, J. A. Bluestone, and A. I. Sperling. 2001. Inducible costimulator regulates Th2-mediated inflammation, but not Th2 differentiation, in a model of allergic airway disease. *J. Immunol.* 167: 1996-2003.

43. Hernandez, H. J., Y. Wang, and M. J. Stadecker. 1997. In infection with Schistosoma mansoni, B cells are required for T helper type 2 cell responses but not for granuloma formation. *J. Immunol.* 158: 4832-4837.

44. Liu, Q., Z. Liu, C. T. Rozo, H. A. Hamed, F. Alem, J. F. Urban, Jr., and W. C. Gause. 2007. The role of B cells in the development of CD4 effector T cells during a polarized Th2 immune response. *J. Immunol.* 179: 3821-3830.

Chapter 4, Conclusions

The initial goal of our first study was to evaluate MCp and basophil responses in two models of Th2 inflammation, *T. spiralis* infection and papain immunization. We found that in response to papain immunization only basophils were recruited to the PLN and neither cell population expanded in any other tissue. In contrast both cell populations expanded in the BM and spleen following *T. spiralis* infection and both were recruited to the MLN. Unlike in other tissues, MCp did not granulate after recruitment to the MLN despite being present between 6 and 11 days post infection. In contrast, progenitors recruited to the small intestine matured into granulated MMC. Rather, MCp in the MLN remained hypogranular and upregulated transcript for IL-4. This was accompanied by IL-4 and IL-6 production, as assessed by intracellular flow cytometry.. Furthermore, MCp were present in higher concentrations than basophils in the MLN, in contrast to the relationship between the concentration of these cell types in the spleen and BM, suggesting they might have a greater potential for influencing the MLN immune response than basophils.

The current understanding of mast cells is that there are two main categories, a long-lived CTMC that is seeded early in life by circulating fetal liver progenitors and a short-lived MMC that matures from circulating bone marrow-derived MCp (1, 2). The MCp constitutively home to some tissues, such as the small intestine (3), while they are only recruited to other tissues like the lung and trachea in the context of T-cell dependant inflammation (4-6). Previously, the MCp that gave rise to mature granulated MMC were invisible cells, only detectable through LDA analysis of tissue. While this technique allowed for quantitation of the recruited

MCp to tissue during inflammation, it did not give any further information about the recruited progenitor cells. Thus, the development of flow cytometric techniques for characterizing and isolating this cell provides a powerful new tool to analyze these cells.

Our finding that MCp recruited to the MLN in the context of inflammation produced cytokines suggests that MCp recruited to other tissues may do the same, thus potentially influencing the local immune response prior to maturing into granulated mast cells. Following OVA/alum sensitization and three inhalational OVA challenges, MCp are recruited to the lung but do not mature into MMC (7). In contrast, after seven challenges mature granulated MMC begin to appear (8). Our first study presented here suggests that the recruited MCp may still serve a function even though they do not granulate. By secreting cytokines and potentially lipid mediators, these cells could shape the lung inflammatory response.

Our second study was a deeper examination of the papain model. Previous reports had indicated that an ancillary CD11c-negative cell expressing MHC-II was necessary for full DC dependent Th2 polarization in this model, and several studies had suggested that the basophil might serve in this capacity. However, none of these studies addressed how basophils, a circulating cell, might encounter peripheral antigen and traffic to the appropriate LN. While subsequent studies by other groups raised doubts and even contradicted the role of basophils as APCs in the papain model, none addressed what the other MHC-II+ cell might be. Thus, we immunized mice with fluorescently labeled papain to determine which MHC-II+ cells in the PLN were acquiring it and found that B cells surprisingly made up the majority of

papain-bearing cells during the first 24 h after immunization and began to acquire papain within an hour after injection. Despite prior reports of basophils serving as APCs in the papain model, at no point did we see any basophil acquisition of papain. Mechanistic studies determined that B cells acted to amplify both Tfh and Th2 responses, and that this amplification involved ICOS-ICOSL interactions between B cells and naïve T cells.

Understanding the mechanisms through which cysteine proteases influence host immune responses is an important step forward in understanding what separates an allergen from an innocuous environmental protein. Cysteine proteases are components of two major allergens, dust mites and grass pollen (9, 10). With dust mites, the cysteine protease DerP1 is a strong target of host IgE responses (11). Cysteine proteases are also common to several families of helminthes, including trematodes and hookworms, and a study of rat infection with the hookworm N. brasiliensis showed that the secreted cysteine protease is specifically targeted by host IgE and IgG1 (12).

In addition to serving as an allergen, cysteine proteases also function as potent adjuvants. DerP1 can provoke an OVA-specific IgE response when injected into a mouse in combination with OVA (13). Papain can similarly serve as an adjuvant to promote strong host Th2 responses and immunoglobulin production directed against OVA (14). Cysteine proteases are not reported to form complexes with OVA, in contrast to other adjuvants such as alum (15). Rather, these studies suggest that cysteine proteases stimulate responses against bystander proteins that the immune system “sees” in close proximity to the protease. Papain is also capable

of provoking a host Th2 and IgE response completely independent of other proteins targeted against papain itself (16). Thus, cysteine proteases have the interesting property of serving as both an antigen and an adjuvant. Interestingly, these cysteine proteases that are targets of IgE responses are also capable of inducing degranulation and cytokine production by mast cells and basophils independent of IgE (17), rendering basophils and mast cells capable of responding to cysteine proteases in both an innate and an adaptive manner.

Despite contradicting the hypothesis that basophils serve as APCs in the papain model, our findings do not exclude other roles for an FcεR1α+ cell in the papain model. Even though a study using basophil-deficient mmcpt8-Cre mice showed that Th2 polarization was intact in the absence of basophils (18), no paper questioning the role of basophils has addressed the finding that treatment of mice with anti- FcεR1α impairs Th2 polarization following both papain and SEA immunization (19, 20). These findings, taken together with our findings that MCp are both present in the spleen at steady state and recruited to the MLN in the context of *T. spiralis* infection, suggest that it may be mast cells rather than basophils contributing to Th2 polarization. Although MCp are not recruited to the PLN in the context of papain immunization they are found in the spleen, and significant uptake of papain by DC and B cells in the spleen can be detected at 24h post-immunization, thus raising the possibility that MCp could play a role in systemic immune responses via the spleen.

One possible way that mast cells or MCp could influence the papain immune response is by acting directly on B cells. Mast cells have been shown to directly

activate B cells in several models (21). In one study, nasal mast cells from patients with perennial allergic rhinitis were cultured in the presence of the *D. farinae*-derived allergenic protein DerFII and tonsillar B cells. These mast cells were able to induce B cell class switching to IgE in an IL-4 independent but IL-13 and CD40L-dependent manner (22). Similarly, human HMC-1 mast cells treated with the adenosine analog NECA are able to induce B cell class switching to IgE. Although the mechanism was not explored in this study, HMC-1 cells were found to express IL-4 and 13 as well as CD40L (23). Together, these studies indicate that mast cells are able to provide B cell help following either surface IgE activation, in the case of DerFII and nasal mast cells, or more innate stimuli, in the case of HCM-1 cells and NECA. However, unlike Tfh-mediated B cell help, mast cell help is dependent on activation of the mast cell rather than cognate interactions between the B cell and the Tfh.

The clear influence of ancillary cells on Th2 responses and immunoglobulin production raises the question of why so many different cell types are required for optimal Th2 responses. One possible answer is the danger associated with misdirected Th2 responses. Th2 responses are mainly directed towards mucosal surfaces such as the lungs and the intestine and these surfaces are important to host survival. Granulocytes associated with IgE responses and recruited to sites of Th2 inflammation have incredibly potent pre-formed mediators and can rapidly synthesize cytokines and lipid mediators. Release of these mediators can cause inflammation and damage to host tissue. Thus, it is important to both prevent inappropriate T cell targeting of innocuous exogenous proteins as well as

preventing immunoglobulin responses. Perhaps by requiring innate activation of multiple cell types, including DC, granulocytes, and B cells, the immune system is somewhat safeguarded against inappropriate responses.

Taken together, our two studies highlight the activity of ancillary cells during LN Th2 inflammation. Although the influence of recruited MCp in the LN during *T. spiralis* infection was not determined, the fact that these cells stain for intracellular cytokines without exogenous stimulation strongly suggests that they are actively producing cytokines in the MLN, which may influence the immune response. B cells in the papain model definitely impact the immune response, as their absence greatly impairs T cell IL-4 responses. However, Th2 responses in the papain model are completely dependent on the DC, which is likely the case in *T. spiralis* infection as well. Thus, the B cell, and potentially the MCp, acts to modify DC-dependent Th2 inflammation rather than directly induce it, suggesting that the primary role of these ancillary cell populations is to fine-tune immune responses.

References

1. Kitamura, Y., M. Shimada, K. Hatanaka, and Y. Miyano. 1977. Development of mast cells from grafted bone marrow cells in irradiated mice. *Nature* 268: 442-443.

2. Hayashi, C., T. Sonoda, T. Nakano, H. Nakayama, and Y. Kitamura. 1985. Mast-cell precursors in the skin of mouse embryos and their deficiency in embryos of Sl/Sld genotype. *Developmental Biology* 109: 234-241.

3. Gurish, M. F., H. Tao, J. P. Abonia, A. Arya, D. S. Friend, C. M. Parker, and K. F. Austen. 2001. Intestinal mast cell progenitors require CD49dbeta7 (alpha4beta7 integrin) for tissue-specific homing. *J Exp Med* 194: 1243-1252.

4. Jones, T. G., J. Hallgren, A. Humbles, T. Burwell, F. D. Finkelman, P. Alcaide, K. F. Austen, and M. F. Gurish. 2009. Antigen-induced increases in pulmonary

mast cell progenitor numbers depend on IL-9 and CD1d-restricted NKT cells. *J Immunol* 183: 5251-5260.

5. Kamal, M., D. Wakelin, A. J. Ouellette, A. Smith, D. K. Podolsky, and Y. R. Mahida. 2001. Mucosal T cells regulate Paneth and intermediate cell numbers in the small intestine of T. spiralis-infected mice. *Clin Exp Immunol* 126: 117-125.

6. Friend, D. S., N. Ghildyal, K. F. Austen, M. F. Gurish, R. Matsumoto, and R. L. Stevens. 1996. Mast cells that reside at different locations in the jejunum of mice infected with Trichinella spiralis exhibit sequential changes in their granule ultrastructure and chymase phenotype. *Journal of Cell Biology* 135: 279-290.

7. Jones, T. G., J. Hallgren, A. Humbles, T. Burwell, F. D. Finkelman, P. Alcaide, K. F. Austen, and M. F. Gurish. 2009. Antigen-Induced Increases in Pulmonary Mast Cell Progenitor Numbers Depend on IL-9 and CD1d-Restricted NKT Cells. *J Immunol* 183: 5251-5260.

8. Xing, W., K. F. Austen, M. F. Gurish, and T. G. Jones. 2011. Protease phenotype of constitutive connective tissue and of induced mucosal mast cells in mice is regulated by the tissue. *Proc Natl Acad Sci U S A* 108: 14210-14215.

9. Grobe, K., W. M. Becker, M. Schlaak, and A. Petersen. 1999. Grass group I allergens (beta-expansins) are novel, papain-related proteinases. *Eur J Biochem* 263: 33-40.

10. Tovey, E. R., M. D. Chapman, and T. A. Platts-Mills. 1981. Mite faeces are a major source of house dust allergens. *Nature* 289: 592-593.

11. Chapman, M. D., and T. A. Platts-Mills. 1980. Purification and characterization of the major allergen from Dermatophagoides pteronyssinus-antigen P1. *J Immunol* 125: 587-592.

12. Kamata, I., M. Yamada, R. Uchikawa, S. Matsuda, and N. Arizono. 1995. Cysteine protease of the nematode Nippostrongylus brasiliensis preferentially evokes an IgE/IgG1 antibody response in rats. *Clin Exp Immunol* 102: 71-77.

13. Gough, L., H. F. Sewell, and F. Shakib. 2001. The proteolytic activity of the major dust mite allergen Der p 1 enhances the IgE antibody response to a bystander antigen. *Clin Exp Allergy* 31: 1594-1598.

14. Sokol, C. L., and R. Medzhitov. 2010. Role of basophils in the initiation of Th2 responses. *Curr Opin Immunol* 22: 73-77.

15. Iyer, S., H. HogenEsch, and S. L. Hem. 2003. Relationship between the degree of antigen adsorption to aluminum hydroxide adjuvant in interstitial fluid and antibody production. *Vaccine* 21: 1219-1223.
16. Sokol, C. L., G. M. Barton, A. G. Farr, and R. Medzhitov. 2008. A mechanism for the initiation of allergen-induced T helper type 2 responses. *Nat Immunol* 9: 310-318.

17. Machado, D. C., D. Horton, R. Harrop, P. T. Peachell, and B. A. Helm. 1996. Potential allergens stimulate the release of mediators of the allergic response from cells of mast cell lineage in the absence of sensitization with antigen-specific IgE. *Eur J Immunol* 26: 2972-2980.

18. Ohnmacht, C., C. Schwartz, M. Panzer, I. Schiedewitz, R. Naumann, and D. Voehringer. 2010. Basophils orchestrate chronic allergic dermatitis and protective immunity against helminths. *Immunity* 33: 364-374.

19. Sokol, C. L., N. Q. Chu, S. Yu, S. A. Nish, T. M. Laufer, and R. Medzhitov. 2009. Basophils function as antigen-presenting cells for an allergen-induced T helper type 2 response. *Nat Immunol* 10: 713-720.

20. Perrigoue, J. G., S. A. Saenz, M. C. Siracusa, E. J. Allenspach, B. C. Taylor, P. R. Giacomin, M. G. Nair, Y. Du, C. Zaph, N. van Rooijen, M. R. Comeau, E. J. Pearce, T. M. Laufer, and D. Artis. 2009. MHC class II-dependent basophil-CD4+ T cell interactions promote T(H)2 cytokine-dependent immunity. *Nat Immunol* 10: 697-705.

21. Merluzzi, S., E. Betto, A. A. Ceccaroni, R. Magris, M. Giunta, and F. Mion. 2014. Mast cells, basophils and B cell connection network. *Mol Immunol*.

22. Pawankar, R., M. Okuda, H. Yssel, K. Okumura, and C. Ra. 1997. Nasal mast cells in perennial allergic rhinitics exhibit increased expression of the Fc epsilonRI, CD40L, IL-4, and IL-13, and can induce IgE synthesis in B cells. *J Clin Invest* 99: 1492-1499.

23. Ryzhov, S., A. E. Goldstein, A. Matafonov, D. Zeng, I. Biaggioni, and I. Feoktistov. 2004. Adenosine-activated mast cells induce IgE synthesis by B lymphocytes: an A2B-mediated process involving Th2 cytokines IL-4 and IL-13 with implications for asthma. *J Immunol* 172: 7726-7733.

Appendix I, Supplemental Information

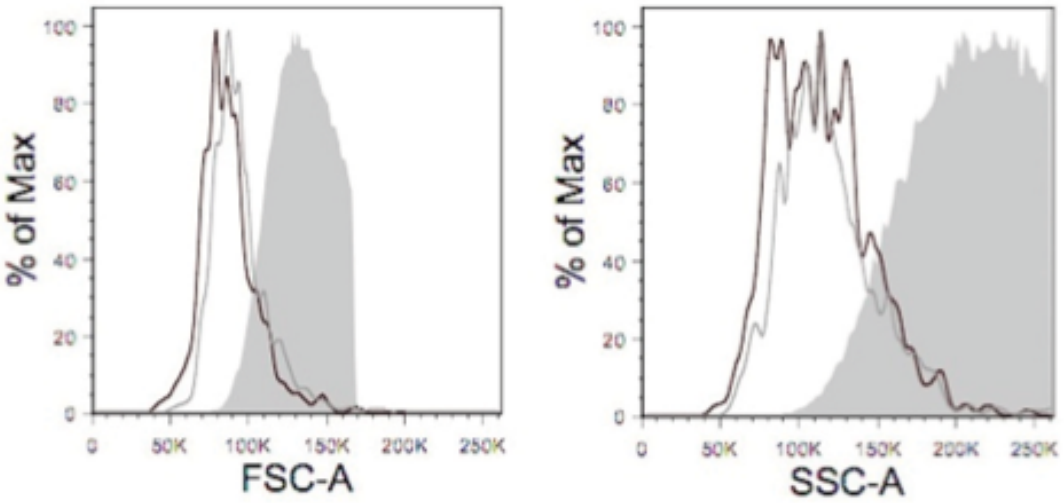

Supplementary Figure 2.1 Comparison of the forward and side scatter profiles of mesenteric LN and splenic MCp with cultured BMMC. Mesenteric LN and spleen MCp populations from d6 T. spiralis-infected mice and 6 wk old BMMC were assessed for forward and side scatter profiles by flow cytometry. The left panel shows LN and spleen MCp and BMMC size as assessed by forward scatter. The right panel shows the granularity as assessed by side scatter from the same 3 populations. The black is LN MCp, the gray line is spleen MCp and the filled histogram is BMMC.

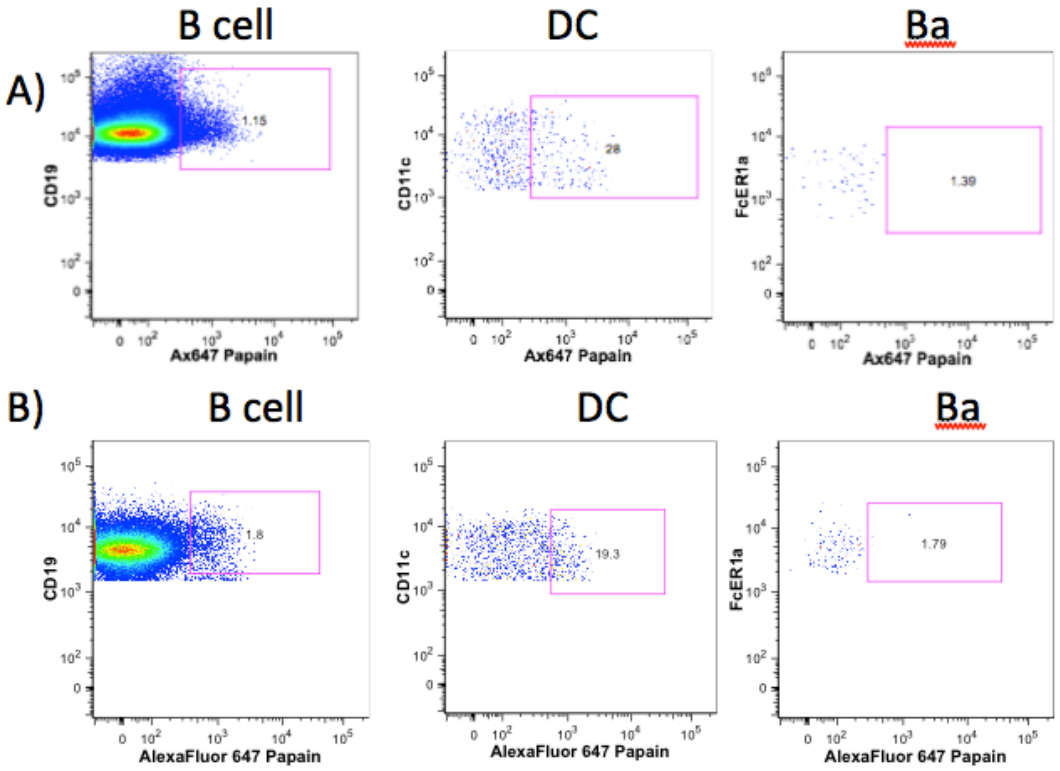

Supplementary Figure 3.1, Papain is acquired by B cells and DC but not Ba in the spleen and PLN of papain immunized mice. Representative FACS plots of B cells (CD19+ MHC-II+), DC (CD11c+ MHC-II+), and basophils, (FcεRI a+ CD49b+), isolated from (A) the LN of mice immunized 3 d prior with AF647 labeled papain, or (B) the spleens of mice immunized 1 d prior with AF647 labeled papain.

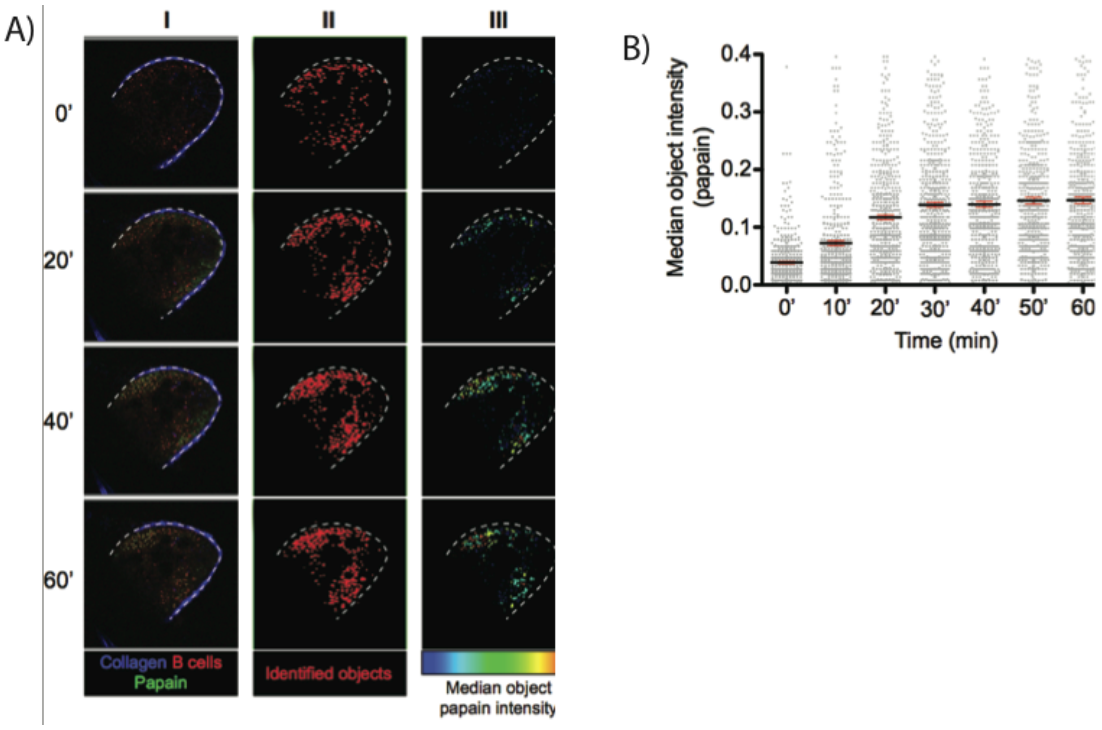

Supplementary Figure 3.2 Intravital microscopy analysis of PLN B cell uptake of labeled papain following footpad injection. **(A)** B cells from CD21-cre_tdTomato mice were adoptively transferred into C57BL/6 recipients, and the PLNs were live-imaged using IV-MPM. AF488-papain was injected into the footpad at t=0 and 150 mm image stacks (3 mm steps) were captured every 2 min for 60 min. Example of CD21 positive object identification at the indicated time points time at a selected z depth (60 mm). Raw images (I) were collected at each z-depth, and then processed by CellProfiler to identify CD21 positive objects (II). Identified objects were then assessed for papain colocalization, and median papain intensity was converted into visual heat-mapping data (III). **(B)** Median papain intensity from objects identified from (A) at the 60 mm depth. Heavy lines indicate the median intensity of papain staining at each given time point and red bars indicate SD. ANOVA $p<0.0001$

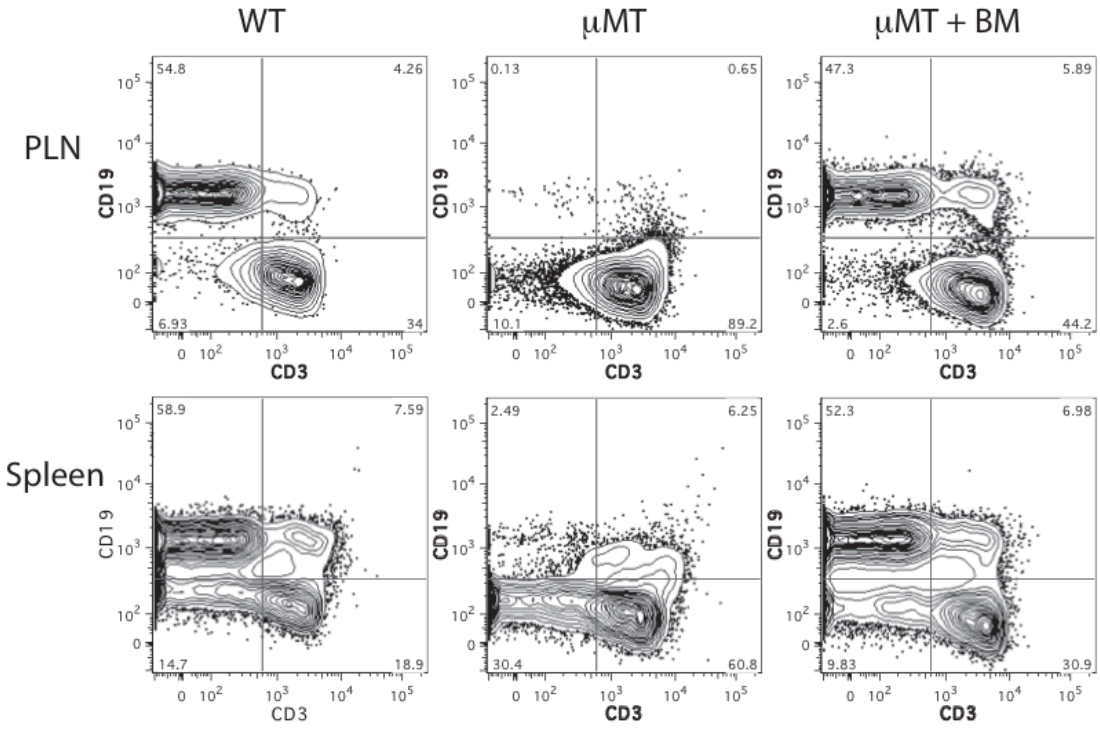

Supplementary Figure 3.3 Assessment of B cell reconstitution following sublethal irradiation. μMT mice were sublethally irradiated and reconstituted with 10^6 WT BM cells. After 8 weeks mice were injected in the rear footpad with papain and the numbers of $CD3^+$ and $CD19^+$ were evaluated in the PLN and spleen. Reconstituted μMT mice were compared to age-matched WT and non-irradiated, non-reconstituted μMT mice. Representative FACS plots are shown. Sublethal irradiation followed by WT BM adoptive transfer was able to restore the B cell compartment in the LN and spleen to near-WT levels.

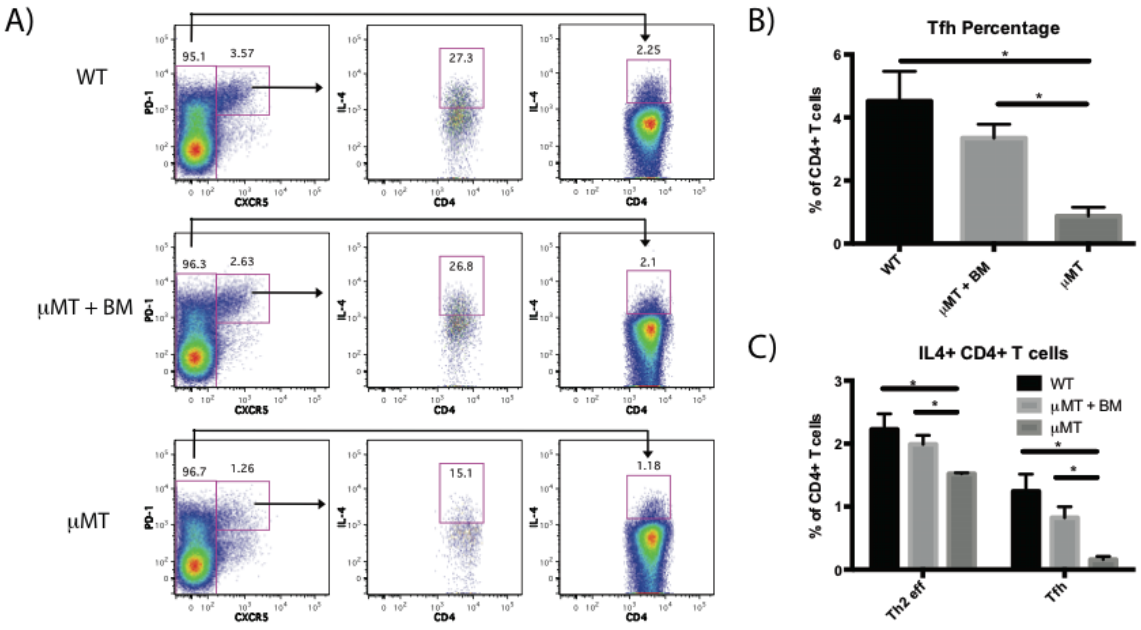

Supplementary Figure 3.4: Analysis of the impact of B cell reconstitution on Tfh and Th2 responses. μMT mice were sublethally irradiated and reconstituted with 10^6 WT BM cells. After 8 weeks mice were injected in the rear footpad with papain and their immune responses were assessed after 5 d. Reconstituted μMT mice were compared to age matched WT and non-irradiated, non-reconstituted μMT mice. **(A)** Representative FACS plots showing the induction of Tfh ($PD1^+$ CXCR5 high) and IL-4 expression by Tfh and effector T cells (CXCR5 low) in WT, sublethally irradiated and reconstituted μMT, or non-irradiated or reconstituted μMT mice analyzed on d 5 post-immunization. **(B)** Quantification of total Tfh as a percentage of all $CD4^+$ T cells in WT, sublethally irradiated and BM-reconstituted μMT, or non-irradiated, non-reconstituted μMT mice. Bars indicate mean ± SEM of n=3 mice per group. **(C)** Comparison of effector Th2 cells ($IL\text{-}4^+$, CXCR5 low) vs $IL\text{-}4^+$ Tfh cells (CXCR5 high, $PD\text{-}1^+$, $IL\text{-}4^+$) as a mean percentage of all $CD4^+$ T cells in WT, sublethally irradiated and BM reconstituted μMT, or non-irradiated, non-reconstituted μMT mice.

(Supplementary Figure 2.4, continued) Bars indicate mean ± SD of n=3 mice per group

Supplemental Movie 3.1 Live imaging of PLN B cell uptake of labeled papain following footpad injection. A C57BL/6 mouse was adoptively transferred with $5x10^6$ CD21-cre _tdTomato B cells and 24 hours later, the recipient was anesthetized and the PLN was exposed for live imaging. AF488-papain was injected into the footpad at t=0, and serial 150 μm image stacks were collected every 2 minutes for 60 minutes. Movie displayed is visualized as a 3 dimensional rendering, and corrected for movement in Volocity image analysis software. Blue indicates collagen, green indicates papain, and red indicates B cells